UNIVERSITY OF CALIFORNIA
RIVERSIDE

Characterization of Novel Luciferin Analogues and Their Evaluation for Engineered
Luciferase Assays

A Dissertation submitted in partial satisfaction
of the requirements for the degree of

Doctor of Philosophy

in

Bioengineering

by

Natalie De Howitt Rivera

December 2018

Dissertation Committee:
    Prof. Michael Pirrung, Co-Chairperson
    Prof. Jiayu Liao, Co-Chairperson
    Prof. William Grover

The Dissertation of Natalie De Howitt Rivera is approved:

_____

_____

Committee Co-Chairperson

_____

Committee Co-Chairperson

University of California, Riverside

Acknowledgements

 I acknowledge,

Prof. Michael Pirrung for teaching a younger version of myself to gather information to construct well founded ideas before jumping into execution, for always holding me against and pushing me to achieve a high scientific standard, and for exposing me to organic chemistry.

Prof. Jiayu Liao for teaching me the ins and outs of protein expression and purification, and for his support throughout my growing process as a scientist.

Prof. Victor Rodgers for seeing the diamond in the rough in me and for the support through the GAAN fellowship which provided funding during the initial stages of my graduate degree pursuit.

Prof. Hui-wang Ai for allowing me to utilize instruments in his lab and for scientific guidance.

Allyson Dorsey, M.Sc., Andrew Carlson, M.Sc., Goutam Biswas, Ph.D., and Zhijian Han, Ph.D. for the synthesis, purification, and characterization of d_2-luciferin, S-luciferin, F_2-luciferin, and iodinated oxyluciferin analogues, respectively.

Dedication

This dissertation is dedicated to my wonderful family -my mother and father, Marta Rivera and Alberto De Howitt, my brother, Alberto De Howitt, my uncle, Richard De Howitt, and my amazing husband, Aaron Cipriano. Your continuous support has made this dissertation possible.

ABSTRACT OF THE DISSERTATION

Characterization of Novel Luciferin Analogues and Their Evaluation for Engineered
Luciferase Assays

by

Natalie De Howitt Rivera

Doctor of Philosophy, Graduate Program in Bioengineering
University of California, Riverside, December 2018
Prof. Michael Pirrung, Co-Chairperson
Prof. Jiayu Liao, Co-Chairperson

The bioluminescence from the luciferase-luciferin reaction has been extensively used in biological assays for the detection and visualization of analytes and cell viability *in vitro* and *in vivo*. Compared to fluorescence, bioluminescence imaging has recently started to explore the engineering of novel pairs of luciferase and luciferin that could broaden the scope of bioluminescence assays. This dissertation describes the work with three luciferin analogues: d_2-luciferin, S-luciferin, and F_2-luciferin, designed to target: 1. The production of inhibitory by-products. 2. A thiol/disulfide redox bioluminescence probe for the detection and visualization in intact cells. 3. The pH dependence of the bioluminescence reaction. Our results with d_2-luciferin showed that the formation of inhibitory by-product,

dehydroluciferin, was reduced from 16%, with luciferin, to 8% with d_2-luciferin. However, these results did not reflect a higher bioluminescence intensity as was expected from the reduction of dehydroluciferin formation. Work with S-luciferin showed that the substitution of a thiol for the hydroxyl group in luciferin decreases the electron donating capacity needed for bioluminescence. Furthermore, results showed that S-luciferin is a poor substrate of luciferase with a K_i of 0.07 μM. We target the pH dependence of luciferin with F_2-luciferin, which has a lower pK_A at the 6'-hydroxyl group allowing the molecule to be ionized around pH 7. Our results showed that F_2-luciferin is a better chromophore at pH 7 with 75% more fluorescence emission compared to luciferin. As a substrate of luciferase, F_2-luciferin showed a bioluminescence intensity optimum at pH 6.5 with a K_M of 0.73 μM. However, the bioluminescence emission intensity is only 12% of that of luciferin. Preliminary docking of S-luciferin and F_2-luciferin into luciferase showed the potential of in silico experiments that could lead to luciferase engineering. These results suggested that further work is needed in order to create novel luciferase-luciferin pairs that could broaden the scope of bioluminescence imaging. Therefore, our next work focused on studying oxyluciferin analogues before developing luciferin analogues with a desired property. Iodinated oxyluciferin analogues were studied for the production of singlet oxygen. From the analogues studied Me_2-I_2-oxyluciferin showed the highest production of singlet oxygen. This preliminary work shows that iodinated luciferin analogues have the potential to produce singlet oxygen through the luciferase reaction.

Table of Contents

List of Figures

List of Tables

List of Abbreviations

AMP	Adenosine monophosphate
ATP	Adenosine triphosphate
BL	Bioluminescence
BRET	Bioluminescence Resonance Energy Transfer
BSA	Bovine Serum Albumin
k_{cat}	Catalytic efficiency
FL	Fluorescence
GFP	Green fluorescence protein
HPLC	High performance liquid chromatography
K_i	Inhibition constant
λ_{max}	Lamda maxima
MRI	Magnetic Resonance Imaging
K_M	Michaelis-Menten affinity constant
pK_A	Negative base-10 logarithm of the acid dissociation constant
NMR	Nuclear Magnetic Resonance
P. pyralis	*Photinus pyralis*
PDT	Photon dynamic therapy
$^1O_2$	Singlet oxygen
SOSG	Singlet Oxygen Sensor Green

Chapter I: Engineering luciferin from the American firefly to create novel luciferase-luciferin assay

I.1 Bioluminescence from the American firefly

Numerous organisms utilize the luciferase-luciferin reaction to produce bioluminescence (BL). Many of these, including bacteria, fungi, fish, jellyfish, and worms have been thoroughly investigated for decades to understand the mechanism and key differences in the BL systems.[1-4] Of these, the luciferase-luciferin reaction from the American firefly (*Photinus pyralis, P. pyralis*) is one of the most studied and well-characterized systems. The American firefly luciferase-luciferin reaction is the focus of the work discussed in this dissertation.

The luciferase-luciferin reaction converts chemical energy into light through the oxidation of luciferin catalyzed by luciferase. The BL reaction can be divided in two steps: adenylation of luciferin, and generation of the excited state of oxyluciferin (Figure I.1). First, luciferin binds into the hydrophobic binding pocket where it gets adenylated by luciferase (Figure I.1, A). Upon binding, luciferase catalyzes the oxidation of luciferyl-adenylate culminating in BL from the excited state of oxyluciferin (Figure I.1, B). Adenylation, which is the first and rate limiting step in the BL reaction, begins by the

displacement of the carboxylic group at the C4 carbon of luciferin and the diphosphate group of ATP. The adenylation step generates the first enzyme-bound intermediate, luciferyl-adenylate.[5, 6] Adenylation increases the acidity of the C4 and allows the subsequent attack of its enolate on molecular oxygen, which forms the hydroperoxy-adenylated intermediate.[5, 7] This step is followed by the nucleophilic attack of hydroperoxide group to create the dioxetanone species. The dioxetanone species is a strained energy-rich ring which is unstable and easily breaks to generate the excited state of oxyluciferin and carbon dioxide.[7-11] Oxyluciferin is the light emitting chromophore in the reaction. Finally, the relaxation of oxyluciferin to the ground state emits light at 562 nm at pH 7.8.[12]
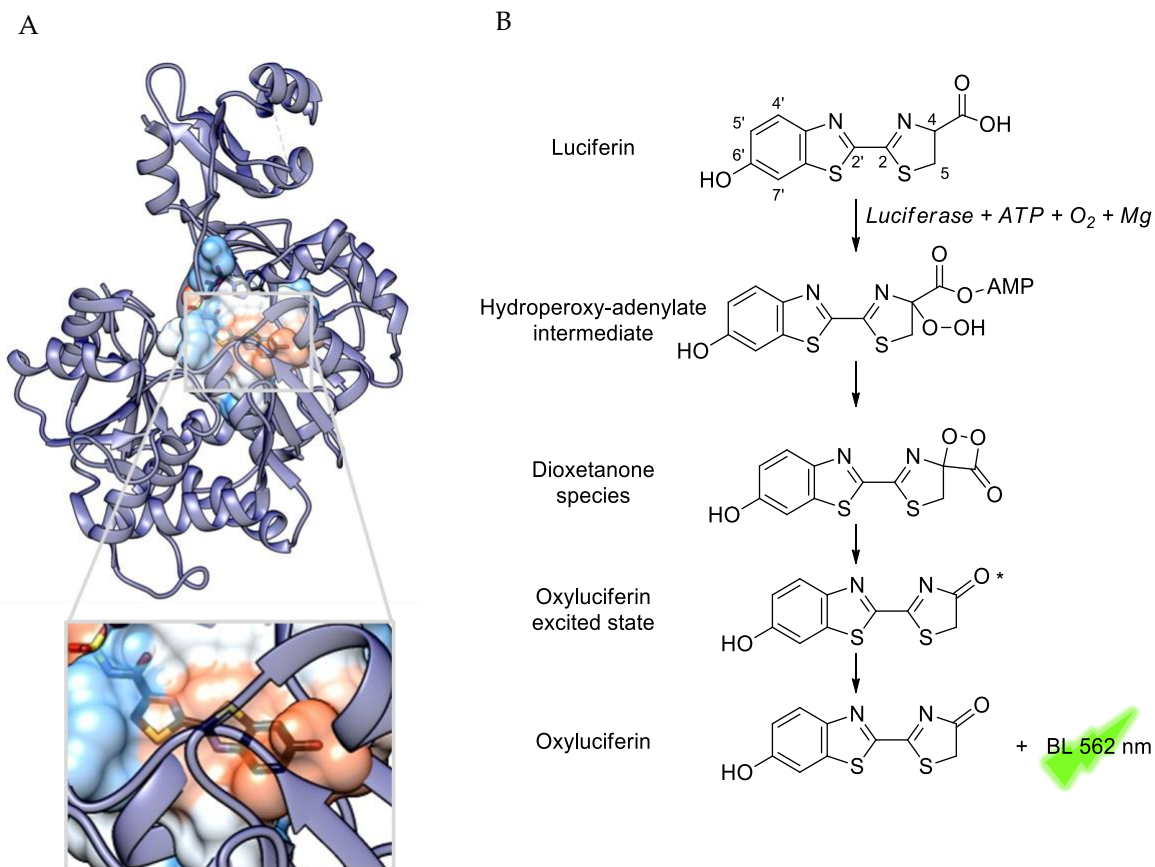
Figure I.1 Scheme for the bioluminescence production by the luciferase-luciferin reaction.
Luciferase (the enzyme) binds with luciferin (the substrate) (A). Here the crystal structure (PDB:4G36) shows the conformation of luciferase with bound luciferyl-adenylate analogue intermediate. Graphic developed using Chimera Software. The inset in (A) highlights the hydrophobic binding pocket of luciferase. BL is generated by a series of molecular changes of luciferin (B). First, luciferase catalyzes the adenylation of luciferin. Then the removal of a proton from the C4 carbon of the adenylate and addition of molecular oxygen transforms luciferyl-AMP into the very reactive dioxetanone intermediate. The dioxetanone possesses a strained four-membered ring that easily breaks down to generate the excited state of oxyluciferin and carbon dioxide (not shown). Lastly, the excited state returns to the ground state while emitting a photon at 562 nm.

Luciferin has two moieties with equally important roles in the production of BL: the benzothiazole and the thiazoline (Figure I.2). The thiazoline moiety is required for the enzyme to catalyze the reaction. The benzothiazole moiety assist in positioning luciferin within the active site of luciferase and plays a leading role in the BL emission wavelength and intensity.[6, 13-16] The generally proposed mechanism for the BL emission wavelength and intensity relies on charge transfers between the moieties. The benzothiazole moiety donates electrons to dioxetanone specie that will break and generate the excited state of oxyluciferin. Modifications to the benzothiazole moiety can impact the BL emission wavelength and intensity and are the focus of many research groups. However, a complete step by step of the BL mechanism that results in the photon emission remains unknown.
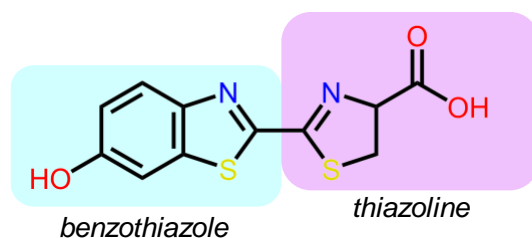
Figure I.2 The two moieties of luciferin: benzothiazole and thiazoline.

The BL from luciferase-luciferin is a widely used bioimaging technique with several advantages over conventional imaging techniques. For example, conventional fluorescence (FL) imaging requires laser excitation which incidentally excites undesired chromophores and generates substantial background. Likewise, common FL chromophores (e.g., dyes, green fluorescence protein (GFP) and its mutants) are susceptible to quenching. Together, the need for an external energy source and quenching of the chromophores limits the use of FL for many bioimaging applications. In contrast, BL results from the biochemical excitation of only the desired chromophore (i.e., oxyluciferin). Furthermore, the quantum yield of the luciferase-luciferin reaction (approx. 0.41)[17] is relatively high compared with the quantum yield of chemiluminescence reactions, which are typically around 0.01. [17, 18] On FL molecules and proteins the quantum yield can vary significantly from low to close to unity, where most molecules are able to emit per excitation.

BL assays are mostly used as gene reporters due to the ability of luciferase to be expressed simultaneously with a desired gene. In the presence of Mg^{2+}, ATP, and molecular oxygen, BL from the luciferase-luciferin reaction provides a genetically encoded probe to visualize, detect, and quantify biological processes within cells and living organisms. The oxidation of luciferin by luciferase generates a quantitative BL signal that is proportional to the concentration of luciferase. The concentration of luciferase usually corresponds to a protein or analyte of interest, cell viability test, and/or detection of the specific cell.[19-21]

Furthermore, cells can be engineered to express luciferase and will emit BL upon addition of luciferin directly into the media or through injection into the organism. This makes BL assays extremely useful for both *in vitro* and *in vivo* studies.

This chapter will highlight developments in luciferin analogues and mutated luciferases, which have been designed to enhance the luciferase-luciferin reaction for novel applications. Advances in luciferin analogues are presented first, followed by efforts to create luciferase mutants that are efficient with luciferin analogues.

I.2 Developments in luciferin and luciferase to optimize pH dependence for biological applications

The first synthesis for luciferin was described around 60 years ago by White et al.[22] Over the last few decades, several luciferin analogues have been developed to address some of the intrinsic limitations of the luciferase-luciferin reaction to enhance the use of BL for biological applications. The luciferase-luciferin reaction is pH dependent, the enzyme is not thermostable, has BL emission at 562 nm, and luciferin does not diffuse easily into cells. Of these, pH dependence and thermostability are critical for biological applications and efforts centered around addressing these limitations will be discussed in this section.

It is well known that the BL emission wavelength and intensity from the luciferase-luciferin reaction is pH dependent. Both luciferin and luciferase contribute to the pH dependence of the reaction; however, the exact mechanism remains elusive since BL results from a multi-step dynamic reaction between a substrate and an enzyme. As a result, both luciferin analogues and luciferase mutants have been developed to study the pH dependence of the luciferase-luciferin reaction. Most studies investigating the pH dependence focused on luciferase mutants rather than luciferin analogues. Likewise, most studies investigated the pH dependence of BL emission wavelength instead of intensity.

I.2.1 *Luciferin analogues to improve pH dependence*

The phenol group in the benzothiazole moiety of luciferin is responsible for the pH susceptibility of the molecule and has a pK_A of 8.7.[6, 17] Interestingly, the BL emission intensity of the wildtype luciferin-luciferase reaction: is highest at pH 8.5, which is close to the pK_A of the 6'-hydroxyl group; and decreases with increasing acidity of the solution. This behavior can be partially attributed to the multiple ionic forms of the molecule, which affect its electronic configuration. Collectively, this indicates that the wildtype luciferase-luciferin system is best used in applications that require basic pH. Unfortunately, most biological applications stipulate neutral pH.

The pK_A of the benzothiazole moiety from luciferin analogues can potentially serve as an indicator of the optimum operating pH. Previous spectroscopic studies showed that the ionization of the 6'-hydroxyl group of luciferin produced a higher FL emission intensity relative to the protonated state. Therefore, it is reasonable to speculate that lowering the pK_A of the 6'-group of luciferin could result in higher emission pH values around or below the aforementioned pK_A. To date, a systematic spectroscopic characterization and pH dependence study of luciferin analogues in response to changes in pK_A of the benzothiazole moiety has not been reported. In fact, the pK_A is often overlooked and the metric often reported is only BL emission of the analogue with luciferase. Most luciferin analogues developed thus far have not managed to increase BL emission intensity at neutral pH, but careful substitutions in the benzothiazole moiety could potentially help achieve this goal.

Luciferin analogues with fluorine or chlorine substitutions at the C7' position were developed to address the emission wavelength pH-dependence of the molecule. Takakura et al. synthesized 7'-fluoro-luciferin, 7'-chloro-luciferin, and 7'-fluoro-5'-hydroxymethyl-luciferin, all of which have a more acidic pK_A at the 6'-hydroxyl group compared with luciferin.[23] Spectroscopic analysis of these luciferin analogues showed that absorbance λ_{max} in acidic and basic conditions remained similar to luciferin. In contrast, the FL emission was pH dependent and showed bathochromic shifts of 10 to 30 nm compared to

luciferin, at acidic and basic conditions. These results confirmed that small substitutions in the benzothiazole moiety could shift the FL λ_{max} of luciferin. The study did not report any emission intensity difference within the analogues or compare to luciferin. Interestingly, when evaluated with luciferase, the BL emission wavelength of 7'-fluoro-5'-hydroxymethyl-luciferin was pH independent, and the relative BL intensity was 2% compared with luciferin.

The luciferin analogue 6'-amino-luciferin addresses the intrinsic pH dependence of luciferin. The amine group used for the substitution at the 6'-position has a lone pair that is able to donate electrons through physiological pH, thus making 6'-amino-luciferin pH independent for biological assays. Interestingly, 6'-amino-luciferin produces a red-shifted BL emission lambda max at 605 nm when catalyzed by luciferase from *P. pyralis* but produces an emission λ_{max} at 550-570 nm when catalyzed by luciferase from *Pyrophorus plagiopthalamus*.[24] Thus, the interaction between the luciferin analogue and the active site of luciferase plays a significant role in dictating the resulting BL properties.

I.2.2 *Luciferase mutants to improve pH and temperature dependence*

Like all enzymes, luciferase has an optimum pH and temperature at which catalytic efficiency (k_{cat}/K_M) of luciferin oxidation is maximum. For the luciferase-luciferin reaction, optimal catalytic efficiency occurs at pH 8.5.[17] As mentioned before, basic conditions are

favorable for some biological applications, including DNA and ATP assays *in vitro*. However, widespread use of BL for biological applications requires optimal k_{cat}/K_M in neutral conditions.

The pH dependence of the BL reaction is influenced by both the catalytic activity and the interaction between the active site hydrogen bonding and the electron donating capacity of the 6'-group on oxyluciferin. The pH dependence of the catalytic activity of luciferase was demonstrated by Takakura et al., who showed varying consumption rates of a pH-independent luciferin analogue with varying pH of the reaction.[23] Specifically, the study showed that the pH independent analogue, 6'-amino-luciferin, was consumed more at pH 8 and consumption decreased with increasing acidity. Furthermore, studies with several luciferase mutants have shown that maximum k_{cat} at approximately pH 8 was conserved, which shows the challenges associated with luciferase pH dependence.[25] Specially, for engineering luciferase-luciferin system that would have optimum BL at neutral pH for biological applications. Other studies with luciferase mutants showed their ability to influence BL emission wavelength in a pH-independent manner but at the cost of lower catalytic efficiency and associated lower BL emission intensity.[25-27]

Other efforts have focused on developing thermostable luciferase mutants for *in vivo* applications. Physiological conditions dictate a working temperature of 37 °C. At this temperature, luciferase loses nearly all activity within 10 minutes.[24] Jathoul et al.

developed a thermostable *P. pyralis* luciferase mutant.[24] Their results showed that the BL

activity of the luciferase mutant remained consistent up to 50 °C. Incidentally, the study

also showed that the BL emission intensity of the luciferase mutant with luciferin was

consistent for pH 8 to pH 6.8. In contrast, under the same condition, the BL emission

intensity of luciferase decreased immediately for conditions slightly more acidic than pH

8. Unfortunately, the BL emission intensities were normalized within each group and a

comparison between wildtype and mutant was not discussed. Thus, the catalytic

efficiencies for wildtype and mutant luciferases from this study cannot be compared.

However, taken together, these results suggest the possibility of further improving

luciferase mutants for catalytic efficiency at neutral pH for biological and physiological

applications.

I.3 Luciferin analogues for biological applications

I.3.1 *Luciferin analogues for in vivo bioimaging*

The yellow-green BL emission at 562 nm from the luciferase-luciferin reaction is not

natively suited for deep tissue bioimaging applications requiring near-red emission.

Efforts to develop red-shifted luciferase-luciferin systems have focused in two general

directions: modifications to the luciferin substrate, and mutations of luciferase. In the first

approach, the electronic properties of the benzothiazole moiety of the substrate (i.e.,

precursor to oxyluciferin) is directly engineered to promote a red-shifted emission. In the second approach, luciferase mutants are used to change the microenvironment of oxyluciferin to influence the emission properties. Despite tremendous efforts and ability to obtain red-shifted emissions, the performance of luciferin analogues with luciferase is extremely poor.[13, 28] Thus, a luciferase-luciferin pair for deep tissue *in vivo* applications remains elusive. BL-based *in vivo* bioimaging and detection could assist in the development of drugs, therapies, and treatments for diseases. In this section, we discuss luciferin analogues intended to achieve a red-shifted emission. The rationale behind the synthesis of these analogues helped guide the work of luciferin analogues presented in this dissertation. Work with luciferase mutants for red-shifted emission has been compiled in other review articles.[29, 30]

I.3.1.a 6′-amino-luciferin

White and McElroy synthesized 6′-amino-luciferin by late 1950s[6, 31] and it was the first luciferin analogue to generate a red-shifted emission. The 6′-amino-luciferin has an amine substitution for the 6′-hydroxyl group. In contrast to the hydroxyl, the amine group has an electron lone pair which it can easily donate to obtain BL emission wavelength independent of pH. The BL from 6′-amino-luciferin is redshifted approximately 30 to 40 nm compared with luciferin, which nearly meets the necessary emission wavelength for deep tissue *in vivo* studies.[6, 28, 32] Therefore, several groups have used the 6′-amino-luciferin

as the starting point to design and create luciferin derivatives with further redshifted emissions to develop BL systems for *in vivo* deep tissue imaging. The 6'-amino-luciferin is routinely used in a variety of biomedical assays and is available as a commercial product.

I.3.1.b Cyclic alkyl-aminoluciferins

In 2010, the Miller research group synthesized a cyclic alkyl-aminoluciferin (CycLuc1) and methylated cyclic alkyl-aminoluciferin (CycLuc2), which are aminoluciferin derivatives with a cyclic alkyl-amine substitution at the 6'-position.[32] (Figure I.3) Cyclization inhibits free rotation of the aryl-amine and ensures a good orbital overlap between the lone pair of N and the conjugated system of the benzothiazole. Thus, the cyclic alkyl-amine substitution results in a stronger electron donating group compared with 6'-amine. The authors reported red-shifted emission wavelengths of: 599 nm for CycLuc1, 607 nm for CycLuc2, and 594 nm for 6'-amino-luciferin when measured with luciferase. The authors measured the BL emission intensity for CycLuc1 and CycLuc2 compared with luciferin and found a significant reduction for both analogs. The authors then compared the characteristic initial light burst for CycLuc1, CycLuc2, and luciferin at equal concentrations and found that the burst for CycLuc1 was twice as high compared with 6'-amino-luciferin but CycLuc2 was lower than 6'-amino-luciferin. In the case of CycLuc1, the high initial burst together with reduced BL emission intensity suggest a high affinity for luciferase followed byproduct inhibition resulting in a mitigated ability to maintain

light emission. Therefore, the authors investigated CycLuc1 further using a commercial

mutant luciferase, Ultra-glow that does not generate the characteristic initial burst yet

allows continuous light production.[32] The results from the Ultra-glow-CycLuc1 pair

showed a 3 to 6-fold increase in BL intensity compared with the Ultra-glow-luciferin and

Ultra-glow-6'amino-luciferin control. Collectively, results from the CycLuc1 analogue

studies suggest that the strategy to develop novel luciferin analogues should also include

developing a mutant luciferase to maximize catalytic efficiency and BL emission at the

targeted conditions. Further studies compared luciferin and CycLuc1 for *in vivo* imaging,

specifically brain imaging.[33]   The *in vivo* results showed superior performance of CycLuc1

with routinely used luciferase. Currently, CycLuc1 is commercially available.
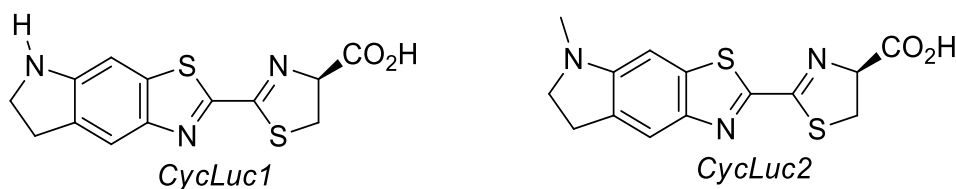
Figure I.3 Cyclic alkyl-aminoluciferin structures.

I.3.1.c 6'-amino-1-seleno-luciferin

In 2012, the Moerner research group synthesized 6'-amino-1-seleno-luciferin, which

contains a selenium atom in exchange of the native sulfur atom at the 1 position.[28] The Se

substitution leverages the heavy atom effect, which provides redshifted emission on FL

chromophores as a result of substituting an atom in the molecule by a heavier atom, such

as replacing oxygen for sulfur or selenium.[34, 35] Spectral characterization of 6′-amino-1-seleno-luciferin analogue showed a 42 nm and 12 nm redshift relative to luciferin and aminoluciferin, respectively. Furthermore, the BL emission with wildtype luciferase for 6′-amino-1-seleno-luciferin showed an increase of 14% and 30% (at wavelengths of 600 nm and above) when compared with aminoluciferin and luciferin, respectively. In contrast, *in vitro* imaging studies using luciferase and 6′-amino-1-seleno-luciferin showed a decrease in BL compared to 6′-amino-luciferin. The authors also investigated the *in vivo* BL emission of 6′-amino-1-seleno-luciferin with cancer cells expressing luciferase and found no significant difference when compared with aminoluciferin during a 30-minute acquisition period. Future studies with 6′-amino-1-seleno-luciferin suggested the possibility of using a ^{77}Se atom to create a stable S = ½ nuclei with chemical shifts detectable by magnetic resonance imaging (MRI). Currently, BL and MRI are used as separate imaging techniques to study tumor models in mice.[21, 36, 37] Thus, 6′-amino-1-seleno-luciferin could provide a BL/MRI platform for a dual imaging modality of tumor models.

I.3.1.d Brominated luciferins

In 2017, the Prescher research group synthesized three brominated luciferin analogues, with a bromo substitution at the C7′, C5′, or C4′positions.[38] In silico modeling studies showed that the active site of luciferase constricts the luciferin molecule at the C4′ and C7′

positions.[38] The authors characterized the FL properties of the three brominated analogues and did not observe a significant difference. In contrast, when evaluated with luciferase at pH 7.6, the BL emission maximum was red-shifted by 25 nm for C7′-Br, 35 nm for C5′-Br, and 50 nm for C4′-Br relative to luciferin. The BL emission intensity was 3.4% for C7′-Br, 46.0% for C5′-Br, and 3.1% for C4′-Br of that produced by luciferin and wildtype luciferase. Based on red-shift and emission intensity results, the C5′-Br analogue was selected for *in vitro* and *in vivo* studies with mice and cells expressing luciferase. Results from the *in vitro* evaluation of C5′-Br showed higher BL intensity at 25 μM compared to luciferin. Additionally, the *in vivo* results showed a slower decay of the emission compared with luciferin. However, the total photons emitted by C5′-Br were lower compared with luciferin at the same concentration. The authors suggested that the three brominated analogues can be used as precursors for the synthesis of other luciferin analogues to achieve the desired performance for *in vivo* bioimaging and/or enhance the scope of BL for other applications.

Despite great progress in the design and synthesis of luciferin analogues that produce red-shifted emissions, a key contribution is likely to come from careful design of the interaction and microenvironment with mutant luciferases. The success of luciferin analogues for *in vivo* applications depends on their ability to: serve as good substrates to luciferase, permeate through the cell wall, and be able to emit from luciferase microenvironment. The latter been the hardest one to predict. Currently, it is known that

the protein microenvironment can affect the BL through deactivation pathways that lead to non-radiative decays and/or disruption of the analogue conformation necessary to allow the charge-energy transfer that results in BL.[38] Thus, development of a luciferin analogue suitable for deep tissue *in vivo* applications should go hand-in-hand with the study and design of luciferase mutants able to create a microenvironment conducive to BL emission with the desired luciferin analogue.

I.3.2 *Luciferin analogues for bioluminescence-based bioanalytic assays*

In addition to bioimaging applications, luciferase-luciferin systems have also been developed for many bioanalytical applications. The first luciferase-luciferin bioanalytical assay relied on using purified luciferase and luciferin from firefly extracts to measure ATP down to 10 picograms.[39] Since then, the luciferase-luciferin ATP assay has been used to test for bacterial contamination, antibiotic efficiency, and cells viability, among other applications.[40-42] The chemical synthesis of luciferin and its analogues, as well as the cloning of luciferase, has opened the scope of luciferase-luciferin assays for detection of specific environments or analytes.[22, 43, 44] A common strategy used in the development of BL analyte detection is a caged luciferin. A caged luciferin is the accepted term for a luciferin with a 6'-substitution that upon reacting with the desired analyte will generate luciferin. The generated luciferin is able to undergo catalysis by luciferase and act as a probe for the desired analyte. Numerous examples of caged luciferins can be found in the

literature and most of them target a specific molecule, like an enzyme, metal, or fatty acid among others. Several luciferin analogues and luciferase pairs used for *in vitro* and *in vivo* bioanalytical assays are described in a review by Smirnova and Ugarova.[45] This section highlights two studies that exemplify recent developments in luciferin-luciferase pairs for BL-based bioanalytical assays.

I.3.2.a Amide-luciferins for detection of FAAH activity

Building on the results from the CycLuc1 luciferin analogue (see Section I.3.1.b), the Miller research group synthesized a CycLuc1 analogue with an amide substitution for the carboxylic acid.[46] The fatty acid amide hydrolase (FAAH) enzyme hydrolyzes fatty acid amides to their respective fatty acids. (Figure **I**.4, A) Thus, the authors rationalized that FAAH could hydrolyze amide-substituted luciferins back to the native carboxylic acid. (Figure **I**.4, B) In the case of CycLuc1-amide, FAAH would hydrolyze the molecule back to the CycLuc1. Similarly, the authors designed and synthesized other amide-substituted analogues capable of being hydrolyzed by FAAH. (Figure **I**.4, C) The authors demonstrated that the amide-substituted luciferin analogues were hydrolyzed and produced BL in the presence of FAAH but did not produce BL when inhibitors of FAAH were added.
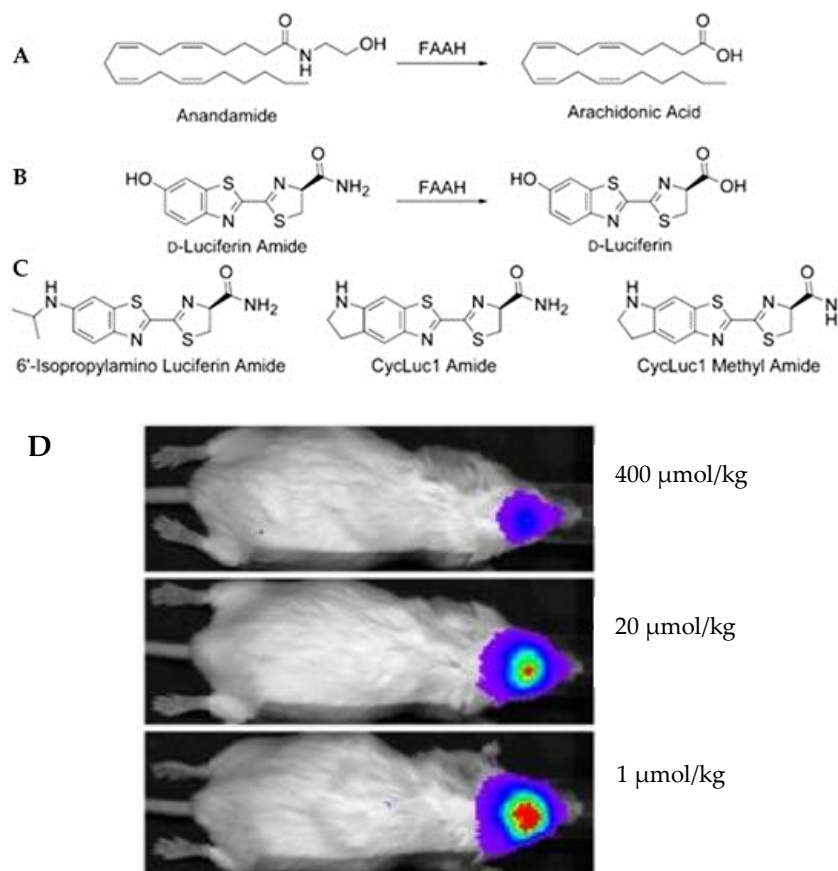
Figure I.4 Amide-luciferin analogues for detection of FAAH activity.
FAAH hydrolyses amides to carboxylic acids (A). FAAH can hydrolyze amide-luciferins (B). Amide luciferins evaluated for FAAH activity in cells and brain (C). *In vivo* BL activity from the brain of CycLuc1-amide at 400-fold lower dose compared with luciferin (D). Figure adapted from Miller et al. J. Am. Chem. Soc. (2015)137, 8684-8687.

Subsequently, CycLuc1-amide, CycLuc1, and luciferin were compared to evaluate *in vivo*

FAAH activity in brain cells expressing luciferase. Results showed that CycLuc1-amide

had a significantly higher BL activity at 400-fold lower dose compared with luciferin.

(Figure **I**.4, D) Furthermore, a higher BL was seen from all the amide-luciferin analogues

compared to their corresponding luciferin on intact cell assays. Presumably, this is due to

the lack of ionization from the amide compared to the carboxylic acid that allows the luciferins to easily penetrate the cell membrane. Previous studies of CycLuc1 with luciferase showed a low K_M compared to luciferin.[47] The authors understand that the results with CycLuc1-amide demonstrate that luciferin analogues with an improved biodistribution and a low K_M can potentially assist the development of novel *in vivo* BL probes.[46, 48]

I.3.2.b Hydroxyamino-luciferin for cell-cell contact

The Prescher research group designed and synthesized a 6'-nitro-luciferin to study cell-cell interactions.[49] The authors rationalized that a nitroreductase enzyme could reduce the nitro substitution to a 6'-hydroxyamino-luciferin. Furthermore, the authors demonstrated that the cell-permeable 6'-hydroxyamino-luciferin produced BL with wildtype luciferase. To demonstrate cell-cell contact based on nitroreductase-mediated BL, the authors prepared cells expressing either nitroreductase or luciferase and plated both cell types in three configurations: 1) in contact with each other, 2) separated but allowed to grow into contact, and 3) 1 mm apart from each other. The 6'-nitro-luciferin analogue was then added to the cells with nitroreductase, and the results showed BL emission for configurations 1 and 2, but not for 3. However, a weak BL emission intensity from the cell-cell contact was presumably due to the limited release and diffusion of the reduced 6'-

hydroxyamino-luciferin. To eliminate these limitations, the authors prepared a cell expressing both nitroreductase and luciferase and observed a 40-fold increase BL signal when 6'-nitro-luciferin was added. The authors did not provide a BL emission spectrum for 6'-hydroxyamino-luciferin analogues, but the reported intensity was lower compared with 6'-amino-luciferin. As mentioned previously, obtaining a BL emission intensity comparable with luciferin, or even 6'-amino-luciferin, continues to be a challenge for luciferin analogues.

I.3.3 *Oxyluciferin as a way to design luciferin analogues for biological applications*

It is well known that luciferin gets oxidized by luciferase to form oxyluciferin, the emitting chromophore in the BL reaction. The majority of the work presented in the literature corresponds to engineered luciferin analogues, since its synthesis has been established for over 50 years. Moreover, luciferin properties as a chromophore serve as a projection of the BL intensity, BL wavelength, and behavior of oxyluciferin. Additionally, is not until more recently that oxyluciferin analogues have been synthesized and studied to help the investigations of the BL reaction and help develop luciferin analogues that could broaden the scope of BL. Therefore, these studies will demonstrate the significant role of the interactions within the luciferase active site and oxyluciferin, the emitter, which will to some extent dictate the final BL outcome.

Additionally, modifications to luciferin are not trivial. They involved the synthesis, characterization, and purification of the molecule without any certainty that they will be a good substrate for luciferase. Recently, Naumov et al. established a synthesis route to oxyluciferin that allows preliminary studies with oxyluciferin analogues as a guide to their optical properties.[50, 51] This could help in the development of new analogues with their optical potential studied beforehand.

I.4 Luciferase mutants for improved biological performance with luciferin and its analogues

The modest quantum yield of the native luciferin-luciferase reaction indicates there is an opportunity to develop luciferase mutants better suited for luciferin or analogues. Back in the 1960s, the efficiency of the native luciferase-luciferin reaction was thought to be high with a quantum yield of close to unity.[43] However, a more recent re-examination with a more precise instrument and accounting for a non-emitting enantiomer of luciferin showed a much lower efficiency with a quantum yield of 0.41.[17] Likewise, many studies have shown that wildtype luciferase does not efficiently generate high-intensity BL with luciferin analogues.[6, 14, 23, 31, 32, 47, 52-55] As mentioned previously, there is a strong relationship between the active site of luciferase and the excitation of oxyluciferin, which is also tightly related to the catalytic efficiency of the enzyme. Collectively, these constraints can help us

to rationally engineer luciferase mutants to improve BL efficiency with luciferin analogues. Already, many groups have reported improved BL using mutated luciferases to catalyze luciferin analogues.[54, 56, 57] Nevertheless, studies have shown that most mutated luciferases lose BL activity with luciferin, which may imply that the brute force approach of random mutagenesis may be partly necessary. This section highlights a few luciferase mutants used to improve BL with luciferin analogues, compared with their performance using wildtype luciferase.

I.4.1 *Ultra-Glo™ luciferase*

Ultra-Glo™ is a luciferase mutant from *Photuris pennsylvanica* commercialized by ProMega Corp. The proprietary enzyme has 62% homology to the *P. pyralis*, with 86% homology in the active site.[58] Furthermore, the enzyme is a thermostable luciferase mutant that eliminates the characteristic initial BL burst and provides a stable BL emission.[24, 58] Presumably, the initial burst is decreased because the enzyme is less susceptible to product inhibition. In a couple of studies, Ultra-Glo and wildtype luciferase were used to measure the BL emission with N-alkylated 6'-aminoluciferins, cyclic alkyl-aminoluciferins: CycLuc1 and CycLuc2, and luciferin.[32, 58] Similar to the results with *P. pyralis* luciferase, these studies showed that the BL emission was red-shifted with lower intensity when compared with luciferin. However, the results showed higher BL emission intensity from Ultra-Glo with CycLuc1 and CycLuc2 when compared with 6'-amino-

luciferin. However, because Ultra-Glo is a commercial product, the gene is not available for cell engineering. Thus, the 6′-aminoluciferin derivates cannot fully leverage their red-shift potential for *in vivo* applications due to the limitations of the mutant enzyme. Nevertheless, the *in vitro* results with 6′-amino-luciferin derivatives and Ultra-Glo showed for the first time that BL efficiency could be improved for luciferin analogues using a mutated luciferase. By doing so, the benefits of the luciferin analogues were maximized to potentially overcome the challenges of BL for imaging and detection.

I.4.2 *Engineered luciferase for cyclic alkyl-amino-luciferins*

The Miller research group generated mutant luciferase libraries to improve the BL emission of CycLuc1 and CycLuc2 cyclic alkyl-amino-luciferin analogues for *in vivo* imaging. The authors focused on six amino acid residues within the active site of luciferase to perform site-directed mutagenesis: phenylalanine 247, arginine 218, leucine 286, tyrosine 340, threonine 251, and serine 347. Figure I.5 shows the amino acids in relation to luciferin within the active site. Phenylalanine 247 plays a role in the π-stacking interaction with luciferin; arginine 218 is proximal to the C4′ and C5′ of luciferin and forms part of the van der Waals network interacting with luciferin; leucine 286 interacts with alkyl side chains on aminoluciferin substrates; tyrosine 340 forms part of the ATP binding site and is located at the interface between the ATP and luciferin binding pockets; threonine 251 side chain makes a van der Waals interaction with the benzothiazole moiety; and, serine

347 forms a hydrogen bond to the benzothiazole nitrogen through the intermediacy of a water molecule. The authors used the six amino acid residues to create mutants that would maintain catalytic activity while giving room and allowing new interactions to help accommodate the 6'-amino-luciferin derivatives. Results from this study showed a significant increase in BL emission intensity for all aminoluciferin analogues when catalyzed by a luciferase mutant with a single lysine substitution for the arginine 218. Furthermore, they showed selectivity for CycLuc1 by a double-substituted luciferase mutant, with an alanine for serine 347 and methionine for leucine 286. The same double-substituted luciferase had poor catalysis for luciferin. Collectively, these results gave first evidence that engineered luciferase mutants have the ability to improve the potential of luciferin analogues for *in vivo* applications.
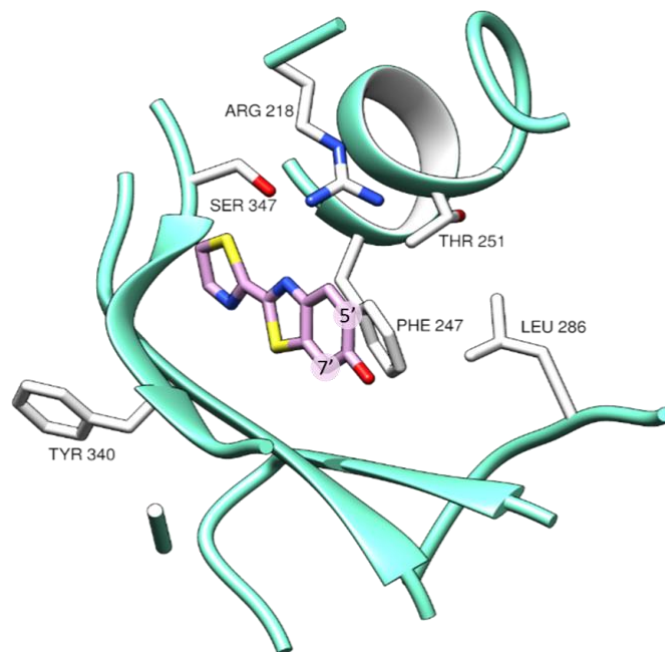
Figure I.5 Scheme for PHE247, ARG218, LEU286, TYR340, THR251, and SER347 in relation to luciferin within the active site of luciferase.
Illustration was developed in Chimera software using PDB 4G36. Specified amino acids side chains shown in white. Luciferin is shown in light purple.

I.4.3 *Coordinated engineering of luciferase and luciferin for multi-imaging modality*

The Prescher research group created luciferase libraries designed for compatibility with their luciferin analogues and intended to provide a multi-imaging modality for *in vivo* imaging.[57, 59] Previous work on luciferase-luciferin BL using luciferases from *P. pyralis* and *Renilla reniformis* was attempted, but the substrate for *Renilla reniformis* has poor cell penetration and stability, making the assay unsuitable for *in vivo* applications.[59, 60] Prescher and co-workers focused on developing luciferase mutants for C4′ and C7′ substituted luciferin analogues. After multiple rounds of mutagenesis and screening, the authors

26

were able to identify luciferase mutants with a 100-fold preference for their C4′ and C7′ substituted analogues. However, the BL intensity output from their engineered luciferase-luciferin pairs was low, and research is being carried further. The ability to engineer luciferase-luciferin pairs with potentially unique BL emission signatures could be useful to investigate multiple biological processes within a single host, e.g., cells, organs, animal model, etc. These results from the Prescher group show the possible impact of engineered luciferases to broaden the scope of BL and compete with systems based on the ubiquitous GFP.

I.5 The future of luciferin analogues and luciferase mutants for biological applications

Decades of research have generated multiple FL techniques, many of which can serve as roadmaps for the development of equivalent BL-based probes and techniques. Research in FL for bioimaging has generated many fluorophores, many of which are the preferred method for staining and observing biological events. However, fluorophores have limited use because they cannot be genetically encoded to provide a response to biological interactions. The discovery of GFP and the ability for genetic encoding made it a very attractive solution to confirm biological interactions and was rapidly adopted by the scientific community. Probes based on GFP have been developed for applications including thiol-disulfide reduction, singlet oxygen production, pH sensors, and analyte

detection. However, work with the luciferin-luciferase reaction to create assays is more challenging than with GFP due to the intricate interplay that allows catalysis by the enzyme while producing excited oxyluciferin with high quantum yield and product release. Nevertheless, engineering of luciferin-luciferase pairs to address current limitations could leverage the high signal-to-noise ratio, capability for genetic encoding, and suitability for long term *in vitro* and *in vivo* studies of BL systems, and potentially provide an alternative to GFP.

In the work described in this dissertation, we designed luciferin analogues aimed to improve the efficiency of luciferase and promote innovative uses of the luciferase-luciferin BL reaction. However, in most cases, the hypothesized outcome of our luciferin analogues was very different to the experimental outcome. Nevertheless, the work with the luciferin analogues described in this dissertation provided novel information about the enzymatic process, interaction, and plasticity of the luciferase-luciferin pairs. The following chapters individually describe the motivation, characterization, properties, and findings of each luciferin analogue: 5,5-deuterated-luciferin, 6'-thiol-luciferin, 5',7'-difluoro-luciferin, and oxyluciferin analogues: 5',7'-diiodo-oxyluciferin, 5',7'-diiodo- 5,5-dimethyl-oxyluciferin, 7'-iodo-oxyluciferin.

I.6 References

1.   Meighen, E. A., Bacterial bioluminescence - organization, regulation, and application of the lux genes. *FASEB Journal* **1993,** *7* (11), 1016-1022.

2.   Stevani, C. V.; Oliveira, A. G.; Mendes, L. F.; Ventura, F. F.; Waldenmaier, H. E.; Carvalho, R. P.; Pereira, T. A., Current status of research on fungal bioluminescence: biochemistry and prospects for ecotoxicological application. *Photochemistry and Photobiology* **2013,** *89* (6), 1318-1326.

3.   Widder, E. A., Bioluminescence in the ocean: origins of biological, chemical, and ecological diversity. *Science* **2010,** *328* (5979), 704-708.

4.   Meyer-Rochow, V. B., Glowworms: a review of *Arachnocampa* spp. and kin. *Luminescence* **2007,** *22* (3), 251-265.

5.   Marques, S. M.; da Silva, J. C. G. E., Firefly bioluminescence: a mechanistic approach of luciferase catalyzed reactions. *IUBMB Life* **2009,** *61* (1), 6-17.

6.   White, E. H.; Worther, H.; Seliger, H. H.; McElroy, W. D., Amino analogs of firefly luciferin and biological activity thereof. *Journal of the American Chemical Society* **1966,** *88* (9), 2015-2019.

7.   Viviani, V. R., The origin, diversity, and structure function relationships of insect luciferases. *Cellular and Molecular Life Sciences* **2002,** *59* (11), 1833-1850.

8.   Wood, K. V., The chemical mechanism and evolutionary development of beetle bioluminescence. *Photochemistry and Photobiology* **1995,** *62* (4), 662-673.

9.   Rhodes, W. C.; McElroy, W. D., Synthesis and function of adenyl-luciferin and adenyl-oxyluciferin. *Federation Proceedings* **1958,** *17* (1), 295-295.

10.   Seliger, H. H.; McElroy, W. D., Chemiluminescence of firefly luciferin without enzyme. *Science* **1962,** *138* (3541), 683-685.

11.   Deluca, M.; McElroy, W. D., Kinetics of firefly luciferin catalyzed reactions. *Biochemistry* **1974,** *13* (5), 921-925.

12.   Suzuki, N.; Sato, M.; Okada, K.; Goto, T., Studies on firefly bioluminescence: 1. synthesis ans spectral properties of firefly oxyluciferin, a possible emitting species in firefly bioluminescence. *Tetrahedron* **1972,** *28* (15), 4065-4074.

13.   Branchini, B. R.; Hayward, M. M.; Bamford, S.; Brennan, P. M.; Lajiness, E. J., Naphthyluciferin and quinolyluciferin - green and red light emitting firefly luciferin analogs. *Photochemistry and Photobiology* **1989,** *49* (5).

14.   White, E. H.; Worther, H.; Field, G. F.; McElroy, W. D., Analogs of firefly luciferin. *Journal of Organic Chemistry* **1965,** *30* (7), 2344-2348.

15.   Denburg, J. L.; Lee, R. T.; McElroy, W. D., Substrate-binding properties of firefly luciferase: I. luciferin-binding site. *Archives of Biochemistry and Biophysics* **1969,** *134* (2), 381-394.

16.   Morton, R. A.; Hopkins, T. A.; Seliger, H. H., Spectroscopic properties of firefly luciferin and related compounds: an approach to product emission. *Biochemistry* **1969,** *8* (4), 1598-1607.

17.   Ando, Y.; Niwa, K.; Yamada, N.; Enomot, T.; Irie, T.; Kubota, H.; Ohmiya, Y.; Akiyama, H., Firefly bioluminescence quantum yield and colour change by pH-sensitive green emission. *Nature Photonics* **2008,** *2* (1), 44-47.

18.   Roda, A.; Guardigli, M.; Michelini, E.; Mirasoli, M., Nanobioanalytical luminescence: Forster-type energy transfer methods. *Analytical and Bioanalytical Chemistry* **2009,** *393* (1), 109-123.

19.   Hochgräfe, K.; Mandelkow, E.-M., Making the brain glow: *in vivo* bioluminescence imaging to study neurodegeneration. *Molecular Neurobiology* **2012**, 1-15.

20.   Bernau, K.; Lewis, C. M.; Petelinsek, A. M.; Benink, H. A.; Zimprich, C. A.; Meyerand, M. E.; Suzuki, M.; Svendsen, C. N., *In vivo* tracking of human neural

progenitor cells in the rat brain using bioluminescence imaging. *Journal of Neuroscience Methods* **2014,** *228,* 67-78.

21.   Danhier, P.; Magat, J.; Leveque, P.; De Preter, G.; Porporato, P. E.; Bouzin, C.; Jordan, B. F.; Demeur, G.; Haufroid, V.; Feron, O.; Sonveaux, P.; Gallez, B., *In vivo* visualization and ex vivo quantification of murine breast cancer cells in the mouse brain using MRI cell tracking and electron paramagnetic resonance. *NMR in Biomedicine* **2015,** *28* (3), 367-375.

22.   White, E. H.; Field, G. F.; McElroy, W. D.; McCapra, F., Structure and synthesis of firefly luciferin. *Journal of the American Chemical Society* **1961,** *83* (10), 2402-2403.

23.   Takakura, H.; Kojima, R.; Ozawa, T.; Nagano, T.; Urano, Y., Development of 5 '- and 7 '-substituted luciferin analogues as acid-tolerant substrates of firefly luciferase. *Chembiochem* **2012,** *13* (10), 1424-1427.

24.   Jathoul, A.; Law, E.; Gandelman, O.; Pule, M.; Tisi, L.; Murray, J., Development of a pH tolerant thermostable *Photinus pyralis* luciferase for brighter *in vivo* imaging. In *Bioluminescence - Recent Advances in Oceanic Measurements and Laboratory Applications*, Lapota, D., Ed. InTech: 2012; pp 119-136.

25.   Koksharov, M. I.; Ugarova, N. N., Random mutagenesis of *Luciola mingrelica* firefly luciferase. Mutant enzymes with bioluminescence spectra showing low pH sensitivity. *Biochemistry-Moscow* **2008,** *73* (8), 862-869.

26.   Koksharov, M. I.; Ugarova, N. N., Thermostabilization of firefly luciferase by *in vivo* directed evolution. *Protein Engineering Design & Selection* **2011,** *24* (11), 835-844.

27.   Kajiyama, N.; Nakano, E., Isolation and characterization of mutants of firefly luciferase which produce different colors of light. *Protein Engineering* **1991,** *4* (6), 691-693.

28.   Conley, N. R.; Dragulescu-Andrasi, A.; Rao, J.; Moerner, W. E., A selenium analogue of firefly d-luciferin with red-shifted bioluminescence emission. *Angewandte Chemie-International Edition* **2012,** *51* (14), 3350-3353.

29.   Viviani, V. R.; Arnoldi, F. G. C.; Neto, A. J. S.; Oehlmeyer, T. L.; Bechara, E. J. H.; Ohmiya, Y., The structural origin and biological function of pH-sensitivity in firefly luciferases. *Photochemical & Photobiological Sciences* **2008,** *7* (2), 159-169.

30.   Ugarova, N. N.; Brovko, L. Y., Protein structure and bioluminescent spectra for firefly bioluminescence. *Luminescence* **2002,** *17* (5), 321-330.

31.   White, E. H.; Worther, H., Analogs of firefly luciferin .3. *Journal of Organic Chemistry* **1966,** *31* (5), 1484-1488.

32.   Reddy, G. R.; Thompson, W. C.; Miller, S. C., Robust light emission from cyclic alkylaminoluciferin substrates for firefly luciferase. *Journal of the American Chemical Society* **2010,** *132* (39), 13586–13587.

33.   Evans, M. S.; Chaurette, J. P.; Adams, S. T., Jr.; Reddy, G. R.; Paley, M. A.; Aronin, N.; Prescher, J. A.; Miller, S. C., A synthetic luciferin improves bioluminescence imaging in live mice. *Nature Methods* **2014,** *11* (4), 393-395.

34.   Ohulchanskyy, T. Y.; Donnelly, D. J.; Detty, M. R.; Prasad, P. N., Heteroatom substitution induced changes in excited-state photophysics and singlet oxygen generation in chalcogenoxanthylium dyes: effect of sulfur and selenium substitutions. *Journal of Physical Chemistry B* **2004,** *108* (25), 8668-8672.

35.   Rodriguez-Serrano, A.; Rai-Constapel, V.; Daza, M. C.; Doerr, M.; Marian, C. M., Internal heavy atom effects in phenothiazinium dyes: enhancement of intersystem crossing via vibronic spin-orbit coupling. *Physical Chemistry Chemical Physics* **2015,** *17* (17), 11350-11358.

36.   Inoue, Y.; Masutani, Y.; Kiryu, S.; Haishi, T.; Watanabe, M.; Tojo, A.; Ohtomo, K., Integrated imaging approach to tumor model mice using bioluminescence imaging and magnetic resonance imaging. *Molecular Imaging* **2010,** *9* (3), 163-172.

37.   Zhang, H. L.; Qiao, H.; Bakken, A.; Gao, F. B.; Huang, B.; Liu, Y. Q. Y.; El-Deiry, W.; Ferrari, V. A.; Zhou, R., Utility of dual-modality bioluminescence and MRI in

monitoring stem cell survival and impact on post myocardial infarct remodeling. *Academic Radiology* **2011,** *18* (1), 3-12.

38.   Steinhardt, R. C.; Rathbun, C. M.; Krull, B. T.; Yu, J. M.; Yang, Y.; Nguyen, B. D.; Kwon, J.; McCutcheon, D. C.; Jones, K. A.; Furche, F.; Prescher, J. A., Brominated luciferins are versatile bioluminescent probes. *Chembiochem* **2017,** *18* (1), 96-100.

39.   Lyman, G. E.; Devincenzo, J. P., Determination of picogram amounts using luciferin-luciferase enzyme system. *Analytical Biochemistry* **1967,** *21* (3), 435-443.

40.   Watanabe, A.; Tamaki, N.; Yokota, K.; Matsuyama, M.; Kokeguchi, S., Monitoring of bacterial contamination of dental unit water lines using adenosine triphosphate bioluminescence. *Journal of Hospital Infection* **2016,** *94* (4), 393-396.

41.   Nguyen, Q. T.; Wallner, U.; Schmicke, M.; Waberski, D.; Henning, H., Energy metabolic state in hypothermically stored boar spermatozoa using a revised protocol for efficient ATP extraction. *Biology Open* **2016,** *5* (11), 1743-1751.

42.   Rossello, G. A. M.; de Urries, M.; Rodriguez, M. P. G.; Grande, M. S.; Domingo, A. O.; Perez, M. A. B., A two-hour antibiotic susceptibility test by ATP-bioluminescence. *Enfermedades Infecciosas Y Microbiologia Clinica* **2016,** *34* (6), 334-339.

43.   White, E. H.; Field, G. F.; McCapra, F., Structure and synthesis of firefly luciferin. *Journal of the American Chemical Society* **1963,** *85* (3), 337-343.

44.   Dewet, J. R.; Wood, K. V.; Helinski, D. R.; Deluca, M., Cloning of firefly luciferase cDNA and the expression of active luciferase in *Escherichia coli*. *Proceedings of the National Academy of Sciences of the United States of America* **1985,** *82* (23), 7870-7873.

45.   Smirnova, D. V.; Ugarova, N. N., Firefly luciferase-based fusion proteins and their applications in bioanalysis. *Photochemistry and Photobiology* **2017,** *93* (2), 436-447.

46.   Mofford, D. M.; Adams, S. T.; Reddy, G.; Reddy, G. R.; Miller, S. C., Luciferin amides enable *in vivo* bioluminescence detection of endogenous fatty acid amide hydrolase activity. *Journal of the American Chemical Society* **2015,** *137* (27), 8684-8687.

47.   Mofford, D. M.; Reddy, G. R.; Miller, S. C., Aminoluciferins extend firefly luciferase bioluminescence into the near-infrared and can be preferred substrates over d-luciferin. *Journal of the American Chemical Society* **2014,** *136* (38), 13277-13282.

48.   Long, J. Z.; LaCava, M.; Jin, X.; Cravatt, B. F., An anatomical and temporal portrait of physiological substrates for fatty acid amide hydrolase. *Journal of Lipid Research* **2011,** *52* (2), 337-344.

49.   Porterfield, W. B.; Jones, K. A.; McCutcheon, D. C.; Prescher, J. A., A "caged" luciferin for imaging cell-cell contacts. *Journal of the American Chemical Society* **2015,** *137* (27), 8656-8659.

50.   Maltsev, O. V.; Nath, N. K.; Naumov, P.; Hintermann, L., Why is firefly oxyluciferin a notoriously labile substance? *Angewandte Chemie-International Edition* **2014,** *53* (3), 847-850.

51.   Ghose, A.; Rebarz, M.; Maltsev, O. V.; Hintermann, L.; Ruckebusch, C.; Fron, E.; Hofkens, J.; Mely, Y.; Naumov, P.; Sliwa, M.; Didier, P., Emission properties of oxyluciferin and its derivatives in water: revealing the nature of the emissive species in firefly bioluminescence. *Journal of Physical Chemistry B* **2015,** *119* (6), 2638-2649.

52.   Viviani, V. R.; Rodrigues Neves, D.; Trabuco Amaral, D.; Prado, R. A.; Matsuhashi, T.; Hirano, T., Bioluminescence of beetle luciferases with 6 '-amino-d-luciferin analogues reveals excited keto-oxyluciferin as the emitter and phenolate/luciferin binding site interactions modulate bioluminescence colors. *Biochemistry* **2014,** *53* (32), 5208-5220.

53.   Woodroofe, C. C.; Meisenheimer, P. L.; Klaubert, D. H.; Kovic, Y.; Rosenberg, J. C.; Behney, C. E.; Southworth, T. L.; Branchini, B. R., Novel heterocyclic analogues of firefly luciferin. *Biochemistry* **2012,** *51* (49), 9807-9813.

54.   Harwood, K. R.; Mofford, D. M.; Reddy, G. R.; Miller, S. C., Identification of mutant firefly luciferases that efficiently utilize aminoluciferins. *Chemistry & Biology* **2011,** *18* (12), 1649-1657.

55.   Miller, S.; Harwood, K.; Reddy, R.; Mofford, D., Expanding the scope of bioluminescence imaging: synthetic luciferins and mutant luciferases. *Molecular Biology of the Cell* **2011,** *22,* 112-120.

56.   Adams, S. T.; Mofford, D. M.; Reddy, G.; Miller, S. C., Firefly luciferase mutants allow substrate-selective bioluminescence imaging in the mouse brain. *Angewandte Chemie-International Edition* **2016,** *55* (16), 4943-4946.

57.   Rathbun, C. M.; Porterfield, W. B.; Jones, K. A.; Sagoe, M. J.; Reyes, M. R.; Hua, C. T.; Prescher, J. A., Parallel screening for rapid identification of orthogonal bioluminescent tools. *ACS Central Science* **2017,** *3* (12), 1254-1261.

58.   Woodroofe, C. C.; Shultz, J. W.; Wood, M. G.; Osterman, J.; Cali, J. J.; Daily, W. J.; Meisenheimer, P. L.; Klaubert, D. H., N-alkylated 6 '-aminoluciferins are bioluminescent substrates for Ultra-Glo and QuantiLum luciferase: new potential scaffolds for bioluminescent assays. *Biochemistry* **2008,** *47* (39), 10383-10393.

59.   Jones, K. A.; Porterfield, W. B.; Rathbun, C. M.; McCutcheon, D. C.; Paley, M. A.; Prescher, J. A., Orthogonal luciferase-luciferin pairs for bioluminescence imaging. *Journal of the American Chemical Society* **2017,** *139* (6), 2351-2358.

60.   Luker, K. E.; Smith, M. C. P.; Luker, G. D.; Gammon, S. T.; Piwnica-Worms, H.; Piwnica-Worms, D. P., Kinetics of regulated protein-protein interactions revealed with firefly luciferase complementation imaging in cells and living animals. *Proceedings of the National Academy of Sciences of the United States of America* **2004,** *101* (33), 12288-12293.

Chapter II: The characterization of 5,5-deuterated-luciferin as a luciferase substrate to reduce an inhibitory byproduct, dehydroluciferin.

II.1 Introduction

Bioluminescence (BL) from the luciferase-luciferin reaction has become a common bioimaging tool that provides high signal-to-noise ratio compared with traditional FL bioimaging. The first measurement of quantum yield for BL emitted by the luciferase-luciferin reaction resulted in a value of 88 ± 25%, which meant that the ratio of reacted luciferin to photons of light emitted through the reaction was fairly efficient.[1, 2] However, the initial apparent quantum yield measurement did not account for optical isomers and racemization of luciferin after extraction and purification from fireflies. This showed that the measurement was incorrect since it suggest an unrealistic quantum yield greater than 100%.[3] Therefore, the quantum yield was re-evaluated for a pure sample of luciferin using a total-photon-flux spectrophotometer. The quantitative evaluation showed a lower quantum yield of 41 ± 7.4%.[4, 5] Therefore, optimizing the luciferase-luciferin reaction to increase the quantum yield from 41% could increase the sensitivity of the BL imaging system and benefit traditional BL assays, for *in vivo* and *in vitro* applications. The molecular structures of the compounds discussed in this chapter are found on Figure II.1.
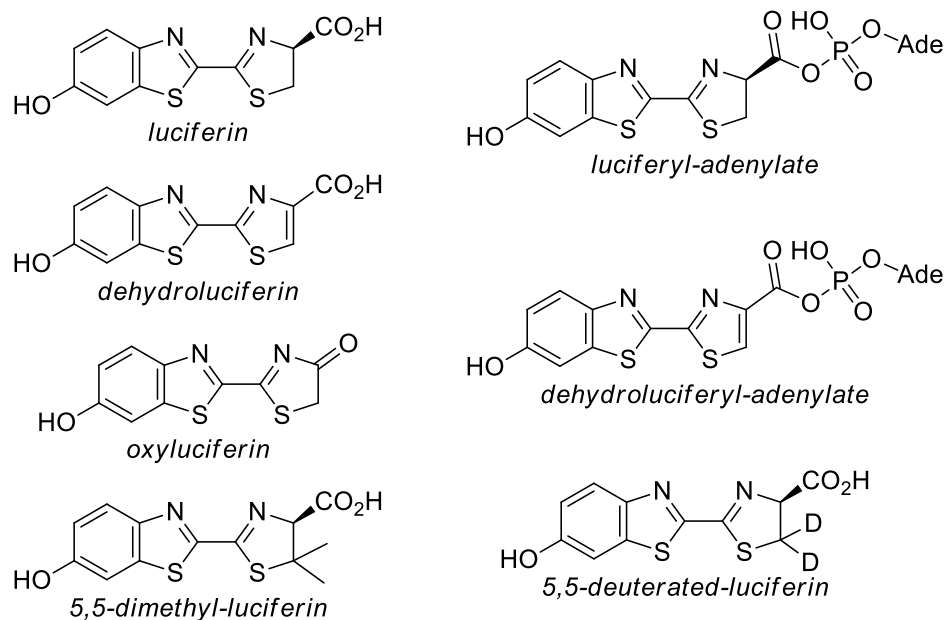
Figure II.1 Molecules in the bioluminescence reaction and luciferin analogues.

One way to achieve a higher quantum yield is to reduce the production of non-emitting byproducts from the luciferase-luciferin reaction. The luciferase reaction can produce either oxyluciferin or dehydroluciferin following the formation of the luciferyl-adenylate intermediate. Oxyluciferin is the light emitting chromophore and the primary product of the BL reaction. Dehydroluciferin, a non-emitting byproduct, results from a side reaction commonly referred to as the "dark reaction" since no light is produced.[6] The detailed mechanism governing the "dark reaction" remains unknown. The current accepted mechanism suggests a deprotonation at the C5 position, which allows the formation of

the double bond characteristic of dehydroluciferin. Furthermore, the production of a dehydroluciferyl-adenylate intermediate that yields dehydroluciferin as byproducts of the luciferase reaction has been confirmed through HPLC and TLC.[7-9] The HPLC results showed that 16% of the luciferin consumed formed dehydroluciferyl-adenylate and dehydroluciferin. Assuming the other 84% of the luciferin is oxidized into oxyluciferin, the approximate ratio of dehydroluciferin to oxyluciferin produced by the reaction is 1:5.25.[7, 10-12] Additionally to the studies on dehydroluciferin production, the co-production of hydrogen peroxide as a byproduct to the "dark-reaction" was proposed and studied. A study by da Silva et al. suggested an equimolar production of hydrogen peroxide and dehydroluciferin during the dark-reaction.

Dehydroluciferyl-adenylate and dehydroluciferin are strong competitive inhibitors of luciferase and are key factors that influence the amount of BL produced. The K_i for dehydroluciferyl-adenylate with luciferase is 3.8 nM.[13] The luciferase inhibition by dehydroluciferin has been reported using two different approaches. In the first approach, dehydroluciferin was pre-incubated in solution with luciferase and cofactors followed by the addition of luciferin. This resulted in a potent inhibition with a K_i of 4 nM. In the second approach, both dehydroluciferin and luciferin were added simultaneously to a solution containing luciferase and cofactors, and resulted in a K_i of 150 nM.[14] In contrast to oxyluciferin as an inhibitor (K_i of 500 nM), the inhibition by the "dark reaction" byproducts can be as much as 100-fold stronger. Both dehydroluciferyl-adenylate and

dehydroluciferin have been associated with the decrease of light emitted after the initial

BL flash peak *in vitro*.[15] Therefore, Coenzyme A is commonly added to produce

dehydroluciferyl-Coenzyme A, which is a weaker non-competitive inhibitor with K_i of

880 nM.[16] Consequently, the amount of free enzyme available for catalysis increases which

decreases the extreme loss of light after the initial BL flash peak *in vitro*.[16, 17]
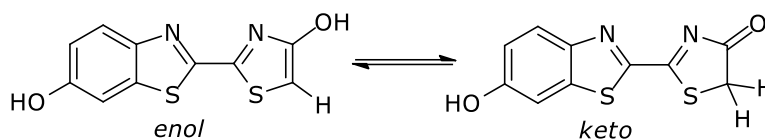
Figure II.2 Oxyluciferin tautomers in its enol and keto form.

The keto-enol tautomerization (Figure **II**.2) of oxyluciferin could influence the quantum

yield of the BL reaction. Recent studies consider the keto-phenolate state of oxyluciferin

as the emitter.[18-22] Previously, it was thought that red and yellow-green BL emission was

produced by oxyluciferin in its keto and enol forms respectively. However, a study used

5,5-dimethyl-luciferin (Figure **II**.1) to form only 5,5-dimethyl-oxyluciferin (i.e.

oxyluciferin in its keto-form). The authors showed that 5,5-dimethyl-oxyluciferin emitted

at both red and yellow-green regions, indicating that the keto-form could be responsible

for both emissions.[23] A challenge with the double methylation in C5 to produce 5,5-

dimethyl-luciferin was that the substitution inhibited the initial adenylation step of the BL

reaction. McElroy et al. showed that excited oxyluciferin can be produced bypassing the adenylation step through the luciferase-catalyzed oxidation of pre-formed luciferyl-adenylate.[24] Thus, a follow-up study used 5,5-dimethyl-adenylated-luciferin to analyze the color modulation mechanism of the BL reaction.[24] The authors were able to investigate the BL emission wavelength, however the kinetics of the luciferase reaction were affected by steric hindrance and the BL emission was reduced by 85% compared with luciferin. Contrary to the expected results of a higher luciferase turn-over, since adenylation is the limiting step in the luciferase reaction, the BL did not increase.

In this study, we focused on evaluating the performance of the 5,5-deuterated-luciferin (d_2-luciferin) with luciferase. The primary isotope effect is the rationale for the double deuteration at the C5 position (β to the site of reaction) to potentially slow deprotonation and the associated production of dehydroluciferyl-adenylate and hydrogen peroxide. The primary isotope effect is based on using a heavier atom, i.e. ^2H = deuterium, to reduce the rate of the reaction where the atom is involved. We hypothesized that using d_2-luciferin as the substrate in the luciferase reaction would produce less dehydroluciferyl-adenylate and improve the luciferase-luciferin assays. First, a reduction in the formation of the potent inhibitor dehydroluciferyl-adenylate and its hydrolyzed product dehydroluciferin should increase the amount of free luciferase available for catalysis. Additionally, a reduction in the C5 enol-keto tautomerization can limit the enol-form, which has been

previously thought could be involved in reducing the BL intensity. The effect of d_2-luciferin on the luciferase-luciferin reaction was determined by the kinetic isotope effect on BL emission over time, the catalytic efficiency, the ratio of the production of dehydroluciferin to oxyluciferin, and the amount of hydrogen peroxide produced. Our results showed that the β-deuteration reduced the ratio of dehydroluciferin to oxyluciferin to 1:11 compared with 1:5.25 with luciferin. The isotope effect calculated from this result is 2.12. However, the BL emission, catalytic efficiency, and hydrogen peroxide production did not show an isotope effect.

II.2 Results

Our work began by synthesizing luciferin and the deuterated analogue, d_2-luciferin. After their purification and spectroscopic characterization, we evaluated d_2-luciferin absorbance and BL emission with respect to luciferin. This was followed by investigating the BL emission intensity and kinetics for d_2-luciferin using luciferase, with luciferin as a control. Then, we quantified the formation of dehydroluciferin and oxyluciferin from the BL reactions using a RP-HPLC method established by Da Silva et al.[7, 10, 25] Furthermore, the established pathway for production of dehydroluciferin shows the simultaneous generation of hydrogen peroxide. Thus, we utilized a fluorescence-based assay to detect hydrogen peroxide produced from the BL reaction with either d_2-luciferin or luciferin.

II.2.1 *Absorbance and bioluminescence emission of luciferin and d₂-luciferin.*

After synthesizing a luciferin analogue, our lab evaluates their absorbance and emission properties to investigates the molecules' ability to emit light as a substrate of luciferase and use it as a model for the oxyluciferin behavior. Therefore, we obtained an absorbance and BL emission spectrum with both molecules at the same concentration at neutral pH. The results did not show a significant difference (Figure **II**.3). These results are expected since the deuteration at the C5 position does not affect the properties of luciferin as a chromophore.
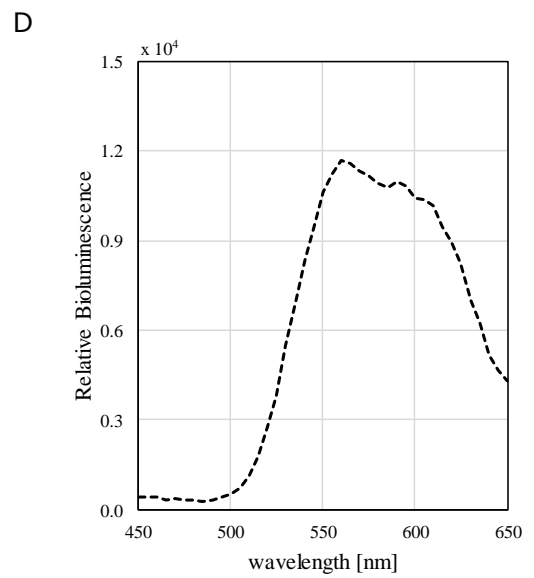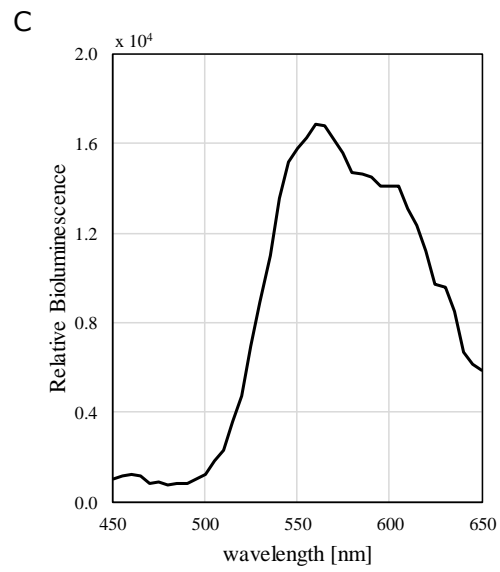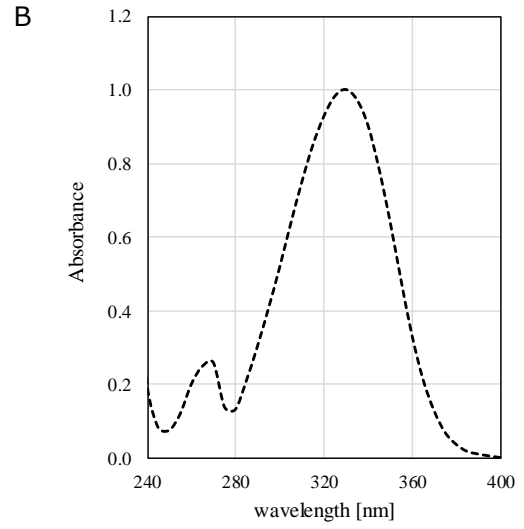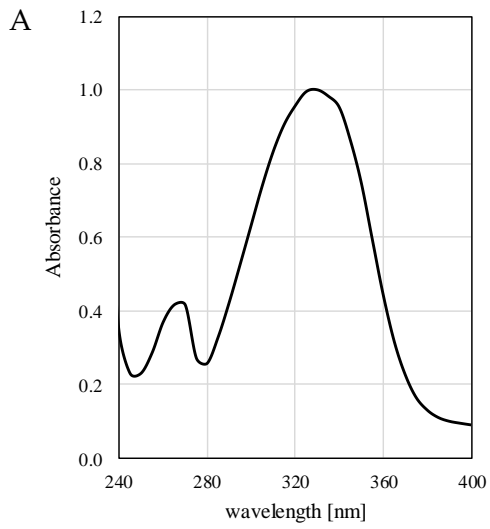
Figure II.3 Absorbance for luciferin (A) and *d₂*-luciferin(B) in water. Bioluminescence emission for luciferin (C) and *d₂*-luciferin (D) at pH 7.

II.2.2 *Bioluminescence decay of luciferin and d₂-luciferin.*

The rationale for creating d_2-luciferin is based on utilizing isotopic substitution of the C5 protons to increase the free luciferase available to catalyze luciferin oxidation by reducing byproduct inhibitors. The C5 protons do not actively participate in the formation of intermediates that result in BL.[11, 23, 26-28] However, the C5 protons play a key role in the formation of dehydroluciferin, one of the byproducts of the reaction.[8, 16, 29-32] Dehydroluciferin is a potent inhibitor of luciferase with an inhibitor constant of 4 nM.[16] Therefore, our lab designed d_2-luciferin to reduce the formation of dehydroluciferin thereby increasing the number of photons produced per time and turnover.

To investigate the ability of d_2-luciferin to produce more BL over time we investigated the time dependence of the BL intensity compared to luciferin (Figure **II**.4). Our results did not show a significant BL increase as was expected. Furthermore, our experiments showed a decrease in the initial characteristic BL flash peak that could only be explained by subtle differences between the synthetic and deuterated luciferin samples. Analyzing the BL emission intensity of d_2-luciferin compared to luciferin at different time points of the reaction reveals that at longer times in the reaction there is slightly less decay of BL emission from the d_2-luciferin reaction, Figure **II**.4 and Table II.1. The slight BL increment over time at this point was presumably able to occur by a reduction in the production of the inhibitor byproduct dehydroluciferin.
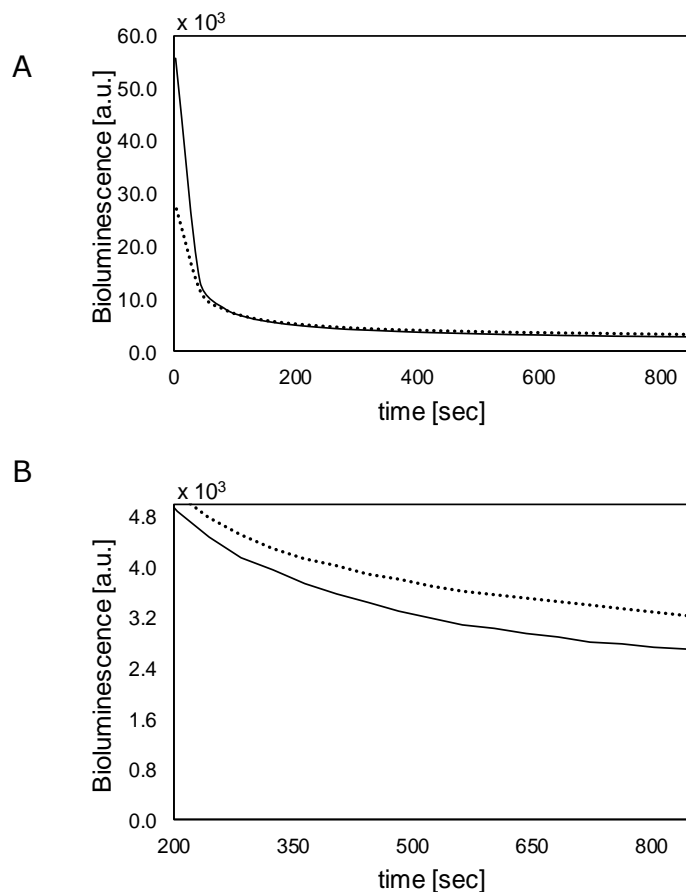
Figure II.4 Time-dependent bioluminescence from luciferin (——) and *d₂*-luciferin (.....).
(A) BL over a period of 900 second (15 minutes), after manual injection of luciferase. The differences in the initial flash peak are due to subtle differences in the samples. (B) Accentuates the 200 to 800 second region to show the slightly lower decay.

Table II.1. Bioluminescence from luciferin and *d₂*-luciferin at specific time after initiating the reaction.

	luciferin	*d₂*-luciferin	Rel. BL*
At initial flash peak+	55.7 ± 3.44	26.9 ± 2.36	48%
At minute 15	2.62 ± 0.46	3.19 ± 0.08	122%
Total BL over 15 minutes	1510.0 ± 5.98	1270.0 ± 4.84	84%
Values show the mean ± SD of triplicates. +Approximately 2 to 3 seconds after manually starting the reaction. *Relative bioluminescence of d₂-luciferin compared to luciferin 100%.

II.2.3 *Luciferase catalytic efficiency with luciferin and d$_2$-luciferin.*

To evaluate any difference within the BL reaction of the *d$_2$*-luciferin from luciferin we focused on evaluating the steady state kinetics for luciferase with its native substrate luciferin and with *d$_2$*-luciferin (Figure **II**.5). The kinetic parameters obtained after nonlinear regression analysis are shown in Table II.2. Steady state kinetics parameters for luciferase with luciferin and *d$_2$*-luciferin., for luciferin and *d$_2$*-luciferin. The calculated K_M and k_{cat} for *d$_2$*-luciferin are slightly lower at 0.48 μM and 2.01 (BL·μmol^{-1}) compared to luciferin, 0.64 μM and 3.90 (BL·μmol^{-1}). The best method to compare luciferin and *d$_2$*-luciferin as a substrate is by determining luciferase catalytic efficiency (k_{cat} / K_M) with each. There was no significant difference between luciferin and *d$_2$*-luciferin. The luciferin value, 6.17 ± 0.78, compared to 4.24 ± 0.41 from *d$_2$*-luciferin. These are similar, compared to other luciferin analogues that show many fold differences. Furthermore, the results are opposite to the expectation that the deuterated substrate should be more efficient. However, these data could be affected by the differences within our *d$_2$*-luciferin sample since its synthesis differs from that of luciferin.

The results discussed above showed a small effect when using *d$_2$*-luciferin in the BL reaction. Therefore, we move on to evaluate the dehydroluciferin production that allows a direct measurement of the byproduct from the luciferase reactions. Since one of our

goals with d_2-luciferin is to reduce the formation of dehydroluciferin as a byproduct of the BL reaction, we used the methods developed by Da Silva et al. to compare dehydroluciferin produced from the BL reactions with d_2-luciferin and luciferin. Furthermore, we analyze the production of hydrogen peroxide, the co-product indicative that dehydroluciferin has formed, by a fluorescence probe, Amplex® Red.
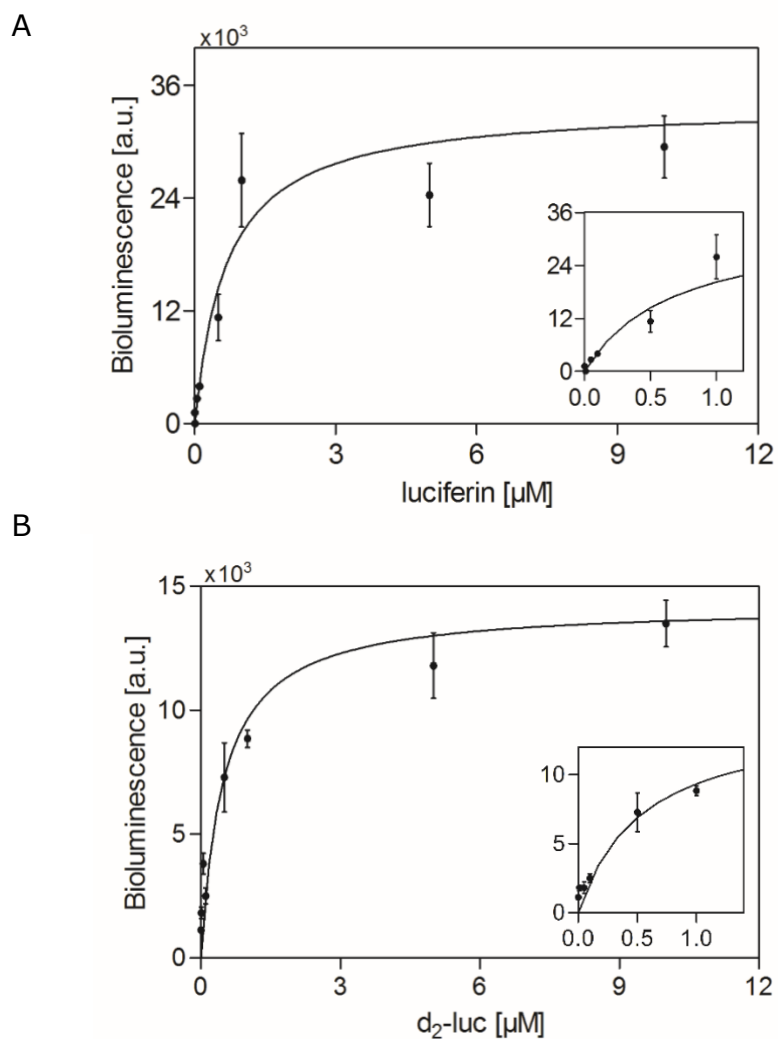
Figure II.5 Luciferase steady state kinetics: luciferin (A) or d_2-luciferin (B) as substrate.

Table II.2. Steady state kinetics parameters for luciferase with luciferin and d_2-luciferin.

	K_M [μM]	[BL·(μmol)$^{-1}$]	k_{cat}/K_M
luciferin	0.64 ± 0.03[a]	3.90 ± 0.32	6.17 ± 0.78
d_2-luciferin	0.48 ± 0.05[a]	2.01 ± 0.23	4.24 ± 0.41

The assays were performed in triplicate, and the values represent the mean ± SD of 4 independent experiments. Each experiment was fit to the Michaelis-Menten equation by non-linear regression (GraphPad 5.0) to determine the K_M. The values of k_{cat} were obtained by dividing the V_{max} values, from the data used to determine the K_M, by the final amount of luciferase (0.25 μmol).

II.2.4 *Commercial dehydroluciferin RP-HPLC calibration curve*

In order to quantify dehydroluciferin produced by BL reactions using HPLC chromatograms, a calibration curve using commercial dehydroluciferin was established. The chromatogram obtained with dehydroluciferin concentrations 1 to 100 μM is shown in Figure **II**.6. The chromatogram from commercial dehydroluciferin shows an impurity peak at 8 minutes that corresponds to luciferin. This was verified with an authentic sample. The plots resulting from height and area of the peaks against the moles of dehydroluciferin were used as a calibration curve (Figure **II**.6, B and C).
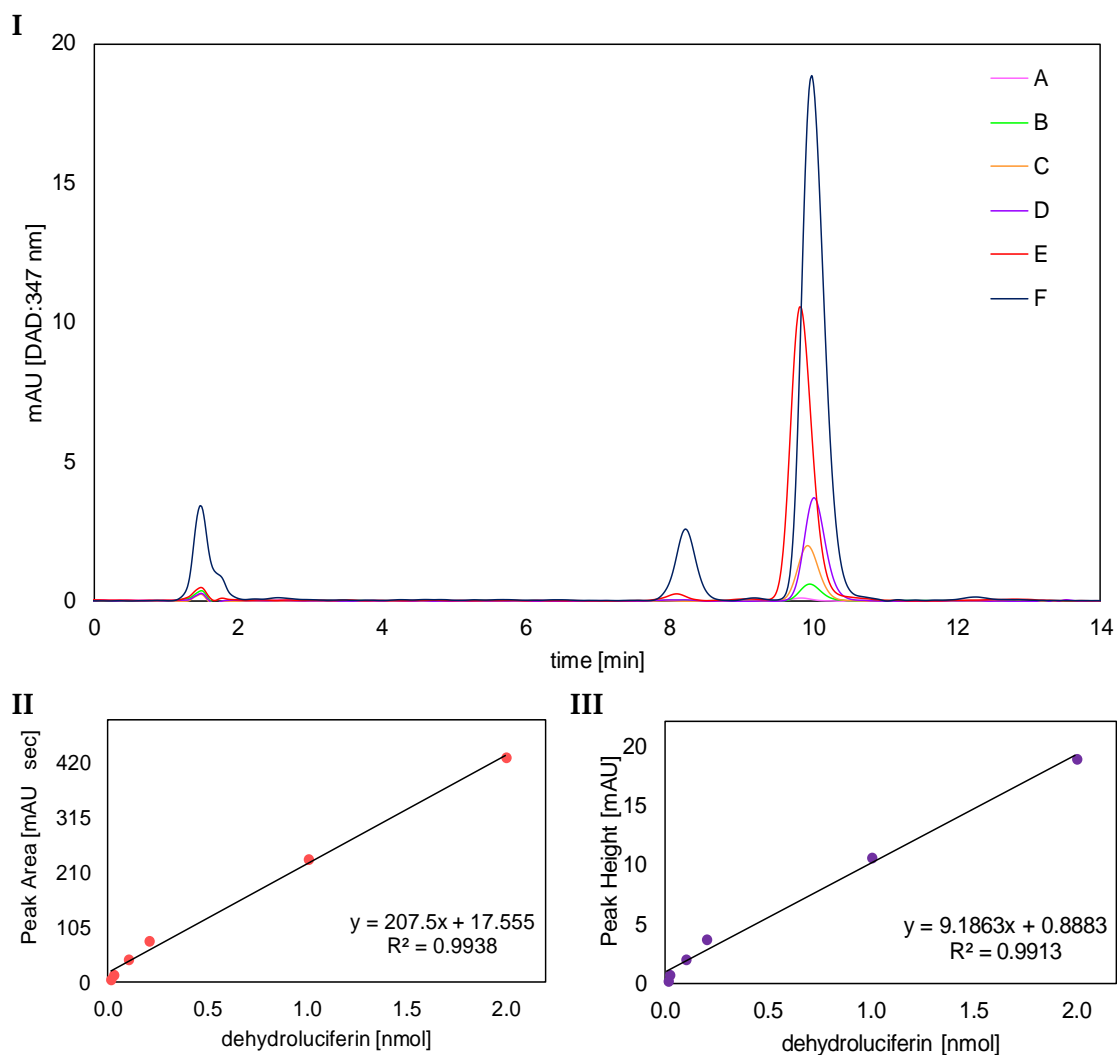
Figure II.6 Calibration standard using commercial dehydroluciferin.
I. Chromatogram showing peaks obtained from solutions of known concentrations of commercial dehydroluciferin at 0.01 nmol (A), 0.02 nmol (B), 0.10 nmol (C), 0.20 nmol (D), 1 nmol (E), and 2 nmol (F). Commercial dehydroluciferin was eluted with 70% 3 mM phosphate buffer at pH 7.0 and 30% methanol. Impurity peaks with retention time of 8 minutes showed absorption spectra characteristic of luciferin. II. Plot for the calibration curve using peak area and moles. III. Plot for the calibration curve using peak height and moles.

II.2.5 *Dehydroluciferin produced from bioluminescence reactions with luciferin and d_2-luciferin.*

The reactions were set up and analyzed as described in the experimental section. The observed chromatographic retention times for luciferin, dehydroluciferin, and oxyluciferin were 7.2, 9.2, and 17.8 minutes, respectively (Figure **II**.7). The identities of these peaks were verified through the instrument's UV/Vis spectra (Figure **II**.8). Peaks at retention time 2 minutes correspond to the solvent-front peak and contains the BL cofactors and EDTA which was used in high concentrations to stop the reaction. Using the dehydroluciferin concentration curve, we calculated the amount of dehydroluciferin produced to be 11.26 ± 0.04 nmol for the luciferin reaction and 4.57 ± 0.30 nmol for the d_2-luciferin reaction. To calculate the amount of oxyluciferin produced we used the literature ratio of 5.25:1 oxyluciferin to dehydroluciferin to establish a correlation between relative mols of oxyluciferin to a peak height and area. Consequently, we calculated oxyluciferin to be 59.15 ± 0.19 nmol from the luciferin reaction, which is 11.26 nmol times 5.25. The obtained oxyluciferin peak area and height from the luciferin reaction in relation to 59.15 nmol was used to calculate the oxyluciferin produced from the d_2-luciferin reaction to be 51.16 ± 0.64 nmol. Results are tabulated in Table **II**.3. The obtained ratio of oxyluciferin to dehydroluciferin produced from the d_2-luciferin was calculated to be 11:1.

Originally, our calculations were done with a 1:4 ratio of dehydroluciferin to oxyluciferin

under the presumption that dehydroluciferin was 20% of oxyluciferin produced.

However, a recent detailed literature review presented lower dehydroluciferin

production at 16%, which yields a ratio of 1 to 5.25, dehydroluciferin to oxyluciferin.[9] The

calculations on the publication associated with this chapter are based on the 1:4

dehydroluciferin to oxyluciferin ratio.[33]
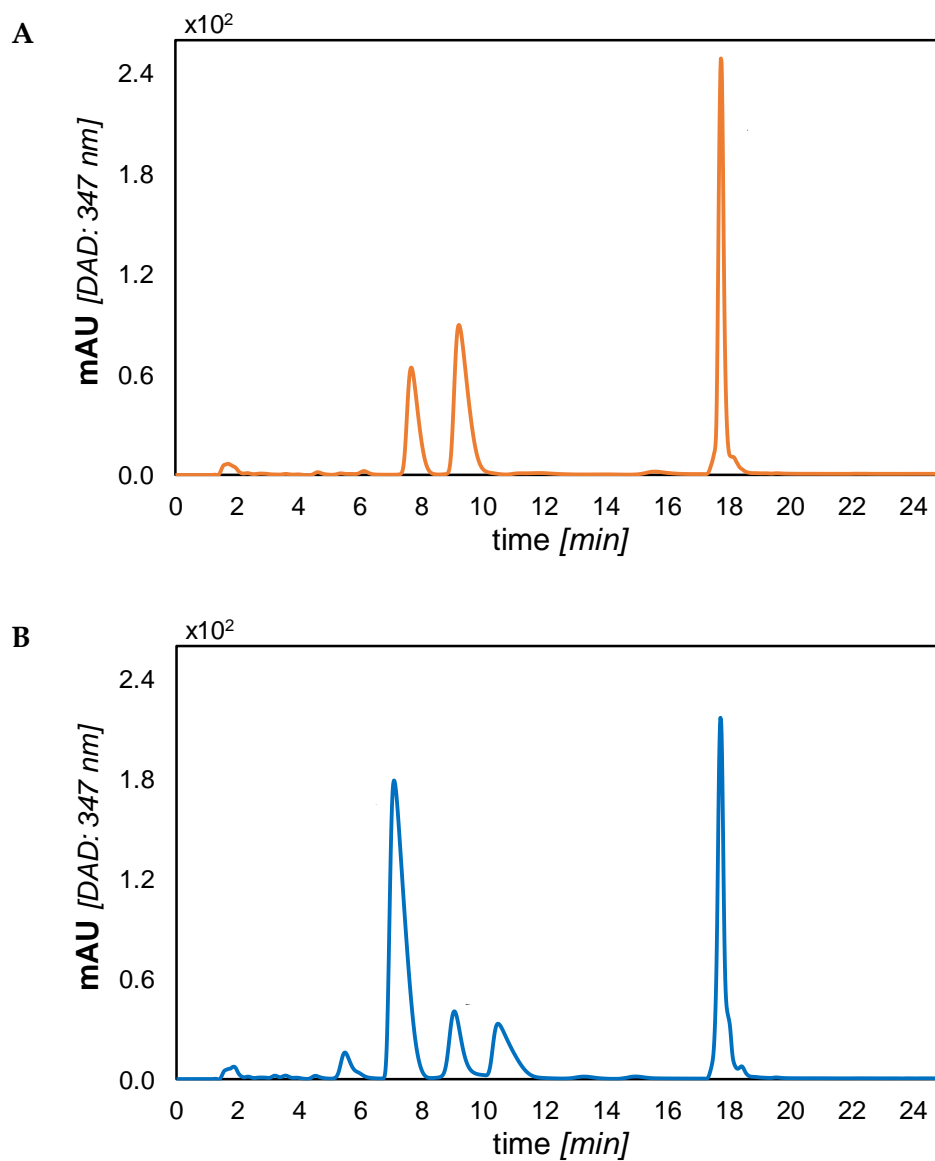
Figure II.7 RP-HPLC Chromatograms of bioluminescence products using luciferin (A) and d_2-luciferin (B).

Chromatograms are at 347 nm which emphasizes luciferin, dehydroluciferin, and oxyluciferin at peaks with retention time of 7.2, 9.2, and 17.8 minutes, respectively. Samples were eluted with 70% 5 mM phosphate buffer pH 7.0 and 30% methanol for the first 10 minutes, then methanol was increased to 85%. Peak with retention time around 2 minutes correspond to solvent, bioluminescence cofactors, and EDTA from previous steps.
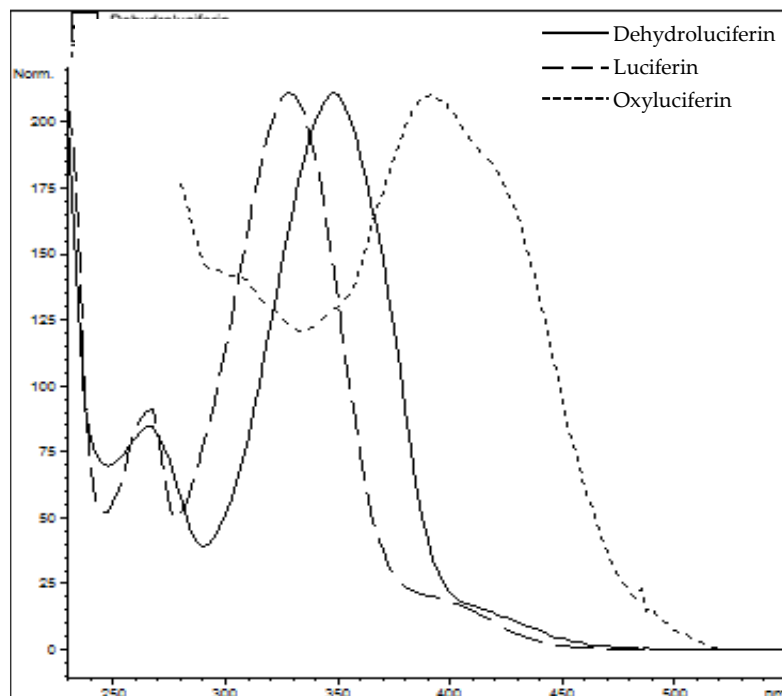
Figure II.8 Absorbance spectra from luciferin, dehydroluciferin, and oxyluciferin from RP-HPLC.

The figure shows the absorbance spectrum corresponding to chromatogram peaks with retention time of 7.2, 9.2, and 18 minutes. Peaks with retention time of 7.2 minutes showed absorbance λ_{max} at 328 nm, corresponding to luciferin. Peaks with retention time of 9.2 minutes showed absorbance λ_{max} at 347 nm, corresponding to dehydroluciferin. Peaks with retention time of 18 minutes showed absorbance λ_{max} at 414 nm, corresponding to oxyluciferin. The graphs were obtained and normalized from integrated peaks by the CHEMSTATION software.

Table II.3. Dehydroluciferin and oxyluciferin production by bioluminescence reactions with luciferin or d_2-luciferin.

luciferin reaction		d_2-luciferin reaction	
dehydroluciferin	oxyluciferin	dehydroluciferin	oxyluciferin
11.31 ± 0.03	59.39 ± 0.15	4.24 ± 0.16	51.39 ± 0.64
11.22 ± 0.50	58.91 ± 2.60	4.96 ± 0.02	50.28 ±1.42
11.26 ± 0.07	59.13 ± 0.40	4.50 ± 0.25	51.80 ± 1.09
11.26 ± 0.04	59.15 ± 0.19	4.57 ± 0.30	51.16 ± 0.64
The values show the nmols of oxyluciferin and dehydroluciferin from three bioluminescence reactions and duplicate RP-HPLC analysis from each reaction. The first 3 rows show the mean and SD of the duplicate analysis per reaction and the last row shows the mean and SD of the 3 reactions.			

II.2.6 *Hydrogen peroxide produced from the bioluminescence reactions of luciferin and d₂-luciferin.*

To investigate the production of hydrogen peroxide we used the molecular probe, Amplex Red, in combination with horseradish peroxidase (HRP). In the presence of hydrogen peroxide, HRP will oxidize Amplex Red in a 1:1 stoichiometric reaction, to resorufin, which is highly fluorescent.[34] First, we obtained a calibration curve using known quantities of hydrogen peroxide (Figure **II**.9). This experiment was followed by analyzing the hydrogen peroxide produced from the BL reaction with either luciferin or d_2-luciferin by taking a sample of the reaction (Table **II**.4). These initial results showed the production of hydrogen peroxide from the BL reaction with both substrates. However, different than expected, the results did not show a difference in the hydrogen peroxide produced from luciferin or d_2-luciferin, which quantified to 0.69 to 0.65 nmol, respectively. Based on the previous literature which relates hydrogen peroxide to dehydroluciferin formed as co-byproducts, we were expecting a significant difference as was seen with the dehydroluciferin produced from the d_2-luciferin reaction, compared to luciferin. To investigate the ratio of hydrogen peroxide to oxyluciferin produced from each substrate we evaluated a BL reaction sample for oxyluciferin by RP-HLPC and hydrogen peroxide by Amplex Red. The results for oxyluciferin are 17.67 ± 0.28 nmol and 13.23 ± 0.23 nmol from the BL reactions of luciferin and d_2-luciferin. Results from the hydrogen peroxide assay are 0.97 ± 0.04 nmol and 0.84 ± 0.03 nmol, from the BL reactions of luciferin and d_2-

luciferin (Table **II**.5). These results were unexpected since they do not follow the

suggested co-production of hydrogen peroxide when dehydroluciferin is formed.[10]

Lastly, we calculated the kinetic isotope effect that the beta deuterium substitution exerted

on the BL reaction from the experiments that have been discussed here.
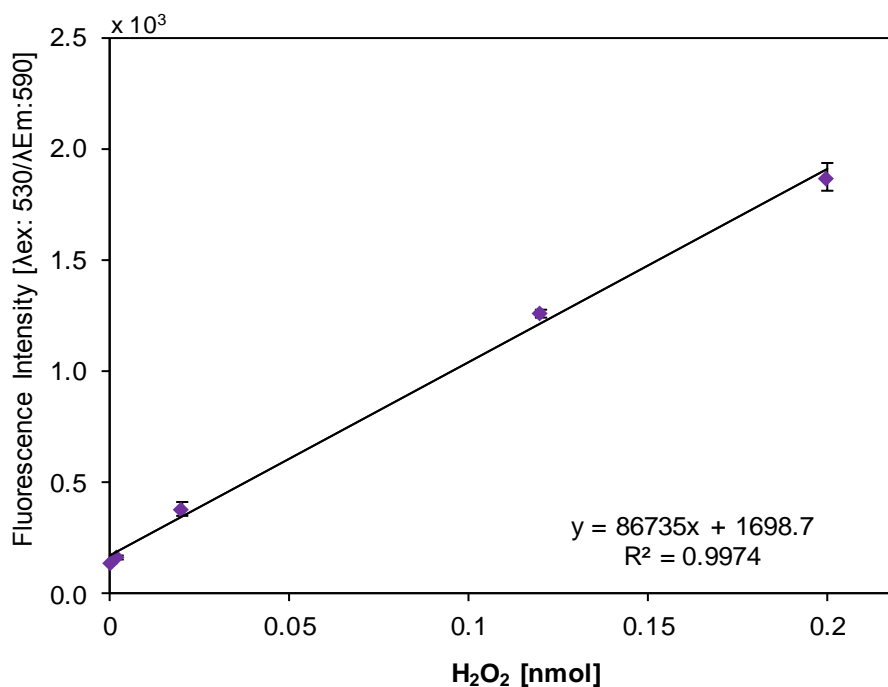
Figure II.9 Calibration curve of fluorescence intensity vs mols of hydrogen peroxide.

Table II.4 Hydrogen peroxide produced from the bioluminescence reactions using luciferin or d_2-luciferin.

luciferin	d_2-luciferin	no substrate
0.697	0.657	0.256
0.694	0.657	0.250
0.688	0.653	0.253
0.693 ± 0.004	0.655 ± 0.002	0.253 ± 0.002

Values in nanomols (mol $\times 10^{-9}$).

Table II.5. Hydrogen peroxide and oxyluciferin produced from the bioluminescence reactions using luciferin or d$_2$-luciferin.

luciferin		d$_2$-luciferin	
hydrogen peroxide	oxyluciferin	hydrogen peroxide	oxyluciferin
0.92 ± 0.07	18.06	0.79 ± 0.01	13.94
0.89 ± 0.02	17.53	0.83 ± 0.03	14.19
0.93 ± 0.07	17.43	0.83 ± 0.03	13.65
0.92 ± 0.03	17.67 ± 0.28	0.82 ± 0.01	13.93 ± 0.22

Values in nanomols (mol $\times 10^{-9}$).

II.2.7 *Beta deuterium isotope effect on the luciferase-luciferin reaction.*

One of the most powerful tools to elucidate the mechanism of enzyme catalyzed reactions is isotope effects, where usually the most obvious information revealed is the rate limiting step. One of the goals with d$_2$-luciferin was to reduce the known side reaction of luciferase that produces dehydroluciferin. Therefore, we calculated the kinetic isotope effect from the experiments performed and discussed previously. Our experiments showed a substantial reduction in the dehydroluciferin produced when d$_2$-luciferin is used in the BL reaction. To determine the isotope effect of the dehydroluciferin per oxyluciferin formed, we divided the amounts of oxyluciferin formed per dehydroluciferin produced to obtain a ratio of 11.19 (Table **II**.3). To calculate the isotope effect, we divided the obtained ratio of the d$_2$-luciferin reaction by the established ratio of 5.25, which generates an isotope effect of 2.12. We have not observed a significant isotope effect in BL emission intensity, luciferase catalytic efficiency, and hydrogen peroxide to oxyluciferin ratio.

II.3 Discussion

We have shown that double deuteration at the luciferin C5 position reduces dehydroluciferin formation from BL reaction to 8% from the established 16%, per turn over. Over the last 50 years numerous publications have demonstrated the production of dehydroluciferyl-adenylate and dehydroluciferin by the luciferase-luciferin reaction and their inhibition towards luciferase catalysis. However, there has not been a thorough investigation of the mechanism involved in the production of these compounds and some suggested intermediates have not been seen. Although our goal of reducing the formation of dehydroluciferin was met, the results did not show a significant increase in BL intensity with d_2-luciferin, compared to luciferin, as was expected. The d_2-luciferin reaction showed a slight increment in BL intensity after the initial characteristic flash peak, where we presume that it is due to the decrease in dehydroluciferin produced that allows higher amounts of free luciferase. This behavior resembles the BL reaction when Coenzyme A is added to the reaction mixture and the light emission is higher at later time points. Figure II.10 shows the Coenzyme A effect in the BL reactions for the first minute. Coenzyme A is usually added to BL assays with cell lysates or purified luciferase at high concentrations of 250-500 μM.[15, 35] However, there is no alternative to reduce dehydroluciferin inhibition on *in vitro* (intact cell) and *in vivo* BL imaging assay besides free Coenzyme A available in the cell. These studies suggest that d_2-luciferin can be of use to decrease dehydroluciferin formation that could inhibit luciferase in any intact cell BL assay that will be measured for

extended periods of time. Further studies could be needed to investigate *d₂*-luciferin as a

possible candidate for the common BL imaging assays *in vitro* and *in vivo* where luciferase

amounts are sensitive and long term BL measurements are a must.
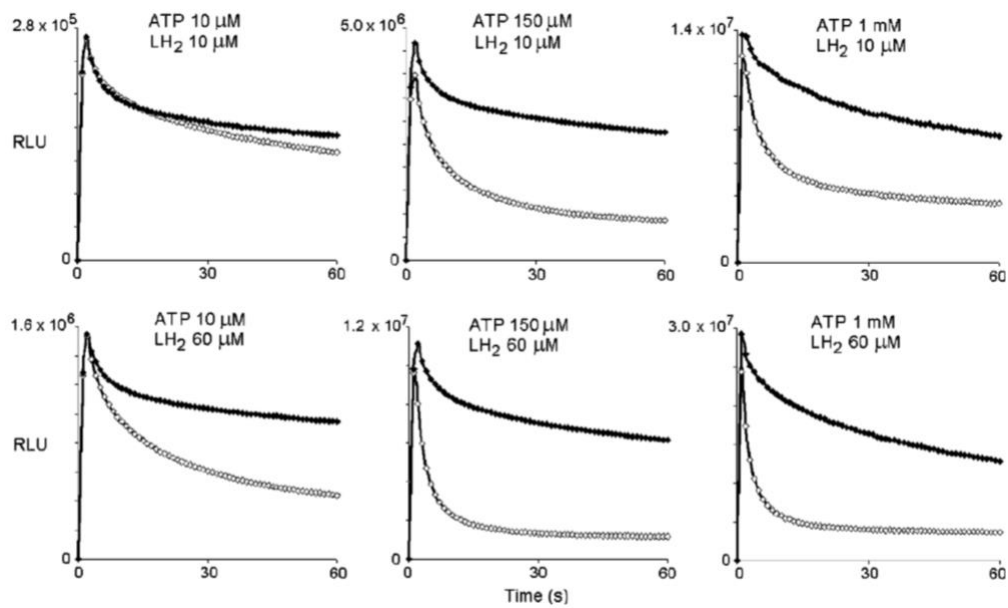
Figure II.10 The stabilizing effect of coenzyme A on bioluminescence.
Mixtures containing ATP and luciferin (LH2) were injected into other mixtures containing Hepes,
MgCl₂, and luciferase (20 nM) supplemented (♦) or not supplemented (◊) with coenzyme A (50
µM). All the indicated quantities are final concentrations. (Figure taken from Da Silva et al., 2005)

Additionally, the work shown here identified the discrepancy in dehydroluciferin

inhibition constants that have been published from different research groups. Two

methods have been reported for determining the inhibition constant. The methods vary

by either previous incubation of dehydroluciferin with luciferase or simultaneous

addition that allows both molecules, luciferin and dehydroluciferin, to compete for the active site. When the inhibition constant is obtained by incubating luciferase with dehydroluciferin the results revealed a inhibition constant in the nM range.[13] However, when the inhibition constant is obtained through the traditional inhibition assay the results show a higher K_i, comparable to oxyluciferin, in the µM range.[14, 36] The commonly observed drastic light decay after the initial flash peak has been attributed to the inhibition of luciferase by its product and byproducts. However, the lack of effect from the decrease in dehydroluciferin produced from the BL intensity suggest further investigations on this theory.

An alternative mechanism to the hydrogen peroxide formation, suggested from the small kinetic isotope effect caused by the deuterated substitution at the β carbon, is discussed in the publication associated to this chapter.

II.4 Materials and methods

Luciferase from firefly (*P. pyralis*) was purified from BL21(DE3) *E. coli* cells transformed with a pET28(b+)-WTLuc vector, following methods reported by Liao et al.[37] Purified luciferase was concentrated using Microcon® (30kDa) from EMD Millipore for experiments that required high enzyme concentration. The luciferase substrates: luciferin and d_2-luciferin, used in the experiments describe here were synthesized by Allyson Dorsey, M.Sc. Commercial dehydroluciferin was purchased from Regis Technologies and used as reference for chromatograms. The purity of synthesized luciferin, d_2-luciferin, and commercial dehydroluciferin were verified by RP-HPLC. The water used to perform experiments, prepare buffers, and solutions was obtained from a Barnstead™ NanoPure™ water purification system with a 18.2 megaohm·cm^{-1} resistance. Stock solutions of each free luciferin acid were prepared by dissolving the compound in water. To assist the dissolving of the compound, the stocks solutions were placed in the ultrasonic bath for 10 to 15 minutes, or until no visible particles were seen. Concentrations of stock solutions for luciferase and luciferins were determined using extinction coefficient 45.6 (mM·cm)$^{-1}$ at 280 nm and 18.2 (mM·cm)$^{-1}$ at 362 nm, respectively, before each experiment.[10, 38, 39] The individual optical measurements for luciferin/d_2-luciferin were obtained from the Varian Cary 50 UV/VIS spectrophotometer at the Analytical Chemistry Instrumentation Facility at UCR. Luciferase was diluted in BSA (1 mg/mL) and Tris-HCl pH 7.8 (20 mM) to desired concentrations. The BL reaction cofactors, ATP and MgSO$_4$ were purchased from RPI

Corp. and Sigma-Aldrich, respectively. Stock solutions of ATP were made at 0.1 M and kept at -20 °C until needed. For $MgSO_4$, 1 M solutions were made and kept at room temperature. The 3-(N-morpholino)propanesulfonic acid, known as MOPS buffer, was purchased from Fisher Scientific. MOPS stocks solutions were made at 1 M and kept at room temperature. For all experiments, a working solution of 0.5 M MOPS was made by adjusting to pH 7 using sodium hydroxide. The BL and FL photon readings were measured by the Synergy Mx BioTek® plate reader. Data for steady state kinetics constants were plotted using GraphPad Prism 5 software. For the hydrogen peroxide assays, both the horseradish peroxidase (HRP) and the Amplex Red compound were purchased from Thermo Scientific. The assay calibration curve was obtained using a commercial 3% hydrogen peroxide. Reverse phase high performance liquid chromatography (RP-HPLC) analyses were conducted using an Agilent Technologies 1100 Series instrument with a C18 column from Alltech™ (4.6×255 mm and 10 μm). Using eluent A: phosphate buffer 7 mM at pH 7.0, 70% and B: methanol (HPLC grade) 30%. The detector was UV/VIS diode array and was set to collect at 215, 328, 347 and 414 nm. Every other run, the HPLC was flushed with water to avoid salt build-up on the column from the phosphate buffer. All experiments were performed at room temperature, 25 °C. Light sensitive Amplex Red was kept wrapped in aluminum foil and any manipulations were done in a dark room.

II.4.1 *Absorbance measurements*

The experiments that are discussed here are dependent on the luciferase and luciferin concentration. Therefore, to corroborate the luciferin's concentration, we used quartz cuvettes to measure the absorbance from 200 to 400 nm, using 1 mL of the stock solutions, and determined the concentration with luciferin's extinction coefficient 18.2 (mM·cm)$^{-1}$ at 328 nm.[40] The concentration was recorded and the measured 1 mL sample was directly used in the experiments. Luciferase concentration was measured using 3 µL of the sample on the NanoDrop spectrophotometer. Absorbance was recorded at 280 nm and concentration was calculated using luciferase' extinction coefficient, 45.6 (mM·cm)$^{-1}$.[10, 38, 39]

II.4.2 *Bioluminescence emission intensity assay*

To compare the d_2-luciferin BL emission intensity to luciferin, we measured the amount of photons produced with both substrates at the same concentration. The samples were prepared by making a 220 µL solution containing 34 µM luciferin in a buffer containing 68 mM MOPS at pH 7.0, 1.7 mM ATP and 11 mM MgSO$_4$. The BL reactions were started by manually adding 30 µL of 0.08 µM luciferase in enzyme diluent to a white 96-well plate containing the sample solution. Reading started 10 seconds after adding luciferase and photons were measured every 30 seconds for a period of 900 seconds, with the integration set to 1 second.

II.4.3 *Bioluminescence concentration dependence assays*

We used BL concentration dependence assays to investigate the catalytic efficiency of both substrates, thus obtaining k_{cat}/K_M for each luciferin. For this experiment, the luciferins at a specific concentration were added to a solution containing final concentrations of 60 mM MOPS buffer pH 7.0, 1.5 mM ATP, and 10 mM $MgSO_4$. The luciferin final concentration ranged from 0.5 to 50 µM. Then, reactions were started by manual injection of luciferase in enzyme diluent to a final concentration of 1 nM. BL was collected for 15 minutes, with integration time of 0.1 second and recording every 30 seconds. To determine each luciferin's K_M and k_{cat}, the steady-state initial velocity was taken from light emitted at the 15 minute time point. GraphPad was used to plot the number of photons produced at 15 minute versus substrate concentration. The plots were analyzed using the nonlinear regression Michaelis-Menten equation fit to determine K_M and the enzyme concentration was entered in the software to determine k_{cat}.

II.4.4 *RP-HPLC analysis of bioluminescence reactions*

To quantify the amount of dehydroluciferin and oxyluciferin produced we followed a method reported by Da Silva et al. where they have identified luciferin, dehydroluciferin, and oxyluciferin from BL reactions using RP-HPLC with phosphate buffer pH 7.0 and 30% methanol as eluents.[7, 10, 25, 41] First, we looked at retention times for synthetic luciferin

and commercial dehydroluciferin in our instrument. Synthetic luciferin was analyzed by manually injecting stock luciferin solution into the HPLC valve (20 μL volume) and eluting under isocratic conditions, 5 mM phosphate buffer pH 7.0 and 30% methanol, at a constant flow rate of 1 mL/minute. In order to compare and quantify the dehydroluciferin produced from the BL reactions, when using luciferin or d_2-luciferin, we verified the retention time and established a concentration curve for dehydroluciferin. A commercial dehydroluciferin stock of 0.1 mM in methanol was diluted to concentrations ranging from 0.01 to 1 μM that were analyzed by RP-HPLC, with the same conditions as stated for luciferin, to record retention time and compose a calibration curve of dehydroluciferin. Before analyzing the BL reactions, the cofactors and enzyme were analyzed individually and collectively (without substrate) by the conditions stated to identify any peaks that are not the products of the BL reaction. Lastly, to analyze the BL reactions for dehydroluciferin and oxyluciferin produced, we used high concentrations of luciferase and substrate. In detail, 300 μL of purified luciferase were added to a Microcon® (30kDa) filter and centrifuged at 10,000 rpm at 4 °C for 30 mins. Luciferase was concentrated before each experiment, and absorbance was used to determine the final concentration. The 500 μL BL reaction solution contained luciferin or d_2-luciferin (50 μM), ATP (1.5 mM), MgSO$_4$ (2 mM), and MOPS pH 7.0 (60 mM). Reactions were initiated by adding concentrated luciferase (20 μM). The reactions were incubated for 1.5 hour at room temperature and stopped by adding 60 μL of EDTA (300 mM). The reaction vials were vortexed for a couple

of seconds and centrifuged for 1 minute at 14,000 rpm. Then, the supernatant was manually injected into the RP-HPLC. The reactions were performed in triplicate and each reaction was analyzed twice by injecting 200 μL into the RP-HPLC valve. To decrease oxyluciferin retention time, after luciferin and dehydroluciferin were eluted (10 minutes into the chromatogram) methanol was increased from 30% to 85% and flow rate from 1 to 1.3 mL/minute. Quantitation of oxyluciferin was done by correlating 1 mol of dehydroluciferin to 5.25 mols of oxyluciferin and assigning the peak area and height to the correlation value.

II.4.5 *Hydrogen peroxide assays*

The production of dehydroluciferin simultaneously results in the production of hydrogen peroxide. Therefore, we wanted to investigate and correlate the production of dehydroluciferin and hydrogen peroxide from the luciferin and d_2-luciferin BL reactions. The methods followed were from Da Silva et al., who analyzed hydrogen peroxide formation using horseradish peroxidase and resorufin (Amplex Red reagent).[10] First, we established a calibration curve to quantify the amount of hydrogen peroxide produced from the BL reactions. The assays were developed under manufacturer specifications. A working solution of 2 μM hydrogen peroxide in PBS was used to prepare the samples with hydrogen peroxide concentration at 0 μM, 0.01 μM, 0.1 μM, 0.6 μM, and 1 μM. The amount of hydrogen peroxide was calculated from the concentrations and used to plot

the FL of Amplex Red vs mols of hydrogen peroxide for each sample. To investigate the

BL reaction for hydrogen peroxide production, the BL reaction solutions were prepared

and stopped under the same conditions as those for RP-HPLC analysis. The incubation

time for the BL reaction was either 30 minutes or 2 hours, depending on the experiment.

The 30 minutes reactions contained luciferase (10 μM), luciferin or d_2-luciferin (50 μM),

ATP (1 mM), MgSO$_4$ (2 mM), and MOPS buffer at pH 7 (60 mM). The 2 hours reactions

contained luciferase (20 μM), luciferin or d_2-luciferin (50 μM), ATP (1.5 mM), MgSO$_4$ (2

mM), and MOPS buffer at pH 7 (60 mM). After reactions were stopped, the rest of the

experiment was performed in a dark room to avoid photooxidation of Amplex Red to

resorufin by light.[30] In the dark room, 12.5 μL of 20 mM Amplex Red stock solution in

DMSO was added to a 500 μL solution containing horseradish peroxidase (72 U/mL) in 1

mM PBS. The stopped reactions were added to a 96 black-well plate containing 100 μL

horseradish peroxidase (0.5 U/mL) and Amplex Red (0.2 mM). After 30 minute incubation

at room temperature protected from light, the fluorescence of resorufin was measured by

excitation at 530 nm and reading emission intensity at 590 nm, which is indicative of

hydrogen peroxide produced.

II.5 References

1.   Seliger, H. H.; McElroy, W. D., Quantum yield in oxidation of firefly luciferin. *Federation Proceedings* **1959,** *18* (1), 321-321.

2.   Seliger, H. H.; McElroy, W. D., Spectral emission and quantum yield of firefly bioluminescence. *Archives of Biochemistry and Biophysics* **1960,** *88* (1), 136-141.

3.   Seliger, H. H.; McElroy, W. D.; Field, G. F.; White, E. H., Stereospecificity and firefly bioluminescence, a comparison of natural and synthetic luciferins. *Proceedings of the National Academy of Sciences of the United States of America* **1961,** *47* (7), 1129-1134.

4.   Ando, Y.; Niwa, K.; Yamada, N.; Enomot, T.; Irie, T.; Kubota, H.; Ohmiya, Y.; Akiyama, H., Firefly bioluminescence quantum yield and colour change by pH-sensitive green emission. *Nature Photonics* **2008,** *2* (1), 44-47.

5.   Helle, P.;   Brau, F.;   Steghens, J.; Bernengo, J., A new low-light-level instrumentation for chemi- and bio-luminescence spectroscopy. In *Bioluminescence and Chemiluminescence*, Bologna, Italy, 1999; pp 195-198.

6.   McElroy, W. D.; Green, A., Function of adenosine triphosphate in the activation of luciferin. *Archives of Biochemistry and Biophysics* **1956,** *64* (2), 257-271.

7.   Fraga, H.;   da Silva, J.; Fontes, R., Chemical synthesis and firefly luciferase produced dehydroluciferyl-coenzyme A. *Tetrahedron Letters* **2004,** *45* (10), 2117-2120.

8.   Fontes, R.;   Dukhovich, A.;   Sillero, A.; Sillero, M. A. G., Synthesis of dehydroluciferin by firefly luciferase: effect of dehydroluciferin, coenzyme A and nucleoside triphosphates on the luminescent reaction. *Biochemical and Biophysical Research Communications* **1997,** *237* (2), 445-450.

9.   Fontes, R.; Ortiz, B.; de Diego, A.; Sillero, A.; Sillero, M. A. G., Dehydroluciferyl-AMP is the main intermediate in the luciferin dependent synthesis of Ap(4)A catalyzed by firefly luciferase. *FEBS Letters* **1998,** *438* (3), 190-194.

10.   Fraga, H.; Fernandes, D.; Novotny, J.; Fontes, R.; da Silva, J. C. G., Firefly luciferase produces hydrogen peroxide as a coproduct in dehydroluciferyl adenylate formation. *Chembiochem* **2006,** *7* (6), 929-935.

11.   Branchini, B. R.; Southworth, T. L.; Murtiashaw, M. H.; Magyar, R. A.; Gonzalez, S. A.; Ruggiero, M. C.; Stroh, J. G., An alternative mechanism of bioluminescence color determination in firefly luciferase. *Biochemistry* **2004,** *43* (23), 7255-7262.

12.   Branchini, B. R.; Southworth, T. L.; Fontaine, D. M.; Murtiashaw, M. H.; McGurk, A.; Talukder, M. H.; Qureshi, R.; Yetil, D.; Sundlov, J. A.; Gulick, A. M., Cloning of the orange light-producing luciferase from *Photinus scintillans*, a new proposal on how bioluminescence color is determined. *Photochemistry and Photobiology* **2017,** *93* (2), 479-485.

13.   Ribeiro, C.; Esteves da Silva, J. C. G., Kinetics of inhibition of firefly luciferase by oxyluciferin and dehydroluciferyl-adenylate. *Photochemical & Photobiological Sciences* **2008,** *7* (9), 1085-1090.

14.   Branchini, B. R.; Magyar, R. A.; Murtiashaw, M. H.; Portier, N. C., The role of active site residue arginine 218 in firefly luciferase bioluminescence. *Biochemistry* **2001,** *40* (8), 2410-2418.

15.   Inouye, S., Firefly luciferase: an adenylate-forming enzyme for multicatalytic functions. *Cellular and Molecular Life Sciences* **2010,** *67* (3), 387-404.

16.   da Silva, L. P.; da Silva, J. C. G. E., Kinetics of inhibition of firefly luciferase by dehydroluciferyl-coenzyme A, dehydroluciferin and L-luciferin. *Photochemical & Photobiological Sciences* **2011,** *10* (6), 1039-1045.

17.   Marques, S. M.; da Silva, J. C. G. E., Firefly bioluminescence: a mechanistic approach of luciferase catalyzed reactions. *IUBMB Life* **2009,** *61* (1), 6-17.

18.   Da Silva, L. P.; Da Silva, J., Theoretical modulation of the color of light emitted by firefly oxyluciferin. *Journal of Computational Chemistry* **2011,** *32* (12), 2654-2663.

19.   da Silva, L. P.; Santos, A. J. M.; Esteves da Silva, J. C. G., Efficient firefly chemi/bioluminescence: evidence for chemiexcitationresulting from the decomposition of a neutral firefly dioxetanone molecule. *Journal of Physical Chemistry A* **2013,** *117* (1), 94-100.

20.   Rebarz, M.; Kukovec, B.-M.; Maltsev, O. V.; Ruckebusch, C.; Hintermann, L.; Naumov, P.; Sliwa, M., Deciphering the protonation and tautomeric equilibria of firefly oxyluciferin by molecular engineering and multivariate curve resolution. *Chemical Science* **2013,** *4* (10), 3803-3809.

21.   Ghose, A.; Rebarz, M.; Maltsev, O. V.; Hintermann, L.; Ruckebusch, C.; Fron, E.; Hofkens, J.; Mely, Y.; Naumov, P.; Sliwa, M.; Didier, P., Emission properties of oxyluciferin and its derivatives in water: revealing the nature of the emissive species in firefly bioluminescence. *Journal of Physical Chemistry B* **2015,** *119* (6), 2638-2649.

22.   Cheng, Y.-Y.; Liu, Y.-J., What exactly is the light emitter of a firefly? *Journal of Chemical Theory and Computation* **2015,** *11* (11), 5360-5370.

23.   Branchini, B. R.; Murtiashaw, M. H.; Magyar, R. A.; Portier, N. C.; Ruggiero, M. C.; Stroh, J. G., Yellow-green and red firefly bioluminescence from 5,5-dimethyloxyluciferin. *Journal of the American Chemical Society* **2002,** *124* (10), 2112-2113.

24.   Rhodes, W. C.; McElroy, W. D., Synthesis and function of adenyl-luciferin and adenyl-oxyluciferin. *Federation Proceedings* **1958,** *17* (1), 295-295.

25.   da Silva, J.; Magalhaes, J.; Fontes, R., Identification of enzyme produced firefly oxyluciferin by reverse phase HPLC. *Tetrahedron Letters* **2001,** *42* (46), 8173-8176.

26.   Viviani, V. R.; Rodrigues Neves, D.; Trabuco Amaral, D.; Prado, R. A.; Matsuhashi, T.; Hirano, T., Bioluminescence of beetle luciferases with 6 '-amino-d-luciferin analogues reveals excited keto-oxyluciferin as the emitter and phenolate/luciferin binding site interactions modulate bioluminescence colors. *Biochemistry* **2014,** *53* (32), 5208-5220.

27.   Niwa, K.; Nakamura, M.; Ohmiya, Y., Stereoisomeric bio-inversion key to biosynthesis of firefly d-luciferin. *FEBS Letters* **2006,** *580* (22), 5283-5287.

28.   Nakamura, M.; Maki, S.; Amano, Y.; Ohkita, Y.; Niwa, K.; Hirano, T.; Ohmiya, Y.; Niwa, H., Firefly luciferase exhibits bimodal action depending on the luciferin chirality. *Biochemical and Biophysical Research Communications* **2005,** *331* (2), 471-475.

29.   Ortiz, B.; Fernandez, V. M.; Sillero, M. A. G.; Sillero, A., Influence of oxygen, dehydroluciferin, luciferin and 6'-ethyl-luciferin on the synthesis of adenosine (5') tetraphospho (5') adenosine (AP(4)A) by firefly luciferase. *Journal of Photochemistry and Photobiology B-Biology* **1995,** *29* (1), 33-36.

30.   Pinto da Silva, L.; Esteves da Silva, J. C. G., Analysis of the performance of DFT functionals in the study of light emission by oxyluciferin analogs. *International Journal of Quantum Chemistry* **2013,** *113* (1), 45-51.

31.   Presiado, I.; Erez, Y.; Simkovitch, R.; Shomer, S.; Gepshtein, R.; da Silva, L. P.; Esteves da Silva, J. C. G.; Huppert, D., Excited-state proton transfer of firefly dehydroluciferin. *Journal of Physical Chemistry A* **2012,** *116* (44), 10770–10779.

32.   Wada, N.; Honda, M.; Suzuki, H., Theory of d-luciferin and dehydroluciferin in acidic or basic solution. *Journal of the Physical Society of Japan* **1985,** *54* (12), 4851-4860.

33.   Pirrung, M. C.; Dorsey, A.; De Howitt, N.; Liao, J., beta-Deuterium Isotope Effects on Firefly Luciferase Bioluminescence. *Chemistryopen* **2017,** *6* (6), 697-700.

34.   Zhao, B. Z.; Summers, F. A.; Mason, R. P., Photooxidation of amplex red to resorufin: implications of exposing the amplex red assay to light. *Free Radical Biology and Medicine* **2012,** *53* (5), 1080-1087.

35.   Reddy, G. R.; Thompson, W. C.; Miller, S. C., Robust light emission from cyclic alkylaminoluciferin substrates for firefly luciferase. *Journal of the American Chemical Society* **2010,** *132* (39), 13586–13587.

36.   Denburg, J. L.; Lee, R. T.; McElroy, W. D., Substrate-binding properties of firefly luciferase: I. luciferin-binding site. *Archives of Biochemistry and Biophysics* **1969,** *134* (2), 381-394.

37.   Malik-Chaudhry, H. K.; Saavedra, A.; Liao, J., A linker strategy for trans-FRET assay to determine activation intermediate of NEDDylation cascade. *Biotechnology and Bioengineering* **2014,** *111* (7), 1288-1295.

38.   Green, A. A.; McElroy, W. D., Crystalline firefly luciferase. *Biochimica Et Biophysica Acta* **1956,** *20* (1), 170-176.

39.   Branchini, B. R.; Magyar, R. A.; Marcantonio, K. M.; Newberry, K. J.; Stroh, J. G.; Hinz, L. K.; Murtiashaw, M. H., Identification of a firefly luciferase active site peptide using a benzophenone-based photooxidation reagent. *Journal of Biological Chemistry* **1997,** *272* (31), 19359-19364.

40.   White, E. H.; Field, G. F.; McCapra, F., Structure and synthesis of firefly luciferin. *Journal of the American Chemical Society* **1963,** *85* (3), 337-343.

41.   Fraga, H.; Fernandes, D.; Fontes, R.; da Silva, J., Coenzyme A affects firefly luciferase luminescence because it acts as a substrate and not as an allosteric effector. *Febs Journal* **2005,** *272* (20), 5206-5216.

Chapter III: The characterization of 6'-thioluciferin as a chromophore and a substrate of luciferase.

III.1 Introduction

Thiol/disulfide redox reactions within eukaryotic and prokaryotic cells oversee many metabolic and biological processes.[1-3] Furthermore, it is well known that thiol/disulfide redox reactions play an important role in: protecting cells against oxidative stress (i.e. reactive oxygen species), signaling, and regulation.[2, 4] The thiol concentration and thiol/disulfide ratio influence the redox potential of the cell and of specific cellular compartments, e.g. mitochondria, endoplasmic reticulum, peroxisomes, and secretory vacuoles. An imbalance of the thiol/disulfide state is associated with a variety of human diseases including diabetes, renal failure, and neurodegenerative diseases, among others.[5-7]

The complexity and ubiquity of the thiol/disulfide system makes it challenging to investigate. Many assays, tools, and methods have been developed to detect and quantify thiols and the disulfide redox-state for *in vitro* and *in vivo* applications.[3] Most of our knowledge about thiol/disulfide biochemical reactions comes from measurements obtained from whole cell lysates, which precludes information from specific

compartments and from the dynamic equilibrium. Therefore, novel redox biosensors that avoid cell lysates are of high importance.

Genetically encoded probes can help target specific compartments within the cell, thereby achieving intact cell measurements and providing information from cellular microenvironments. Two green fluorescent protein (GFP) derivatives, redox-sensitive yellow-fluorescent protein (rxYFP) and redox-sensitive GFP, generated a great interest for monitoring dynamic redox changes in intact cells.[8-10] The introduction of two cysteine residues to the beta-barrel surface of GFP facilitates the formation of a reversible disulfide bridge or oxidized state, which results in a 2.2-fold reduction in emission.[11] Later work showed that the redox-sensitive GFPs expressed in cells can respond to oxidative stimuli through the glutaredoxin (Grx) catalyzed mechanism. Thus, genetically encoded probes for glutathione redox potential can function when Grx is present in sufficient concentrations in a cell or in a specific compartment.[12]

Engineering of novel luciferin analogues from the American firefly can provide a BL-based genetically encoded probe for analyte detection and imaging within cellular microenvironments.[13] BL is obtained when luciferase catalyzes the oxidation of luciferin. In the presence of adenosine triphosphate (ATP), Mg^{2+}, and O_2, luciferase produces oxyluciferin (i.e. oxidized luciferin) in its excited state, which then emits upon relaxation.[14] Luciferin engineering has created novel BL imaging techniques to enable visualization of specific analytes, such as metals, carbohydrates, and enzymes.[15-23] For analyte detection

and visualization, luciferin is usually modified in two ways: (1) alteration of the carboxylic acid [18], and/or (2) extension at the 6′ group.[14] In both cases, the alterations react selectively with the analyte to generate luciferin and emit upon oxidation by luciferase. Benefits of BL-based methods for analyte detection include: no need for external energy source, a high-signal-to-noise ratio that provides a reliable bio-imaging probe, and the ability to perform experiments at different time points.

Despite recent work on luciferins to broaden the scope of BL, to our knowledge, there has not been any investigation to create a luciferase-luciferin pair to monitor thiol/disulfide redox-state of biological molecules. The work presented here shows the characterization of 6′-thioluciferin (S-luciferin), the first luciferin analogue designed to monitor thiol/disulfide redox-state. The publication associated with this chapter discusses the synthesis and structural characterization of S-luciferin (manuscript in preparation). The rationale behind S-luciferin follows a similar approach to the "caged" luciferin examples, where the intensity of the BL emission will depend on the thiol/disulfide redox state of the S-luciferin (Figure **III**.1). We expect that under reductive environment, luciferase will catalyze the S-luciferin oxidation that will result in BL. On the contrary, an oxidative environment will promote disulfide formation and reduce or inhibit the BL signal. Thus, S-luciferin will create a BL system that allows the *in vivo* detection and bioimaging of thiol/disulfide redox-state within specific cellular compartments.
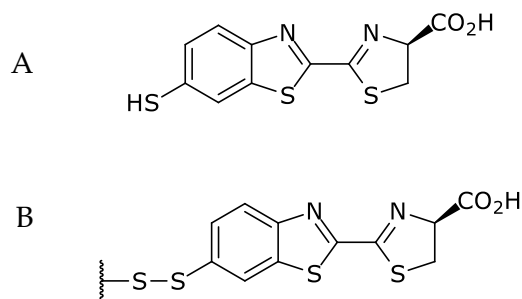
Figure III.1 The reduced (A) and oxidized (B) form of the 6'-thioluciferin molecule.

Previous experimental and theoretical work showed that the optical properties of luciferin can be an indicator of the optical properties of oxyluciferin, given their similarity. Therefore, our work began by evaluating the absorbance and fluorescence of S-luciferin in a reductive environment. We then characterized S-luciferin with purified luciferase for pH dependence, BL intensity, and steady-state enzyme kinetics. The results showed a poor fluorescence emission and BL intensity for S-luciferin compared with luciferin. Possible explanations for the observed low emission are provided in the discussion.

III.2 Results

We investigated the optical properties and performance of S-luciferin as a substrate for luciferase. Emission intensity of luciferin analogues is highly dependent on the electron donating ability of the 6'-group, see Chapter 1. Additionally, the pK_A impacts the ability of S-luciferin to be reduced/oxidized. Thus, our work started by computing the pK_A of the 6'-thiol group of S-luciferin.

III.2.1 *Computational pK$_A$ for S-luciferin*

We computed the pK_A of the 6'-thiol group of S-luciferin using the Marvin Sketch Software pK_A plugin. We first computed the pK_A of the 6'-hydroxyl group of luciferin and compared it to experimental values to determine a percent error. The results with luciferin produced a pK_A of 9.22 for the 6'-hydroxyl (Figure **III**.2, A), which was somewhat in agreement with an experimentally determined value of pK_A 8.7 found in the literature.[24] Taken together, these values resulted in a systematic error of 0.52 pK_A units. Furthermore, the predicted pK_A for the 6'-thiol group of S-luciferin was 5.73 (Figure **III**.2, B), which shows a lower pK_A of the 6' group compared with luciferin. These results suggest that ionization of the 6'-thiol, and the associated electron donating capacity that has been found to be helpful for light emission, will occur around biologically-relevant neutral pH. To further characterize the emission capacity of S-luciferin, we evaluated the optical properties.
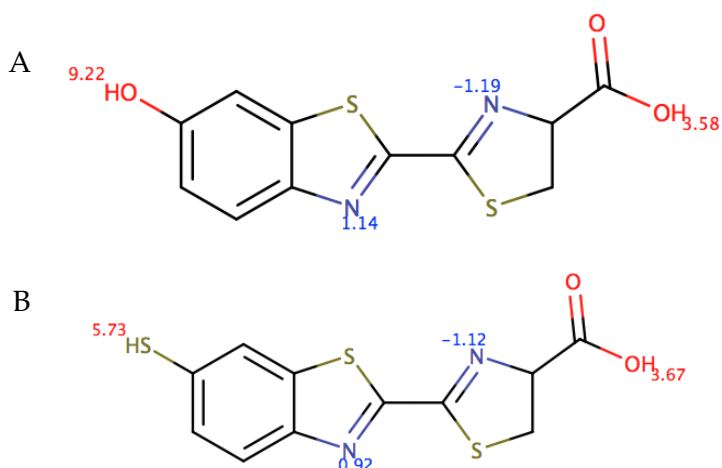
Figure III.2 Computational pK_A for luciferin (A) and S-luciferin (B).
Computation was performed using the Marvin Sketch Software.

III.2.2 *Characterization of the optical properties of S-luciferin*

We investigated the absorbance and fluorescence of S-luciferin. The substitution of the 6′-hydroxyl group of luciferin by 6′-thiol was designed to create a luciferin able to detect thiol/disulfide redox environments. Moreover, it is known that substitution of the 6′-hydroxyl group of luciferin can results in a shifted λ_{max}.[25] Results from absorbance and fluorescence measurements showed a λ_{max} at 300 nm for S-luciferin, which is a 30 nm blue shift compared with luciferin (Figure **III**.3). Furthermore, the shape of the absorption peak for S-luciferin was broad and did not show the characteristic features of luciferin or its analogues (Figure **III**.3, A). To investigate further, we analyzed our sample through HPLC.
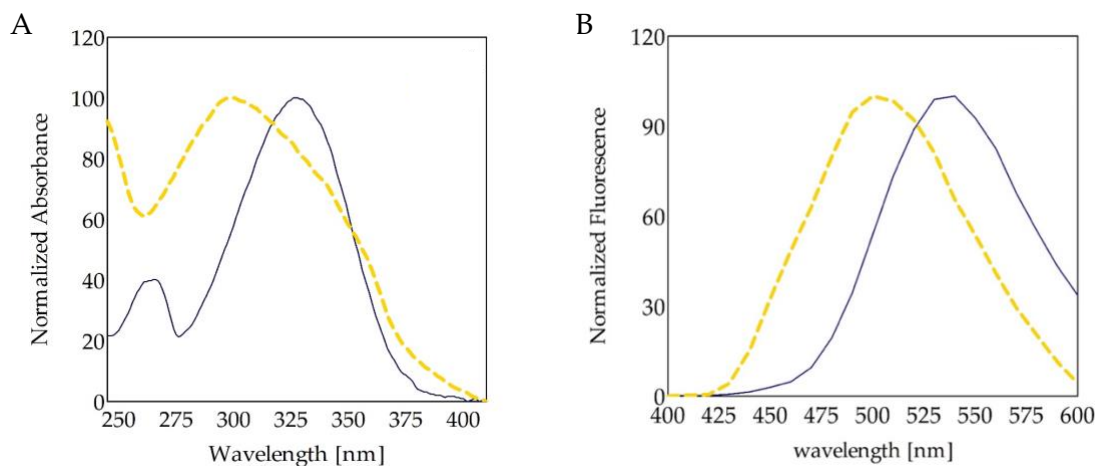
Figure III.3 Normalized absorbance (A) and fluorescence (B) spectra of luciferin (——) and S-luciferin (---).

HPLC and UV/Vis analysis were used to investigate the absorption of S-luciferin. The chromatogram of S-luciferin showed three peaks with retention times at 1.9, 3.6, and 5.5 min (Figure **III**.4). The chromatogram peaks were then analyzed by UV/Vis to identify the products (Figure **III**.5). Our results showed that the peaks at 1.9, 3.6, and 5.5 min corresponded to the solvent, reduced S-luciferin, and dimerized S-luciferin, respectively. Results from UV/Vis analysis showed that the individual absorption peaks for reduced and dimerized S-luciferin had the characteristic shape and features of luciferin. Thus, the broad absorption peak obtained for the stock solution of S-luciferin (Figure **III**.3, A) was a combined spectrum of reduced and dimerized S-luciferin. Hereafter we refer to "stock S-luciferin" to the solutions containing S-luciferin in its reduced and dimerized form. Furthermore, the UV/Vis spectrum of stock S-luciferin was used to estimate the extinction

coefficient at absorbance λ_{max}. The results showed that S-luciferin has an extinction

coefficient of 3.2 $(mM \cdot cm)^{-1}$ at 300 nm, which is far lower than the 18.2 $(mM \cdot cm)^{-1}$ at 330

nm for luciferin.
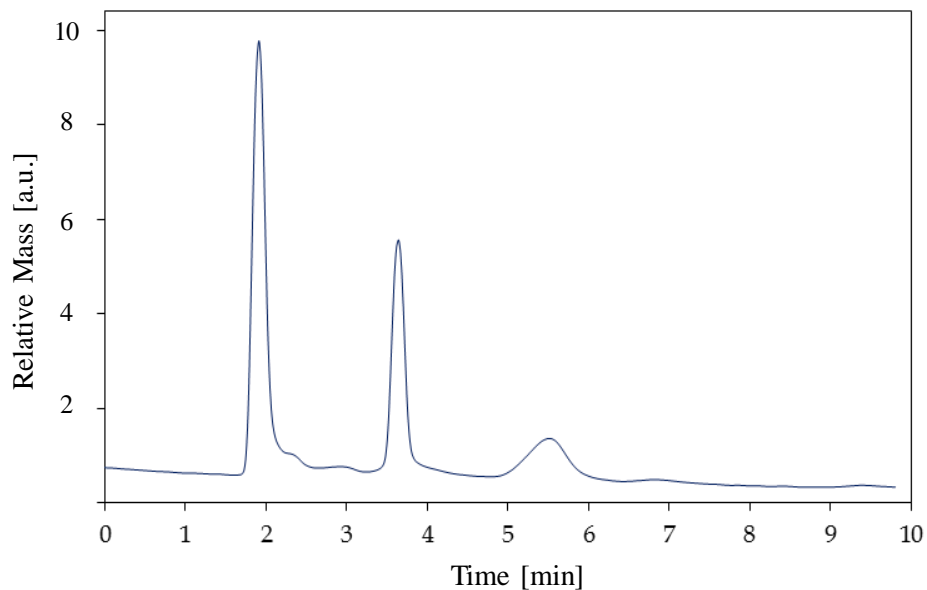
Figure III.4 Chromatogram of stock (i.e. as prepared) S-luciferin.
S-luciferin was eluted with 10% acetonitrile and 90% water under isocratic conditions. The
chromatogram was obtained at 300 nm.
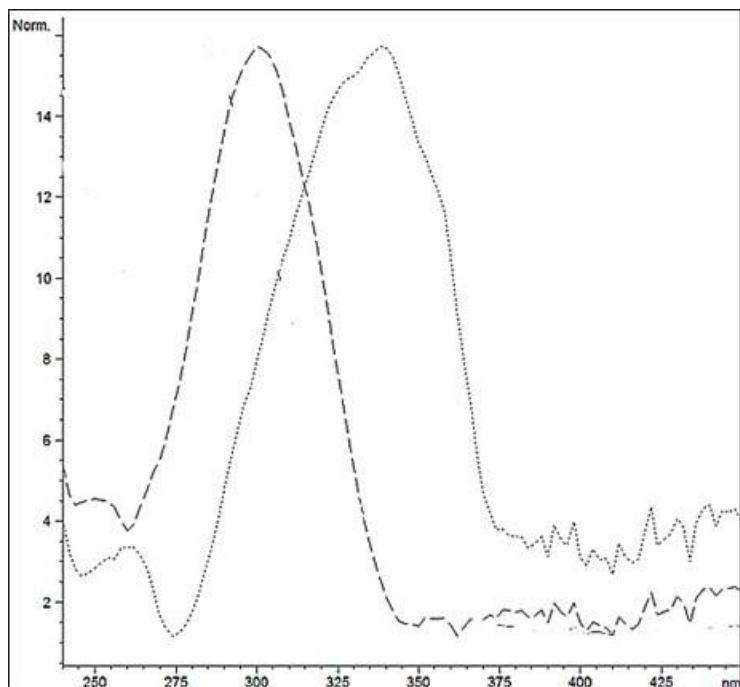
Figure III.5 Absorbance spectra of reduced S-luciferin (_ _ _), and dimerized S-luciferin (……..) from RP-HPLC elutes.
The figure shows the absorbance spectrum corresponding to chromatogram peaks with retention time 3.6, and 5.5 minutes. The sample was eluted with 10% acetonitrile and 90% water under isocratic conditions. The chromatogram was obtained at 300 nm. The graphs were obtained and normalized with CHEMSTATION software. The y-axis shows normalized absorbance, and x-axis wavelength in nm. The solid line shows the absorbance from the solvent peak with retention time at 1.9 min.

We then evaluated the fluorescence emission of reduced S-luciferin by adding a commonly used reducing agent tris(2-carboxyethyl)phosphine (TCEP) to our sample. The fluorescence emission was measured for stock S-luciferin, reduced S-luciferin due to addition of TCEP, and for luciferin. Our results showed a 30 nm blue shift for reduced S-luciferin when compared to luciferin (Figure **III**.6). Interestingly, the fluorescence intensity of reduced S-luciferin was much lower compared with both stock S-luciferin

80

(which contained both reduced and dimerized molecules) and luciferin. We observed a

75% reduction of fluorescence intensity of reduced S-luciferin compared with luciferin.

Despite measuring a reduction in fluorescence intensity, we continued to use TCEP to

obtain reduced S-luciferin since luciferase would not produce enough BL from stock S-

luciferin to be measured. We presumed that luciferase will not accept the disulfide as its

substrate.
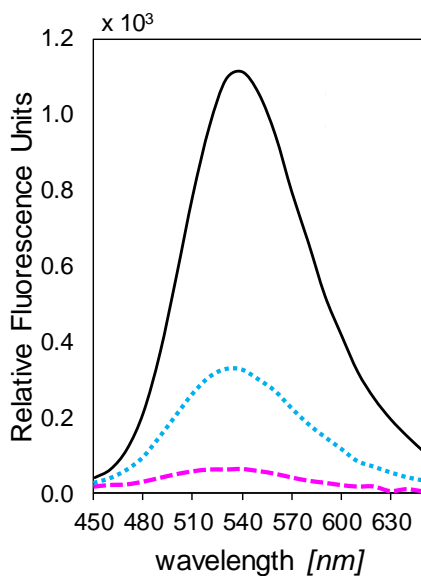
Figure III.6 Relative fluorescence intensity of luciferin (——), reduced S-luciferin (_ _ _), and stock S-luciferin (......).
All compounds were used at a concentration of 10 μM. Reduced S-luciferin was obtained by addition of 0.1 mM TCEP. The excitation source was set to 328 nm for luciferin and 300 nm for S-luciferin.

III.2.3 *Bioluminescence intensity from reduced S-luciferin*

We evaluated the performance of reduced S-luciferin as a substrate for luciferase. We started with a control experiment by investigating the influence of TCEP on the BL intensity produced by luciferin with luciferase. Our results showed a concentration dependent decrease in BL intensity with increasing concentration of TCEP from 5 mM concentration (Figure III.7). Specifically, the BL intensity decreased 12% when increasing TCEP from 1 to 5 mM, and BL intensity was totally lost when increasing from 10 to 50 mM. Therefore, we determined that the TCEP at 1 mM during the S-luciferin reaction experiments was not affecting the luciferase reaction. After determining the TCEP concentration that would not have a negative effect on the BL reaction, we continued to determine the pH dependence of the BL reaction of S-luciferin with luciferase.
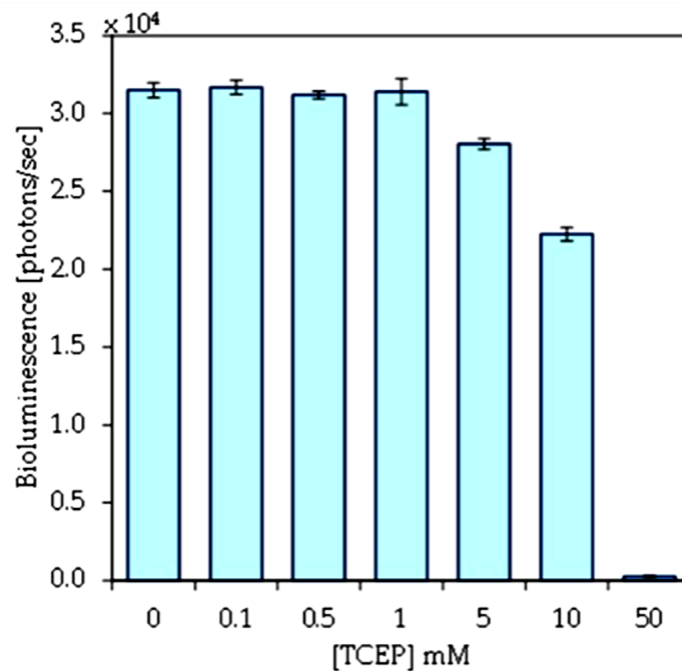
Figure III.7 The TCEP-concentration dependence of the bioluminescence intensity for luciferin as substrate for luciferase.
Readout was performed after manual injection of luciferase with final concentration of 1 nM to the reaction mixture. The reaction mixture final concentration was composed of 1 mM ATP, 10 mM MgSO$_4$, 50 mM Tris-HCL buffer at pH 7.8, and TCEP at each concentration. The assays were performed in triplicate and error bars represent standard deviations within the triplicates.

We evaluated the pH-dependent BL intensity of reduced S-luciferin with luciferase to determine an optimum reaction pH and associated steady-state kinetics. (Figure **III**.8 and Figure **III**.9) Results for pH dependence of the BL reaction with reduced S-luciferin showed an optimum at pH 9.4. (Figure III.8) Compared with the optimum pH of luciferin which is 8.5 (see Chapter 1), the optimum pH of reduced S-luciferin was more alkaline. We then measured the BL intensity of reduced S-luciferin within a concentration range with luciferase at pH 9.4 to determine a K_M of 0.5 µM (Figure **III**.9). The plot for saturation

kinetics showed a bell-shaped curve that could be indicative of a substrate inhibitor. To further investigate the interaction of S-luciferin with luciferase investigate, we treated S-luciferin as an inhibitor of the BL reaction, discussed in section III.2.4. It should be noted that high concentrations of luciferase were used for the steady-state kinetics experiments with reduced S-luciferin. Similar concentrations of luciferase cannot be used with luciferin because the instrument will saturate, thus the K_M of reduced S-luciferin cannot be directly compared to its K_i.
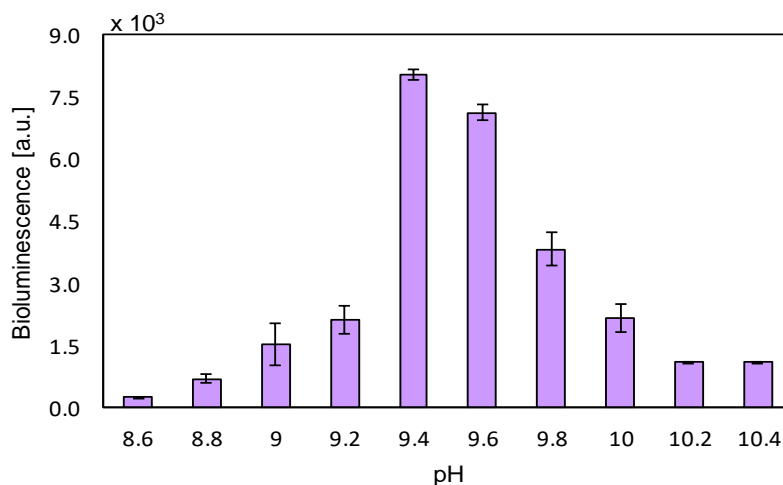
Figure III.8 Luciferase pH dependence with S-luciferin.
BL readings were performed after manual injection of luciferase for a final concentration of 1 μM. The BL reaction mixture contained 1.5 mM ATP, 10 mM MgSO₄, 60 mM Glycine-NaOH buffer at the desired pH, and 0.5 μM reduced S-luciferin using 1 mM TCEP. Assays were performed in triplicate and the error bars represent standard deviations within the triplicates. Refer to Figure IV.4 for luciferase pH dependence with luciferin.
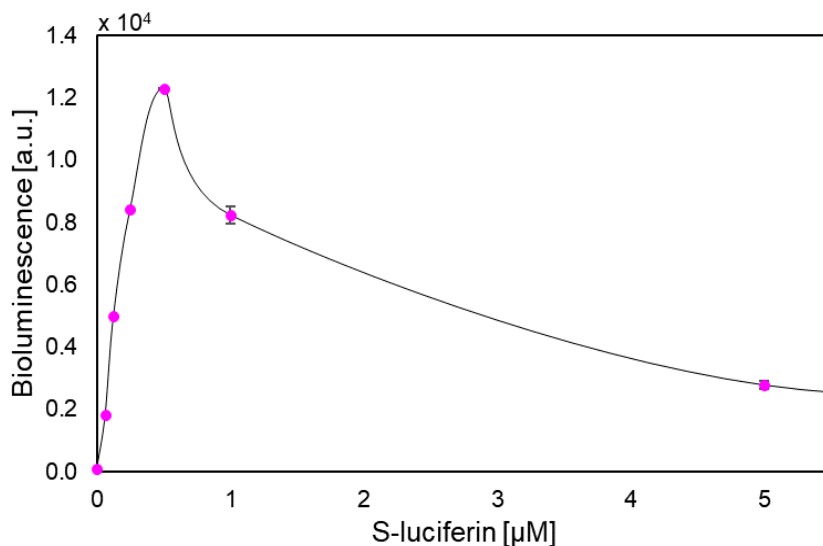
Figure III.9 Steady state kinetics with S-luciferin.
The assay was performed at pH 9.4 with S-luciferin concentrations ranging from 0 to 5 μM, 0.5 μM luciferase, and 1.5 mM TCEP. Initial velocities were taken from light emission 3 minutes after initiating the reaction to avoid the light flash common with luciferase. The assays were performed in triplicate and error bars represent standard deviations.

We compared the BL intensity of reduced S-luciferin with the BL intensity produced by luciferin, both at their respective optimum pH and K_M concentrations. We utilized a 100-fold higher concentration of luciferase for measurements with reduced S-luciferin compared with measurements for luciferin. Therefore, the BL intensity for luciferin was scaled by 100 to account for the difference in enzyme concentration. For the conditions evaluated, our results showed that the BL intensity with reduced S-luciferin was 0.01% compared with luciferin. (Figure **III**.10)
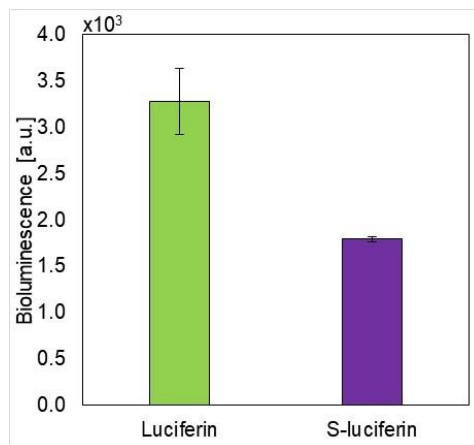
Figure III.10 Bioluminescence intensity from luciferin (■) and reduced S-luciferin (■).
Each substrate was used at its K_M concentration and optimal pH: 0.5 µM and pH 9.4 for reduced S-luciferin, and 1 µM and pH 7.8 for luciferin. The concentration of luciferase used was 1 and 0.001 µM for S-luciferin and luciferin, respectively. Value represent the average of triplicates and error bars indicate the standard deviation.

III.2.4 *Inhibition constant of reduced S-luciferin*

We investigated the ability of the active site of luciferase to accept reduced S-luciferin to determine if reduced BL was due to poor binding as a substrate to the active site. To do so, we evaluated the inhibition by reduced S-luciferin against luciferin (Figure **III**.11). Our results showed an increase in the K_M of luciferin with increasing concentration of reduced S-luciferin (Figure **III**.12). This result showed reduced S-luciferin is a competitive inhibitor of luciferase and confirmed binding of reduced S-luciferin to the active site. We also calculated the inhibition constant of reduced S-luciferin and obtained a K_i of 0.07 µM. It should be noted that no BL is observed from the inhibitor in this assay.
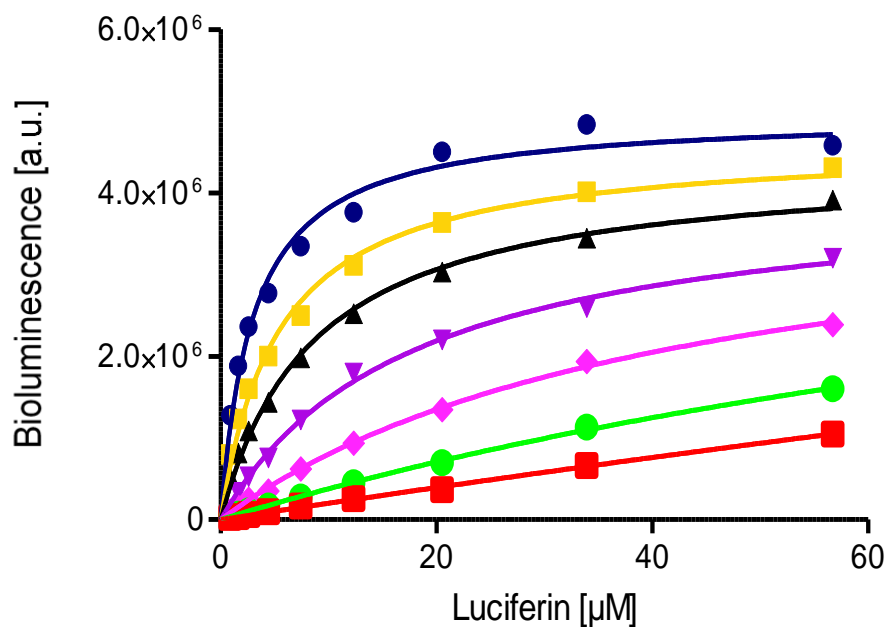
Figure III.11 Competitive inhibition of luciferase by reduced S-luciferin.
S-luciferin concentration at 0 µM (●), 0.1 µM (■), 0.3 µM (▲), 0.6 µM (▼), 1.2 µM (◆), 2.4 µM (●), and 5.0 µM (■). Luciferin concentrations ranged from 0.1 to 57 µM. BL measurements were obtained from reactions containing 10 nM luciferase, 1.5 mM TCEP, 1.5 mM ATP, 5 mM $MgSO_4$, and 60 mM Tris-HCl buffer at pH 9.4. The lines represent the non-linear regression fit calculated through GraphPad software.
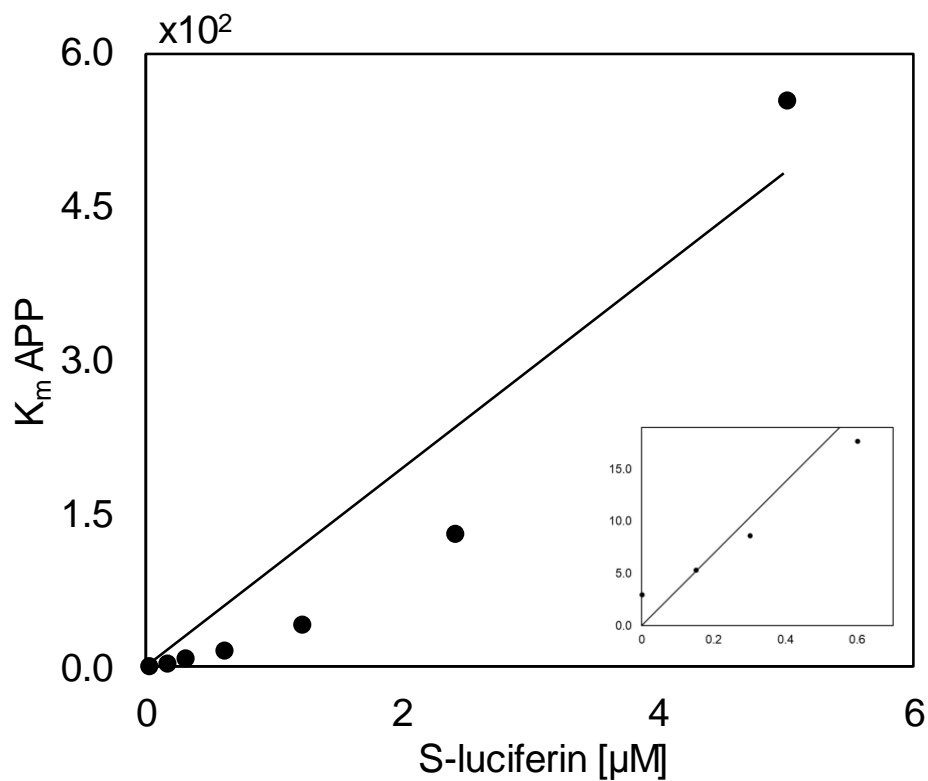
Figure III.12 The effect of S-luciferin on luciferin apparent K_M.
Graph shows apparent K_M corresponding to a specific S-luciferin concentration. The increase in K_M is characteristic of a competitive inhibitor. Insert emphasizes the S-luciferin concentration from 0 to 0.6 μM. Apparent K_M was calculated using GraphPad software.

III.2.5 *Docking of reduced S-luciferin*

We investigated a simulated binding of reduced S-luciferin towards the active site of luciferase using preliminary computational studies. Computational studies to analyze protein structures or protein-ligand interactions have become routine in protein and enzyme research workflow. We used AutoDock4 software to examine the simulated interaction between reduced S-luciferin and the active site of luciferase to further

investigate the experimentally observed binding. Our preliminary computational studies focused on addressing whether the ionic state of reduced S-luciferin influenced its ability to interact with the active site. We performed in silico docking simulations of reduced S-luciferin in its thiol and thiolate within the active site of luciferin (

Figure III.13). Interestingly, our results showed that the thiol-luciferin did not aligned well with the active site of luciferase. In contrast, the coordinates of thiolate-luciferin were similar to the crystallographic structure of luciferin bound in the active site of luciferase. These preliminary simulations suggest that the thiolate S-luciferin binds similar to luciferin.
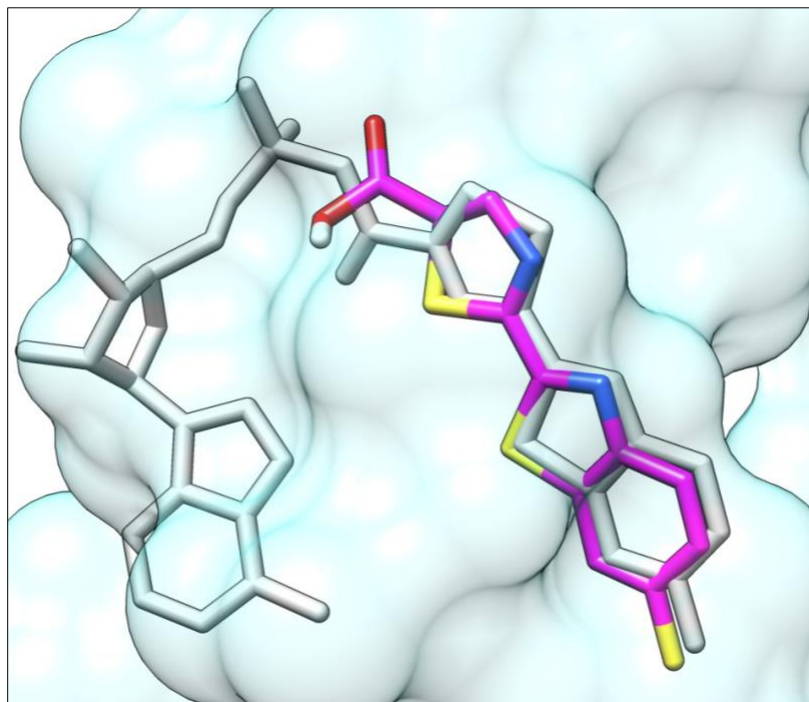
Figure III.13 Illustration of thiolate S-luciferin docked within the active site of luciferase.
Thiolate S-luciferin (shown in color) overlaid with the adenylated-luciferin analogue from the crystal strucutre (shown in gray) within the active site of luciferase (gray surface in the background). PDB-ID: 4G37 was used to dock luciferin and S-luciferin. Luciferin was run through the simulation as reference to evaluate the docking parameters.

III.3 Discussion

The 6′-thiol substitution has a detrimental effect on the chromophore properties of S-luciferin. Our results showed that the 6′-thiol substitution decreased the absorbance extinction coefficient and the FL intensity compared with luciferin. The 6′-thiol substitution also caused a blue-shift in the absorbance and emission of the chromophore

relative to luciferin. Moreover, our results showed that reduced S-luciferin was a poor substrate for luciferase. However, it is not uncommon for luciferin analogues to be poor substrates to luciferase.[26]

Two thiol-based substituted luciferins, similar to S-luciferin, were recently synthesized and characterized by the Miller group. Both 6′-methylthio-luciferin and 6′-methylsulfinyl-luciferin have sulfur substitutions at the 6′ position. On the one hand, the absorbance of the 6′-methylthio-luciferin was slightly redshifted (approximately 10 nm) compared to luciferin. Furthermore, 6′-methylthio-luciferin showed a blue shifted emission of approximately 40 nm relative to luciferin, and a 70% decrease in the FL quantum yield relative to 6′-amino-luciferin.[27] On the other hand, the absorbance of the 6′methylsulfinyl-luciferin was blue shifted 30 nm relative to luciferin, and no FL emission was observed.[27] The absorbance and emission characteristics of 6′-methylsulfinyl-luciferin are similar to our results for S-luciferin. Comparison of the electron donating capacity of the methylthio, methylsulfinyl, and thiol to the hydroxyl group suggest that the decrease in the electron donating capacity of the 6′-S-R substitutions in luciferin directly affects their FL emission.

We speculate that the poor electron donating ability of the thiol group may result in the reduced absorption and FL emission of S-luciferin. The thiol group is a poor electron donor relative to hydroxyl, and electron rich donor groups are needed for emission. Promega Corporation has a commercial luciferin analogue with no substitution at the 6′ position (Figure **III**.14) with characteristics similar to S-luciferin. The luciferin analogue

6′-deoxy-luciferin (Figure **III**.14, A) is oxidized at the 6′ position to generate luciferin in the presence of a cytochrome enzyme. The produced luciferin is then used to generate BL and quantify the cytochrome enzymatic activity. Like S-luciferin, 6′-deoxy-luciferin lacks an electron donating group at the 6′ position, which also causes the molecule to have an approximate 30 nm blue shift in FL emission (Figure **III**.14, B and C) compared with luciferin. White et al. synthesized 6′-methoxy-luciferin to investigate the effect of the 6′-group on the optical properties of luciferin. The methoxy group is a poorer electron donor compared with the hydroxyl. Published values show that the fluorescence quantum yield of 6′-methoxy-luciferin decreases significantly compared to luciferin.[24] The authors showed that the decrease was such that it did not allow a measurement of FL emission. Values for optical properties of luciferin and luciferin analogues with poor electron donating groups at C6′ were compiled for ease of comparison, Table **III**.1. Taken together, the poor electron donating ability of C6′ groups in luciferin analogues may be responsible for the FL emission blue shift and the decrease in intensity observed for S-luciferin and these commercial analogues.

A

B

C
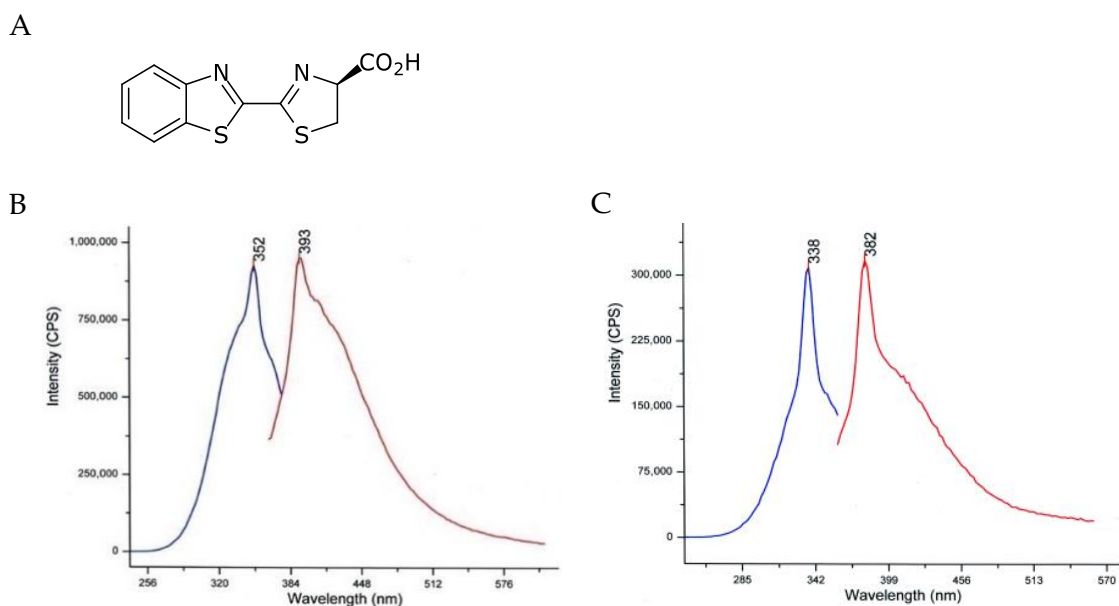
Figure III.14 Luciferin analogue 6'-deoxy-luciferin sold commercially by Promega Corporation: molecular structure (A), and excitation and fluorescence emission spectra in methanol (B) and 50 mM potassium phosphate pH 7.4 (C).
Blue and red traces in (B) and (C) represent excitation and fluorescence emission, respectively, for 5 μM concentration of the substrate. Graphs were obtained from Promega Corporation.

Table III.1 Compilation of spectroscopic data for luciferin and luciferin analogues with poor electron donating groups at the C6'position based on their absorbance and fluorescence properties.

	Absorbance [nm]	Extinction coefficient [(mM·cm)$^{-1}$]	FL [nm]		FL Quantum Yield
			water	methanol	
Luciferin [a, b]	330	18.2	540	415	0.62
6'-methylsulfinyl-luciferin [c]	300	NA	NA	NA	NA
6'-methylthio-luciferin [c]	342	NA	494	465	0.33*
6'-deoxy-luciferin [a]	295	16.6	382	393	NA
6'-methoxy-luciferin [a, b]	325	18.6	NA	NA	0.03
S-luciferin	300	3.2	510	NA	NA

[a]Values from White et al., 1965 in ethanol. [b]Values from Seliger et al.,1969 in water. [c]Values from Miller at *al.*, 2017 in methanol. *Value is relative to aminoluciferin at 1. NA, not available.

S-luciferin, like the other 6'-S-R luciferin analogues in the literature,[27] show inhibition of luciferase. The Miller group did not provide inhibition constants, therefore a comparison to our S-luciferin cannot be made. In addition to being a poor chromophore, S-luciferin was also a poor substrate for luciferase and its extremely low emission did not allow the measurement of BL emission spectra. However, it is not uncommon for luciferin analogues to be bad substrates for luciferase. Therefore, synthesis of future luciferin analogues should go in parallel with engineering of luciferases to construct a BL-based system to monitor the thiol/disulfide redox for imaging and detection of redox measurements in cellular compartments. In addition, a detailed photophysics study of S-luciferin or S-oxyluciferin would be helpful to understand the excitation pathway of the luciferin analogue.

III.4 Materials and methods

III.4.1 *Reagents*

General methods are discussed in Chapter 2. Luciferase from firefly (*P. pyralis*) was cloned, expressed, and purified in our lab. Experiments with reduced S-luciferin were carried out using the reducing agent tris(2-carboxyethyl) phosphine (TCEP), which was acquired from RPI Corp. A solution of 100 mM TCEP was prepared fresh before each experiment. The substrate S-luciferin was synthesized, purified, and characterized by Andrew Carlson. HPLC grade acetonitrile obtained from Fisher Scientific was used for all RP-HPLC measurements.

For the BL reaction cofactors: ATP was purchased from RPI Corp and $MgSO_4$ was purchased from Sigma-Aldrich. For ATP, solutions were prepared at 0.1 M concentration and stored at -20 °C until needed. For $MgSO_4$, solutions were prepared at 1 M concentration and stored at room temperature. Commercial luciferin used on control experiments was obtain from Research Products International.

III.4.2 *Computational pK_A*

The pK_A of the 6'-group from luciferin and S-luciferin was calculated using the calculator plugins from Marvin Sketch 14.7.28, 2014 software.

III.4.3 *Absorbance and fluorescence measurements.*

The absorption spectrum for stock S-luciferin was first obtained using a 3 μL solution in water and a NanoDrop2000c spectrophotometer. Detailed characterization of stock S-luciferin was carried out using reverse phase high performance liquid chromatography (RP-HPLC). RP-HPLC measurements were conducted using an Agilent Technologies 1100 Series instrument with a C18 column from Alltech™ (4.6 x 255 mm and 10 μm). The detector was a UV/VIS diode array monitoring 300 nm. The retention times were determined by manually injecting 20 μL of stock solution into the HPLC valve, flowing at a constant rate of 1.5 mL/min, and eluting with 10% acetonitrile in water under isocratic conditions. Peaks in the chromatogram was analyzed for UV/Vis absorbance using the CHEMSTATION software.

Fluorescence measurements for stock S-luciferin were obtained using black 384-well plates and a Synergy Mx microplate reader (BioTek®) with excitation at 300 nm for S-luciferin or 328 nm for luciferin. All fluorescence measurements were carried out using an integration time of 0.1 second and 10 μM concentration for luciferin and S-luciferin.

III.4.4 *Bioluminescence assays of reduced S-luciferin*

The amount of photons produced by the BL reaction with reduced S-luciferin was investigated. A solution of luciferase was prepared in enzyme diluent containing 20 mM

Tris-HCL and 1 mg/mL BSA. A reaction cocktail was prepared: 0.5 μM solution of stock S-luciferin, 1.5 mM ATP, 10 mM $MgSO_4$, and 1.5 mM TCEP, and added into a white 96-well plate. To evaluate the pH dependence, 60 mM glycine-sodium hydroxide buffer was used for pH 8.6 to pH 10.4. The BL reactions were started by manually injecting 30 μL of 0.08 μM luciferase into the wells containing 270 μL of reaction mixture that included reduced S-luciferin and cofactors. The BL readings, sum of photons over 1 second, were measured using a Synergy Mx BioTek® plate reader. The sensitivity of the PMT was adjusted as needed.

We determined the steady-state kinetics of reduced S-luciferin with luciferase. Since the BL intensity of S-luciferin was very low, we increased the concentration of luciferase to obtain enough BL emission. A 2 μM luciferase solution in enzyme diluent was added to a 96-well plate containing the reaction cocktail: 0 to 5 μM reduced S-luciferin, 1 mM TCEP, and at pH 9.4. BL reactions were started and measured as described above. GraphPad Prism 5 software was used to plot the total number of photons as a function of substrate concentration and plots were analyzed using a nonlinear regression fit.

To compare the BL intensity of S-luciferin with luciferin we used a 100-fold higher concentration of enzyme for the BL reaction with S-luciferin and then scaled the BL by 100. The following was used for S-luciferin: 1 μM luciferase solution in enzyme diluent;

and reaction cocktail with 0.5 μM reduced S-luciferin, 1 mM TCEP, and pH 9.4. The following was used for luciferin: 0.001 μM luciferase solution in enzyme diluent; and reaction cocktail with 1 μM reduced S-luciferin and pH 7.8, without TCEP. BL reactions were started and measured as described above.

III.4.5 *Steady-state kinetic measurements to determine the inhibition constant*

We determined the inhibition constant of reduced S-luciferin by measuring the apparent K_M of luciferin, with concentrations ranging from 0 μM to 57 μM, in the presence of 0 μM to 5 μM of S-luciferin. A reaction cocktail was prepared with: luciferin or S-luciferin at the designated concentration, 5 mM ATP, 30 mM $MgSO_4$, 120 mM glycine-sodium hydroxide buffer at pH 9.4, and 5 mM TCEP, and added into a white 96-well plate. Water was added to each well to make the total volume 258 μL. The BL reactions were started by manually injecting 42 μL of 0.07 μM luciferase into the reaction cocktail. BL reactions were measured and analyzed with non-linear regression as described above to determine the K_i.

III.4.6 *Docking of reduced S-luciferin*

The crystal structure of luciferase from *P. pyralis* with an adenylated-luciferin analogue was obtained from the Protein Data Bank (PBD code 4G37) and used for docking simulations. We delimited the active site of luciferase to the amino acids within 10 Å away

from the luciferin structure. The active site of luciferase was modeled without solvents, counterions, and substrates. Modeling of the active site was carried out with energy minimization using the Amber (PARM99) forcefield in UCSF Chimera Software.[30] Affinity grids on the active site were constructed using AutoGrid4. The isotropic grid map consisted of 40-x, y, z grid points with 0.603 Å spacing.

AutoDock4 was used to simulate docking of luciferin, thiol S-luciferin, and thiolate S-luciferin into the active site of luciferase. The amino acids in the active site were kept rigid and the bond C2-C2' in all luciferins was allowed to rotate. The VEGA ZZ Software was used to build and calculate partial charges on the luciferins prior to modeling.[31] AutoDock4 Tools interface was used to keep polar hydrogens and add Gasteiger partial charges to the active site. Docking was performed using a global genetic algorithm combined with local minimization in VEGA ZZ Software and Lamarckian genetic algorithm to explore conformational changes of the luciferins within the active site.

The resulting conformations were clustered into similar binding energy with a root mean square deviation (RMSD) clustering tolerance of 2 Å. The conformations were then ranked based on lowest binding energy and alignment with the crystallographic structure of the adenylated-luciferin analogue. The resulting conformations were used for analysis and comparison with luciferin.

III.5 References

1.   Go, Y.-M.; Jones, D. P., Thiol/disulfide redox states in signaling and sensing. *Critical Reviews in Biochemistry and Molecular Biology* **2013,** *48* (2), 173-191.

2.   Van Laer, K.; Hamilton, C. J.; Messens, J., Low-molecular-weight thiols in thiol-disulfide exchange. *Antioxidants & Redox Signaling* **2013,** *18* (13), 1642-1653.

3.   Comini, M. A., Measurement and meaning of cellular thiol:disufhide redox status. *Free Radical Research* **2016,** *50* (2), 246-271.

4.   Schwarzlaender, M.; Dick, T. P.; Meyer, A. J.; Morgan, B., Dissecting redox biology using fluorescent protein sensors. *Antioxidants & Redox Signaling* **2016,** *24* (13), 680-712.

5.   Giustarini, D.; Tsikas, D.; Colombo, G.; Milzani, A.; Dalle-Donne, I.; Fanti, P.; Rossi, R., Pitfalls in the analysis of the physiological antioxidant glutathione (GSH) and its disulfide (GSSG) in biological samples: an elephant in the room. *Journal of Chromatography B-Analytical Technologies in the Biomedical and Life Sciences* **2016,** *1019*, 21-28.

6.   Ballatori, N.; Krance, S. M.; Notenboom, S.; Shi, S.; Tieu, K.; Hammond, C. L., Glutathione dysregulation and the etiology and progression of human diseases. *Biological Chemistry* **2009,** *390* (3), 191-214.

7.   Johnson, W. M.; Wilson-Delfosse, A. L.; Mieyal, J. J., Dysregulation of glutathione homeostasis in neurodegenerative diseases. *Nutrients* **2012,** *4* (10), 1399-1440.

8.   Meyer, A. J.; Dick, T. P., Fluorescent protein-based redox probes. *Antioxidants & Redox Signaling* **2010,** *13* (5), 621-650.

9.   Ostergaard, H.; Henriksen, A.; Hansen, F. G.; Winther, J. R., Shedding light on disulfide bond formation: engineering a redox switch in green fluorescent protein. *Embo Journal* **2001,** *20* (21), 5853-5862.

10.   Hanson, G. T.; Aggeler, R.; Oglesbee, D.; Cannon, M.; Capaldi, R. A.; Tsien, R. Y.; Remington, S. J., Investigating mitochondrial redox potential with redox-sensitive green fluorescent protein indicators. *Journal of Biological Chemistry* **2004,** *279* (13), 13044-13053.

11.   Ostergaard, H.; Tachibana, C.; Winther, J. R., Monitoring disulfide bond formation in the eukaryotic cytosol. *Journal of Cell Biology* **2004,** *166* (3), 337-345.

12.   Ren, W.; Ai, H. W., Genetically encoded fluorescent redox probes. *Sensors* **2013,** *13* (11), 15422-15433.

13.   Umezawa, Y., Genetically encoded optical probes for imaging cellular signaling pathways. *Biosensors & Bioelectronics* **2005,** *20* (12), 2504-2511.

14.   Li, J.; Chen, L. Z.; Du, L. P.; Li, M. Y., Cage the firefly luciferin! - a strategy for developing bioluminescent probes. *Chemical Society Reviews* **2013,** *42* (2), 662-676.

15.   Ioka, S.; Saitoh, T.; Maki, S. A.; Imoto, M.; Nishiyama, S., Development of a luminescence-controllable firefly luciferin analogue using selective enzymatic cyclization. *Tetrahedron* **2016,** *72* (47), 7505-7508.

16.   Zheng, Z.; Wang, L.; Tang, W.; Chen, P. Y.; Zhu, H.; Yuan, Y.; Li, G. Y.; Zhang, H. F.; Liang, G. L., Hydrazide d-luciferin for *in vitro* selective detection and intratumoral imaging of Cu2+. *Biosensors & Bioelectronics* **2016,** *83*, 200-204.

17.   Hsu, H. T.; Trantow, B. M.; Waymouth, R. M.; Wender, P. A., Bioorthogonal catalysis: a general method to evaluate metal catalyzed reactions in real time in living systems using a cellular luciferase reporter system. *Bioconjugate Chemistry* **2016,** *27* (2), 376-382.

18.   Mofford, D. M.; Adams, S. T.; Reddy, G.; Reddy, G. R.; Miller, S. C., Luciferin amides enable *in vivo* bioluminescence detection of endogenous fatty acid amide hydrolase activity. *Journal of the American Chemical Society* **2015,** *137* (27), 8684-8687.

19.   Henkin, A. H.; Cohen, A. S.; Dubikovskaya, E. A.; Park, H. M.; Nikitin, G. F.; Auzias, M. G.; Kazantzis, M.; Bertozzi, C. R.; Stahl, A., Real-time noninvasive imaging of fatty acid uptake *in vivo*. *Acs Chemical Biology* **2012,** *7* (11), 1884-1891.

20.   Yuan, Y.; Wang, F. Q.; Tang, W.; Ding, Z. L.; Wang, L.; Liang, L. L.; Zheng, Z.; Zhang, H. F.; Liang, G. L., Intracellular self-assembly of cyclic d-luciferin nanoparticles for persistent bioluminescence imaging of fatty acid amide hydrolase. *ACS Nano* **2016,** *10* (7), 7147-7153.

21.   Ke, B. W.; Wu, W. X.; Liu, W.; Liang, H.; Gong, D. Y.; Hu, X. T.; Li, M. Y., Bioluminescence probe for detecting hydrogen sulfide *in vivo*. *Analytical Chemistry* **2016,** *88* (1), 592-595.

22.   Ke, B. W.; Wu, W. X.; Wei, L.; Wu, F. B.; Chen, G.; He, G.; Li, M. Y., Cell and *in vivo* imaging of fluoride ion with highly selective bioluminescent probes. *Analytical Chemistry* **2015,** *87* (18), 9110-9113.

23.   Van de Bittner, G. C.; Bertozzi, C. R.; Chang, C. J., Strategy for dual-analyte luciferin imaging: *in vivo* bioluminescence detection of hydrogen peroxide and caspase activity in a murine model of acute inflammation. *Journal of the American Chemical Society* **2013,** *135* (5), 1783-1795.

24.   Morton, R. A.; Hopkins, T. A.; Seliger, H. H., Spectroscopic properties of firefly luciferin and related compounds: an approach to product emission. *Biochemistry* **1969,** *8* (4), 1598-1607.

25.   White, E. H.; Worther, H.; Seliger, H. H.; McElroy, W. D., Amino analogs of firefly luciferin and biological activity thereof. *Journal of the American Chemical Society* **1966,** *88* (9), 2015-2019.

26.   Reddy, G. R.; Thompson, W. C.; Miller, S. C., Robust light emission from cyclic alkylaminoluciferin substrates for firefly luciferase. *Journal of the American Chemical Society* **2010,** *132* (39), 13586–13587.

27.   Sharma, D. K.; Adams, S. T.; Liebmann, K. L.; Miller, S. C., Rapid access to a broad range of 6'-substituted firefly luciferin analogues reveals surprising emitters and inhibitors. *Organic Letters* **2017,** *19* (21), 5836–5839.

28.   Ohulchanskyy, T. Y.; Donnelly, D. J.; Detty, M. R.; Prasad, P. N., Heteroatom substitution induced changes in excited-state photophysics and singlet oxygen generation in chalcogenoxanthylium dyes: effect of sulfur and selenium substitutions. *Journal of Physical Chemistry B* **2004,** *108* (25), 8668-8672.

29.   Rodriguez-Serrano, A.; Rai-Constapel, V.; Daza, M. C.; Doerr, M.; Marian, C. M., Internal heavy atom effects in phenothiazinium dyes: enhancement of intersystem crossing via vibronic spin-orbit coupling. *Physical Chemistry Chemical Physics* **2015,** *17* (17), 11350-11358.

30.   Pettersen, E. F.; Goddard, T. D.; Huang, C. C.; Couch, G. S.; Greenblatt, D. M.; Meng, E. C.; Ferrin, T. E., UCSF chimera - A visualization system for exploratory research and analysis. *Journal of Computational Chemistry* **2004,** *25* (13), 1605-1612.

31.   Pedretti, A.; Villa, L.; Vistoli, G., VEGA: a versatile program to convert, handle and visualize molecular structure on Windows-based PCs. *Journal of Molecular Graphics & Modelling* **2002,** *21* (1), 47-49.

Chapter IV: The characterization of 5',7'-difluoroluciferin as a chromophore and substrate of luciferase.

IV.1 Introduction

One of the known limitations for the luciferase-luciferin reaction is its pH dependence. The optimum pH for the reaction was initially thought to be at pH 7.8; however, a more recent evaluation determined the optimum pH to be 8.5.[1, 2] Additionally, this result showed an approximately 50% decrease of BL intensity at neutral pH, compared to pH 8.5.[1] Furthermore, numerous studies have shown that a decrease in pH decreases BL intensity and causes an emission wavelength shift from the known yellow-green (562 nm) to a red emission (616 nm) (Figure IV.1).[1, 3] As discussed in Chapter I, oxyluciferin (i.e. oxidized luciferin) can be divided into two moieties: benzothiazole and thiazol (Figure I.2). The benzothiazole moiety plays a key role in positioning luciferin in the active site, and in determining the final BL emission intensity and wavelength.[2, 4-7] Therefore, perturbations to the benzothiazole moiety, such as oxyluciferin ionic states, can directly affect the BL output.

Early investigations using luciferin analogues were devoted to studying the oxidation and kinetic mechanism of the reaction, and the variation of the BL emitted wavelength.[2, 3, 8-11]

For example, field pioneer E. White made substitutions on the benzothiazole moiety of initial luciferin analogues and showed redshifted BL emission wavelength from 6'-amino-luciferin and 4'-hydroxyl-luciferin.[2, 12] The amine substitution for the 6'-hydroxyl group provides the chromophore with an electron pair readily able to donate into the conjugated system. Thus, 6'-amino-luciferin was the first pH independent luciferin analogue that provided a redshifted BL emission.[2, 13] However, the catalytic activity of luciferase with luciferin analogues (including 6'-amino-luciferin) is known to be lower compared to luciferin.[2, 14] Fewer efforts have been dedicated to decrease the pH dependence of luciferin while aiming to recover the BL intensity at neutral pH, which is where most biology happens.
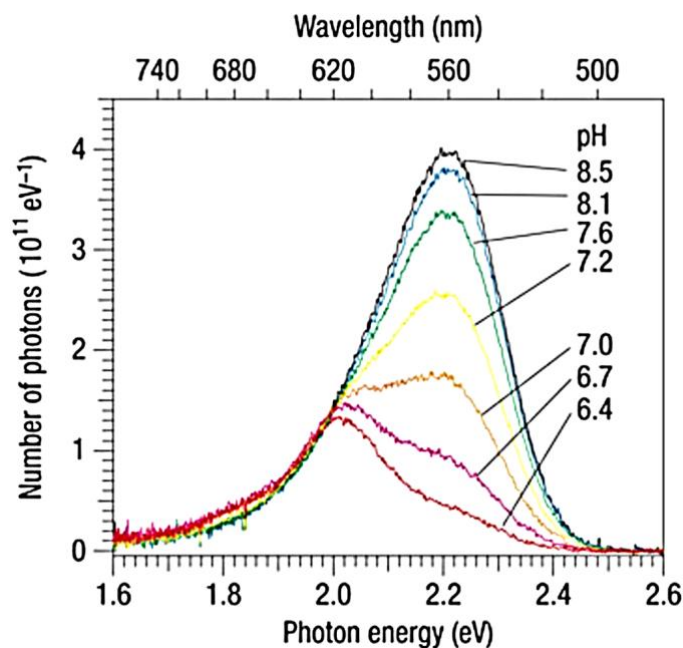
Figure IV.1 Quantitative measurement for luciferase-luciferin reaction.
Quantitative luminescence spectra for 2.98×10^{11} luciferin molecules at various pH values: black, pH 8.5; blue, pH 8.1; green, pH 7.6; yellow, pH 7.2; orange, pH 7.0; pink, pH 6.7; red, pH 6.4. The vertical axis is scaled by the absolute number of emitted photons in units of eV^{-1}. *(Figure and caption taken from Akiyama et.al, Nature Photonics, 2008)*

This chapter discusses the characterization of 5′,7′-difluoroluciferin (F_2-luciferin) as a chromophore and a substrate for luciferase. The synthesis of F_2-luciferin is discussed in the publication associated with this chapter. This analogue is designed to target the pH dependence of luciferin by decreasing its pK_A below neutral pH. We postulate that keeping the 6′-hydroxyl group ionized will decrease the pH dependence and increase the BL emission intensity for biological assay applications.

IV.2 Results

IV.2.1 *Computational pK_A for luciferin and F$_2$-luciferin.*

The premise of the F$_2$-luciferin focused on decreasing its pK_A at the 6′-hydroxyl. Therefore,

we used computational methods to corroborate a decrease in pK_A for luciferin and F$_2$-

luciferin (Figure IV.2). The calculated pK_A for the 6′-hydroxyl of luciferin was 9.2. The pK_A

predicted by the Marvin Sketch software was in resonable agreement with an

experimentally determined value of pK_A 8.7 found in the literature.[7] As expected, the

calculated pK_A for the 6′-hydroxyl from F$_2$-luciferin was lower at 6.5, which is nearly 3 log

units below luciferin's calculated pK_A. These results suggest that F$_2$-luciferin will be

ionized near or at neutral pH, which should produce a higher luminescence. The

ionization facilitates the electron donating capacity to the conjugated system which

enhances luminescence. This behavior has been described for other chromophores and

the fluorescence of luciferin.[7, 15, 16]
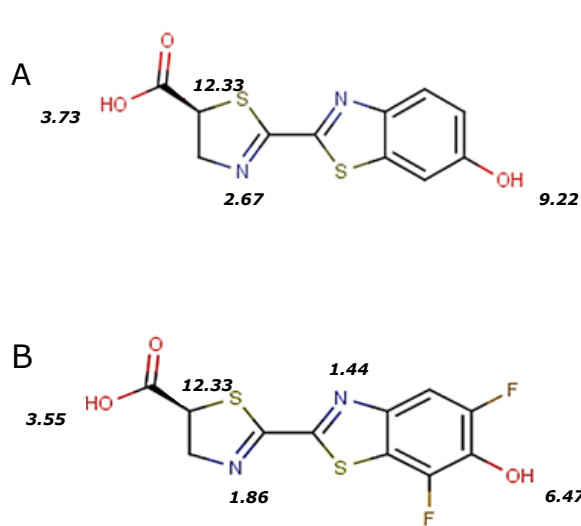
Figure IV.2 Computational pK_A for luciferin (A) and F₂-luciferin (B).
Computation was performed using the Marvin Sketch Software.

IV.2.2 *Absorbance and fluorescence spectra of luciferin and F₂-luciferin at pH 4 and pH 7.*

Previous studies have shown that the luciferin electronic properties are similar to that of the corresponding oxyluciferin. Additionally, investigating luciferin properties as a fluorophore can provide experimental insight that could help evaluate if the designed analogue will have the desired BL.[17, 18] Therefore, our next step was to carry out FL studies at an acidic and neutral pH to evaluate the capacity of F₂-luciferin to produce higher luminescence intensity compared with luciferin (Figure IV.3). We investigated acidic and neutral pH values because in acidic conditions both molecules are protonated, whereas in neutral conditions luciferin is protonated while F₂-luciferin is mostly ionized. We started

by measuring the absorbance of F_2-luciferin and luciferin to determine the absorbance λ_{max}, which was used to excite each molecule in fluorescence. Our results did not show a significant difference in absorbance maximum in the acidic environment; however, the fluorescence intensity for F_2-luciferin was twice the value compared with luciferin. In contrast, at neutral pH there was a 30 nm redshift in the absorbance maximum compared to luciferin. Impressively, the fluorescence intensity of F_2-luciferin at neutral pH was 6 times greater than luciferin. Taken together, these results indicate that F_2-luciferin is a better fluorophore at neutral pH than luciferin.
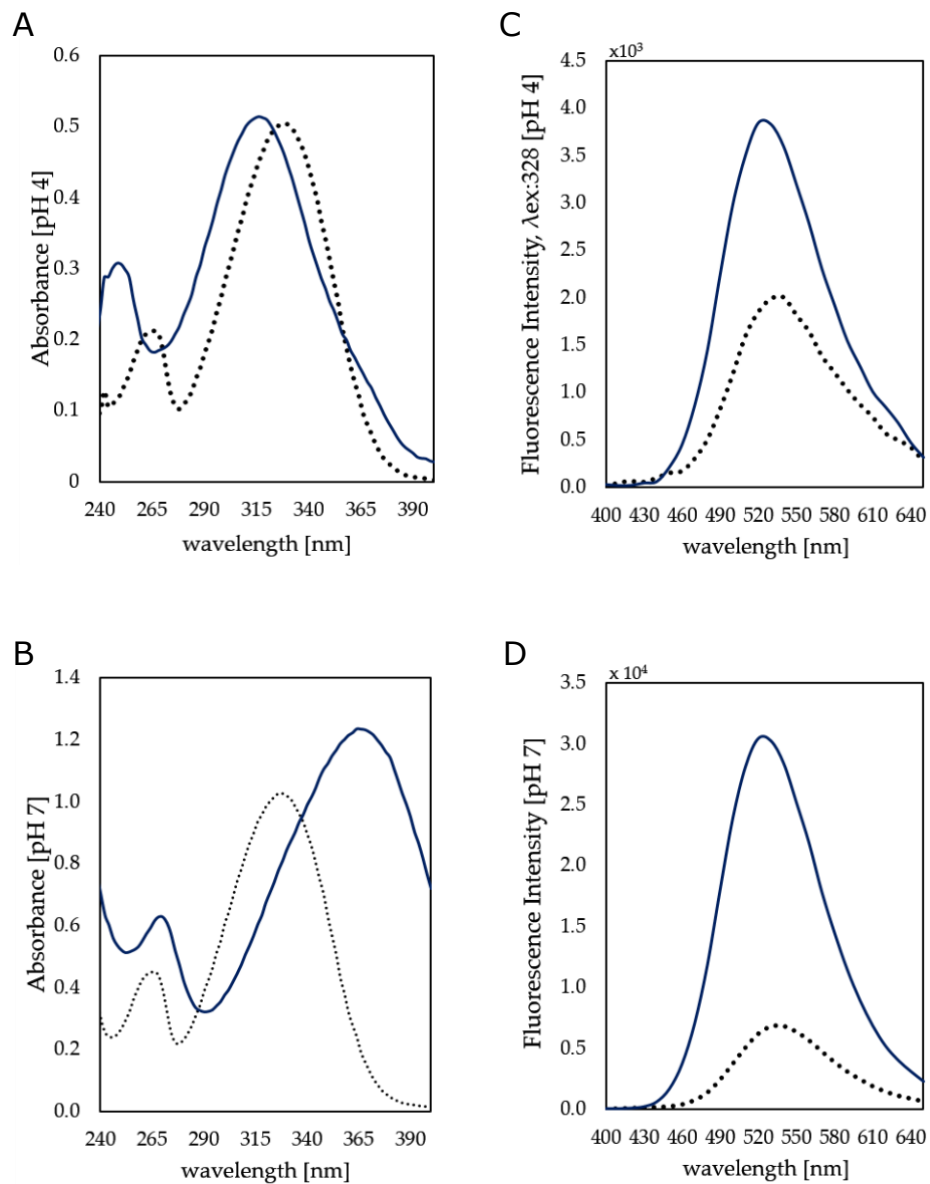
Figure IV.3 Absorbance and fluorescence spectra of luciferin (…..) and F₂-luciferin (____) at pH 4 and pH 7. Overlap of absorbance graphs at pH 4 (A), and pH 7 (B). Overlap of fluorescence graph at pH 4 (C) and pH 7 (D)

Measurements were performed with each chromophore at the same concentration in 50 mM MES buffer at the designated pH.

110

IV.2.3 *Bioluminescence intensity from luciferin and F₂-luciferin.*

After verifying that the 5′,7′ fluorination decreased the pK_A and produced a higher fluorescence at neutral pH, we evaluated the BL intensity of luciferin and F₂-luciferin at pH 5.5 to 7.8 using luciferase. (Figure IV.4) The BL intensity of luciferin showed its characteristic behavior of decreasing intensity with decreasing pH. In contrast, F₂-luciferin showed a bell-curve behavior within the pH range evaluated with optimum at 6.5. These results highlighted that optimum pH for the BL of luciferin and F₂-luciferin is in close proximity to their respective pK_A values. Furthermore, these results showed 1,000-fold drop in BL emission intensity from F₂-luciferin compared to luciferin.
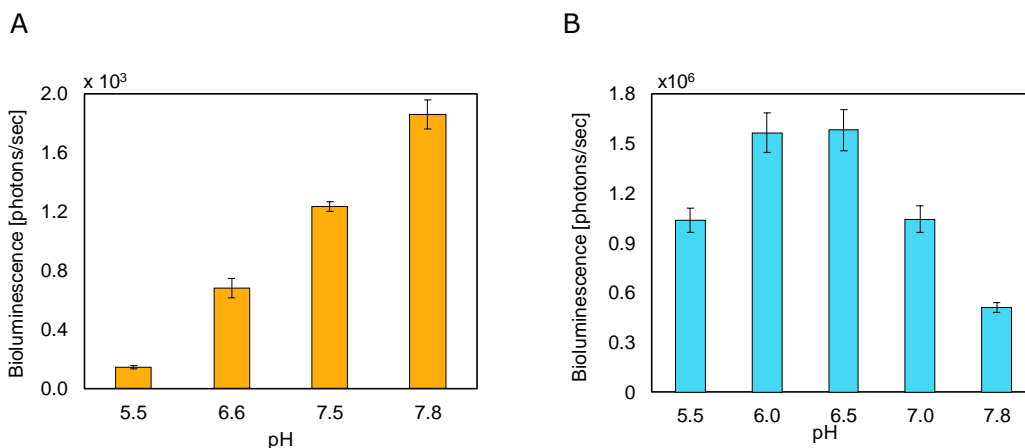
Figure IV.4 The pH dependence of the bioluminescence intensity for luciferin (A) and F₂-luciferin (B) with luciferase.
Readout was performed after manual injection of luciferase (to a final concentration of 1 nM) into a reaction mixture containing ATP, MgSO₄ buffer and either luciferin or F₂-luciferin (to a final concentration of 5 μM). Assays were performed in triplicate and error bars represent standard deviations within the replicates. The difference in the y-axis units is due to a change in the sensitivity of the instrument between the readings to detect lower BL from F₂-luciferin.

111

Luciferases that have a 67% to 80% sequence identity to the *P. pyralis* have the capacity to oxidize luciferin and produce BL.[19, 20] Among them, the luciferases from Japanese fireflies (*Luciola cruciate* and *Luciola lateralis*) have been modified to create a thermostable luciferase.[21, 22] The thermostable luciferase retains 80% of luciferase activity at 50 °C after 20 min and 65% after 60 min, which makes it a good luciferase alternative for *in vivo* studies. We evaluated the pH dependence of BL intensity of F_2-luciferin and luciferin using the thermostable luciferase (Figure IV.6). Overall, the results showed the same pattern obtained using the luciferase from *P. pyralis*. Specifically, F_2-luciferin had an optimum around pH 6 whereas the optimum for luciferin was closer to pH 8. These results suggested that the pH dependence of F_2-luciferin is consistent within *P. pyralis* and *luciola* luciferases.
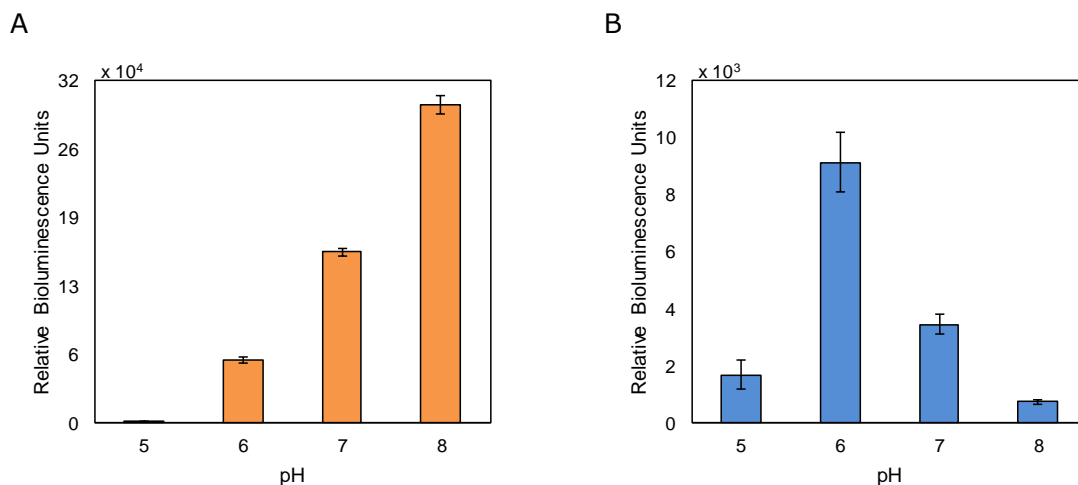
Figure IV.5 The pH dependence of the bioluminescence intensity from luciferin (A) and F₂-luciferin (B) with thermostable luciferase from Kikkoman.
Measurements were made with final concentrations of substrates at 5 μM and luciferase at 25 nM. Assays were performed in triplicate and error bars represent standard deviations within the replicates.

IV.2.4 *The pH dependence of bioluminescence emission spectra for luciferin and F₂-luciferin.*

To further characterize F₂-luciferin with luciferase we obtained the BL emission spectra at pH 5, 6, 7, 8, and compared the results with luciferin (Figure **IV**.4). At the acidic pH values of 5 and 6 the BL emission maxima were at 610 nm for both molecules. However, at pH 7 the emission maximum for F₂-luciferin was redshifted 30 nm relative to the maximum of luciferin (600 nm and 570 nm, respectively). At pH 8 the emission maxima coincided for both molecules at 560 nm, but F₂-luciferin showed a broader redshifted peak.
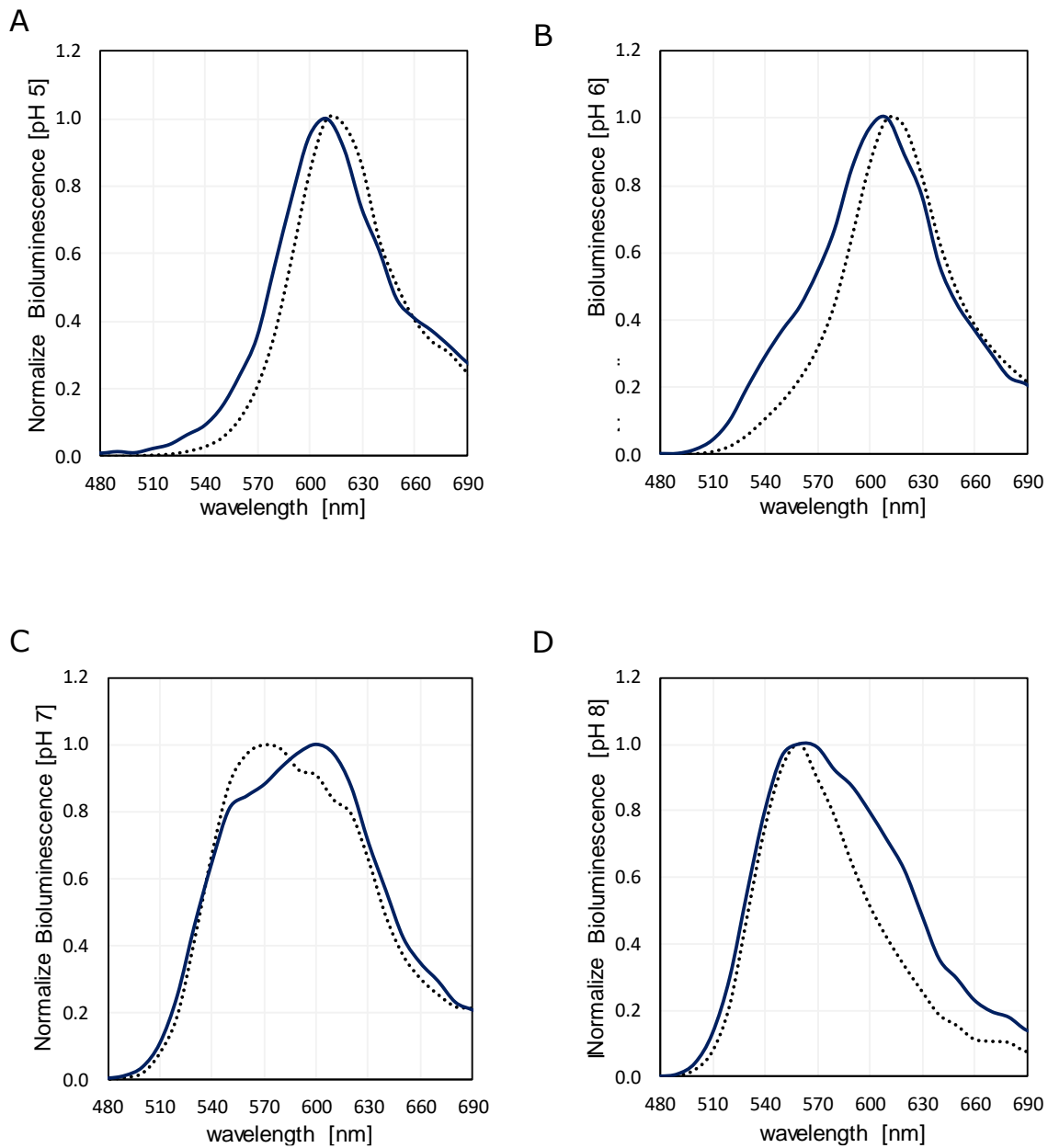
Figure IV.6 Bioluminescence spectra from luciferin (.....) and F₂-luciferin (⎯) with luciferase at pH 5 (A), pH 6 (B), pH 7 (C), pH 8 (D).

Data was normalized at λ_{max} for each chromophore for easier visualization.

IV.2.5 *Steady-state kinetic parameters for F₂-luciferin.*

Collectively, results from the pH-dependence and BL intensity experiments using F₂-luciferin as a substrate showed a decrease in BL emission compared to luciferin. As mentioned in Chapter I, most luciferin analogues in the literature tend to be poor substrates for luciferase. To evaluate the enzymatic activity of luciferase with F₂-luciferin, we determined the affinity constant (K_M) and inhibition constant (K_i). Non-linear regression analysis was used to determine the K_M of F₂-luciferase with luciferase (Figure IV.7). The K_M for F₂-luciferin was 0.73 μM at its optimal pH, whereas luciferin had a K_M of 1.34 μM.
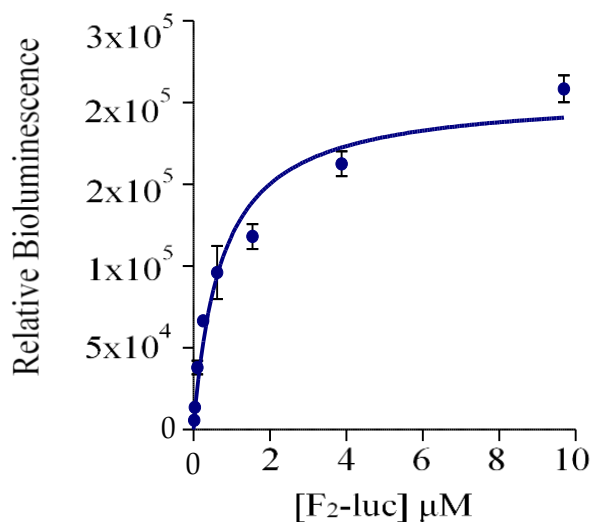
Figure IV.7 Saturation plot for determining the K_M of F₂-luciferin at pH 6.5.
The line represents the non-linear regression fit calculated through GraphPad Software.

To further investigate the interaction of luciferase with F_2-luciferin, we decided to study it as an inhibitor of luciferase (Figure IV.8). Note that this experiment is possible due to the significantly low BL from F2-luciferin at this concentration and allows its used as an inhibitor. Our results showed that increased concentrations of F_2-luciferin decreased the V_{max} of the reaction (Figure IV.8.A). The apparent K_M increased with increasing concentration of F_2-luciferin, which indicated that F_2-luciferin is a competitive inhibitor to luciferin. The calculated K_i for F_2-luciferin was 1.56 μM, which shows moderate inhibition compared to product inhibitors.
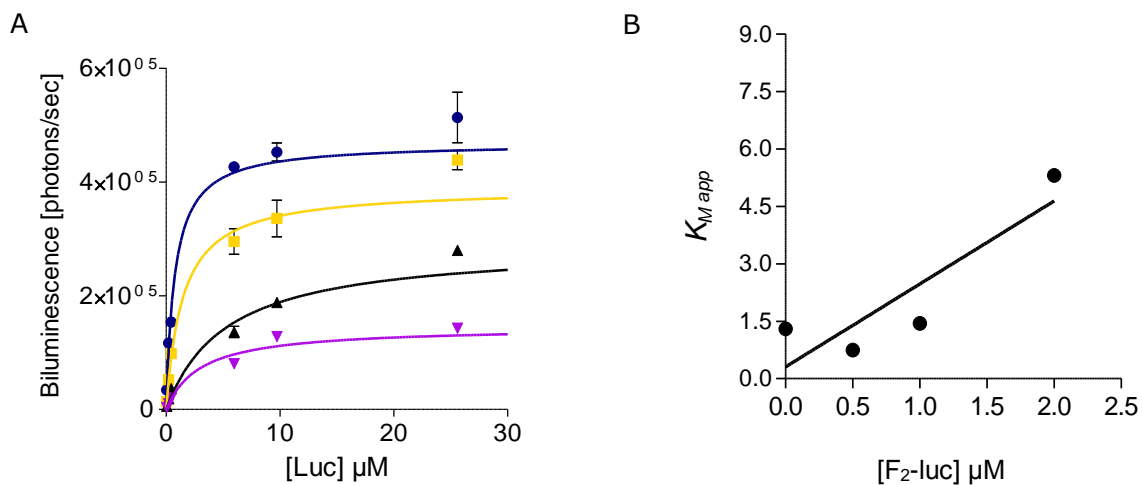
Figure IV.8 F_2-luciferin luciferase inhibition plots effect on V_{max} (A) and apparent K_M (B).
A) F2-luc concentration at 0.5 μM (●), 1 μM (■), 2 μM (▲), 10 μM (▼). Luciferin concentrations ranged from 0.1 to 25 μM. Reactions were initiated by adding luciferase to a final concentration of 1 nM to wells containing luciferin, cofactors: ATP, MgSO₄, and MOPS buffer pH 7 for final concentrations of 1.5 mM, 10 mM, and 50 mM, respectively. The lines represent the non-linear regression fit calculated through GraphPad Software. B) Plot shows calculated apparent K_M with F2-luciferin at the specific concentration used, 0.5, 1, and 2 μM. The 10 μM concentration was omitted to facilitate calculation since it induced more than 70% inhibition.

Using F_2-luciferin and luciferin at their respective experimentally determined K_M concentration and optimum pH, we compared the BL intensity emitted from each substrate. Results showed that F_2-luciferin produced 12% BL intensity relative to luciferin. The measured BL intensity for F_2-luciferin was similar to the 11% reported for 7'-fluoro-luciferin, a fluorinated luciferin analogue reported in the literature.[13] In contrast, 5'-fluoro-luciferin, another fluorinated luciferin analogue, produced 86% BL intensity relative to luciferin.[23]

Table IV.1 Steady state kinetics parameters for luciferase with luciferin and F_2-luciferin

	K_M [μM]	K_i [μM]*
luciferin	1.34	---
F_2-luciferin	0.73	1.56

* Preliminary inhibition constant determined with four concentrations of F_2-luciferin.

IV.2.6 *F_2-luciferin docking and modeling in luciferase active site.*

To further explain the decrease in catalytic activity of F_2-luciferin with luciferase, we turned to naïve docking simulations. Initially, we hypothesized that the 5' and 7' substitution of hydrogen for fluorine would not affect catalysis since both atoms are similar in size and these positions are far from to the catalytic site of the molecule (thiazoline moiety, Figure **I**.2) We compared the simulation results, from the docking model, to the crystallographic structure from the luciferase-luciferin active site. The

computational results confirmed that the 5 most energetically-favorable conformations of luciferin aligned with the reference crystal structure (Figure IV.9.A). However, the most energetically favorable conformation of luciferin did not directly overlay with the luciferin coordinates in the crystal structure (Figure IV.9.A). These results validated the model and allowed us to evaluate the docking of F_2-luciferin into the active site. The preliminary simulation for F_2-luciferin showed that the most energetically-favorable conformations did not align with the reference crystal structure (Figure IV.9.B). Instead, it showed F_2-luciferin binding in the opposite direction within the binding site. These results suggest an opportunity to design in silico the binding site of luciferase to promote F_2-luciferin use as its substrate. Further and detailed simulations are needed to evaluate the interaction within the active site and F_2-luciferin. Furthermore, simulations with F_2-luciferin, adenylated-F_2-luciferin and F_2-oxyluciferin can potentially be descriptive of the overall reaction and assist the engineering of luciferase to accept F_2-luciferin as its substrate.
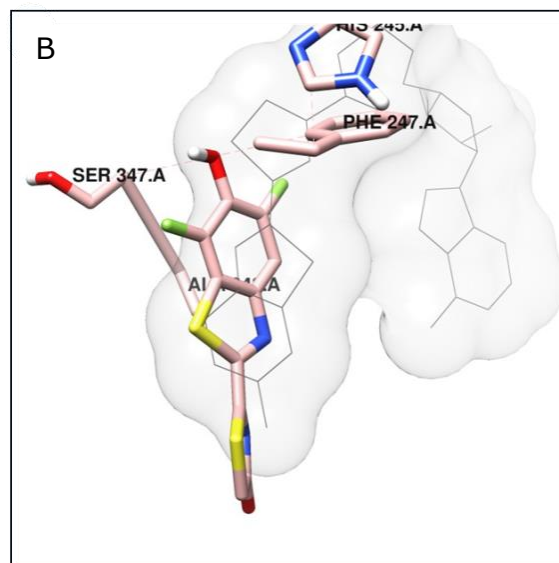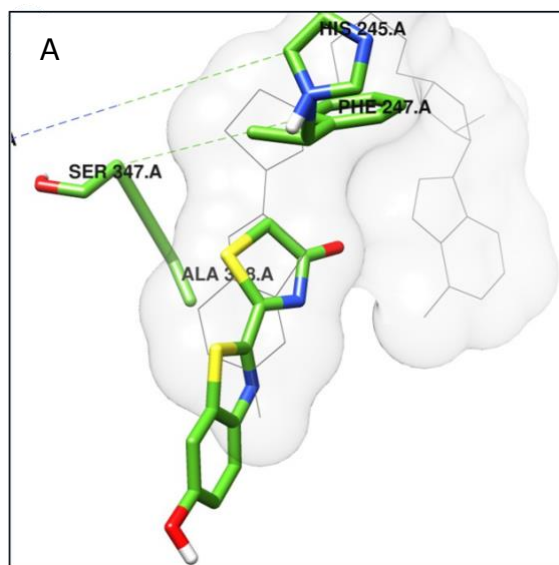
Figure IV.9 Most favorable docking conformation from luciferin (A) and F₂-luciferin (B).
PDB-ID: 4G36 was used to docked luciferin and F₂-luciferin. The gray surface area denotes the adenylated-luciferin analogue from the original PDB.

IV.3 Discussion
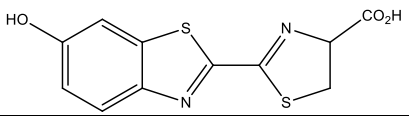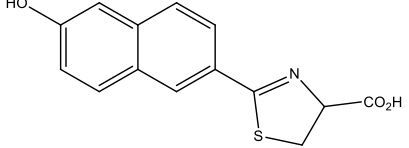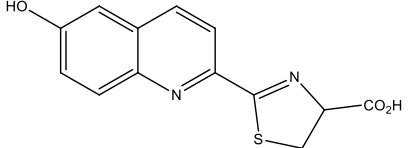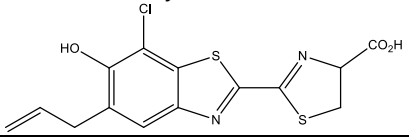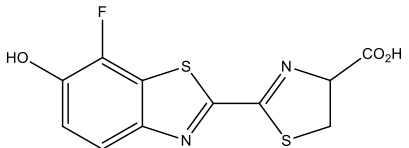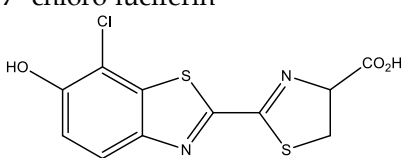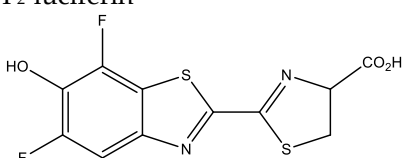
The work presented here showed the performance of F$_2$-luciferin as a substrate of luciferase for higher BL emission intensity, relative to luciferin, at neutral pH. We focused on decreasing the pK_A of the 6'-hydroxyl group in luciferin to influence the ionization behavior of the molecule at neutral pH, to provide pH independent BL emission. We verified one of our hypotheses that postulated a higher fluorescence emission intensity for F$_2$-luciferin compared with luciferin. Through studies of F$_2$-luciferin as a fluorophore we confirmed that F$_2$-luciferin was a better fluorophore at neutral pH compared with luciferin.

We found a correlation between the pK_A values of the 6'-hydroxyl groups of F$_2$-luciferin and luciferin and their optimum pH for BL. Our results showed that F$_2$-luciferin had an acidic shift in optimum (pH 6.5) relative to the luciferin (pH 7.8). Interestingly, the optimum pH for F$_2$-luciferin coincided with the computationally determined pK_A of its 6'-hydroxyl group (pK_A 6.5). To our knowledge, there is no previous report in literature suggesting an association between the pK_A of the 6'-hydroxyl group and optimum pH for BL emission. We found several luciferin analogues in the literature for which experimentally determined pK_A values and optimum pH values for BL were reported and compiled them in Table IV.2. These values suggest a relationship between pH dependence of the luciferase-luciferin reaction and the pK_A of 6'-hydroxyl group. Specifically,

naphthyl-luciferin and quinolyl-luciferin showed a strong agreement between their pK_A values (9.4 and 8.5, respectively) and their optimum pH values for BL (9.3 and 8.6, respectively).[24] Furthermore, studies with mono-fluorinated and -chlorinated luciferin analogues prepared for BL assays at acidic conditions showed a similar trend.[13] Collectively, the proposed relationship between pK_A of the 6′-hydroxyl group and optimum pH of the molecule for BL could be utilized in the development new luciferin analogues.

It has been proposed that hydrogen bonds are responsible for stabilizing the ionized 6′-hydroxyl group for the characteristic green (562 nm) BL emission from the luciferase-luciferin reaction.[25] Recently, Branchini et al. proposed the role of hydrogen bonds in the stability of the ionized 6′-hydroxyl group during the generation of the excited state.[26] In the context of the proposed pK_A-optimum pH relationship, we speculate that the hydrogen bond might play a role in the generation of the singlet excited state of oxyluciferin when the pK_A of the 6′-hydroxyl group and pH of the solution are similar. Further investigations could lead to the development of luciferin analogues with high BL intensity at desired pH values.

Table IV.2 Luciferase substrates with the pK_A of the 6′-hydroxyl and the pH for optimum BL intensity in close proximity.

	pK_A of 6′-hydroxyl	BL optimum pH	Reference
luciferin 	8.7	8.5	[1]
naphthyl-luciferin 	9.4	9.3	[24]
quinolyl-luciferin 	8.5	8.6	[24]
7′-chloro-5′allyl-luciferin 	6.7	7.0	[13]
7′-fluoro-luciferin 	7.1	8.0	[13]
7′-chloro-luciferin 	6.7	7.4	[13]
F₂-luciferin 	6.5	6.0-6.5	[27]

We highlighted the opportunity for engineering the active site of luciferase to improve functionality with luciferin analogues, especially F_2-luciferin. Results from recent studies using halogenated luciferins suggested that substitutions at the 4' and 7' positions were in close proximity to the enzyme backbone.[28] Analysis of modeling F_2-luciferin within the active site showed that the 7' fluorinated substitution is in close proximity to the protein and may impact the activity of luciferase (Figure IV.10). Alternatively, the literature suggests that a single halogenated substitution at the 5' position does not cause a drastic negative effect on the BL production with wild-type luciferase. Results from the evaluation of 5'-F, 7'-F, 5'-Br, and 7'-Br substituted luciferins showed that a substitution only at the 5' position did not have a significant effect (relative to the 7' substitution) on luciferase activity.[13, 28] Specifically, the 5' F and 5' Br substituted luciferins retained 86% and 46% luciferase activity, respectively, compared with 11% and 3% for their respective 7' substitution counterparts. We speculate that the proximity of the 7' position to the binding pocket may be involved in the reduced enzymatic activity and should be investigated further. Future work should focus on investigating permutations of any substitutions (avoiding the 7' position) in combination with a luciferase library to maximize the BL intensity of the designed chromophores.
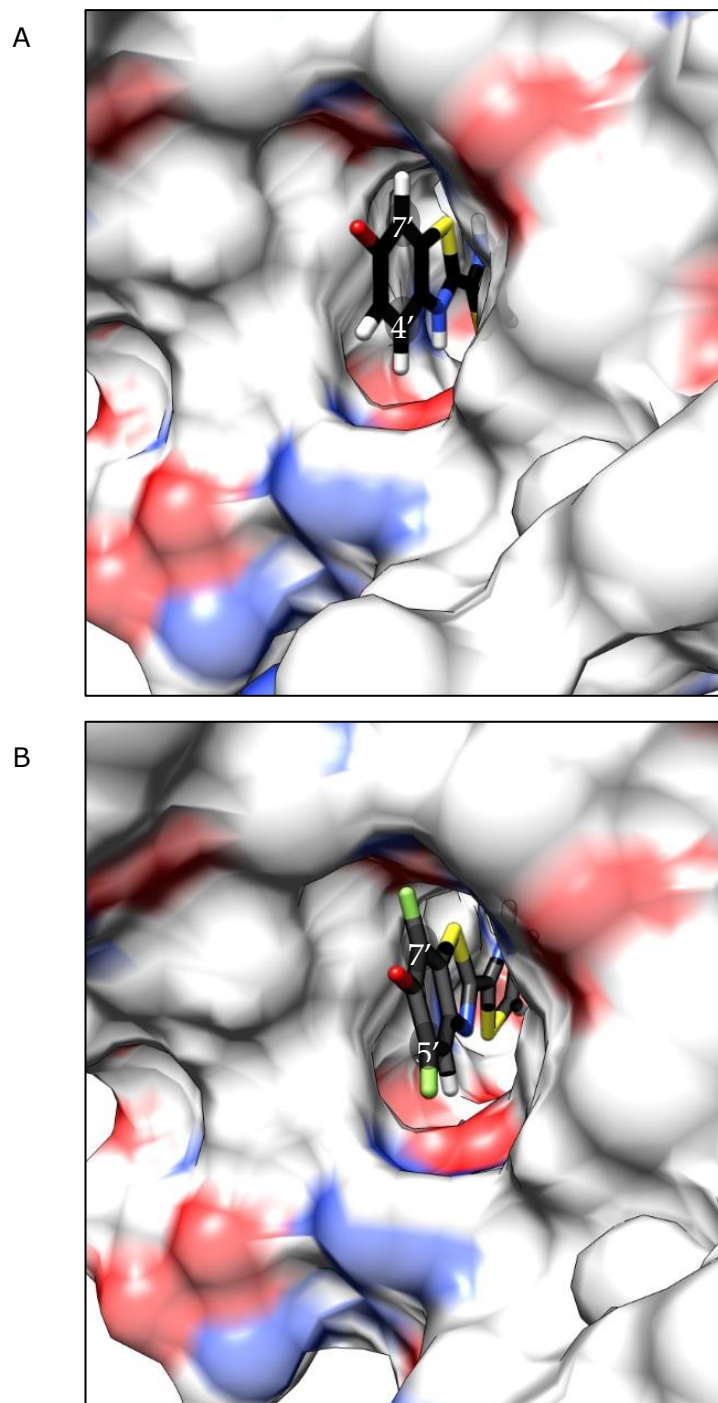
Figure IV.10 Illustration of luciferin (A) and F₂-luciferin (B) within luciferase active site.
The luciferin coordinates on the PBD-ID: 4G36 was used to position F₂-luciferin in the active site.
Illustration was developed in Chimera Software.

IV.4 Materials and methods

IV.4.1 *Materials and general methods*

Luciferin, $MgSO_4$, and ATP were obtained from Sigma-Aldrich. The luciferin analogue F_2-luciferin was synthesized by Goutam Biswas, Ph.D. in our lab; a detailed synthesis and structure characterization can be found elsewhere.[27] Prior to BL experiments, the working stock concentrations of F_2-luciferin or luciferin were determined using a Nanodrop 2000c UV-Vis spectrophotometer with 2 μL of solution. The concentrations of each molecule were calculated using the extinction coefficient of luciferin (18.2 $mM^{-1} \cdot cm^{-1}$ at 328 nm). Similarly, the concentration of luciferase was determined using a reference value for its extinction coefficient (45.6 $mM^{-1} \cdot cm^{-1}$ at 278 nm).[29-31] MOPS and MES buffer stock solutions were prepared at 1 M and stored at room temperature. Working buffer solutions were made at 0.5 M and adjusted to the designated pH using 5 M NaOH solution. Purified water (18.2 MΩ resistance) was used for all experiments. All experiments were carried out at room temperature. All experiments were run in triplicate to obtain a mean and standard deviation.

IV.4.2 *Computational pK_A*

The pK_A of the 6'-hydroxyl from luciferin and F$_2$-luciferin was calculated using the calculator plugins from Marvin Sketch 14.7.28, 2014.

IV.4.3 *Absorbance and fluorescence measurements*

The absorbance and fluorescence of luciferin and F$_2$-luciferin were measured in 20 μM MES at pH 4 (acidic) and in 10 mM MOPS at pH 7 (neutral). Absorbance and fluorescence measurements were taken for the same sample. Absorbance measurements were taken using standard 10 mm quartz cuvettes in a Cary-Vis spectrophotometer. Fluorescence measurements were taken using black 96-well plates at λ_{ex} = 328 nm and 365 nm, for luciferin and F$_2$-luciferin respectively, in a BioTek Synergy Mx microplate reader.

IV.4.4 *Assay for pH dependence of bioluminescence emission intensity and spectra*

A cocktail-mix containing the substrate (F$_2$-luciferin or luciferin) and co-factors was prepared and aliquoted into white 96-well plates. To evaluate the pH dependence, Tris-HCl was used for pH 8.0-7.0, MOPS for 6.0-6.9, and MES for pH 5.0-5.9. Final assay concentrations were: luciferin or F$_2$-luciferin, 5 μM; ATP, 1 mM; MgSO$_4$, 10 mM; and Tris-HCl, MOPS, or MES, 50 mM.

For BL emission intensity, the reactions in each well were manually initiated immediately before measurement by loading 5 μL of luciferase (final concentration, 1 nM). The plates were introduced into the Synergy Mx microplate reader, the reaction proceed for 10 minutes to reach steady state, and the BL was measured using the luminescence end-point reading in the software.

For BL emission spectra, the reactions in each well were manually initiated immediately before measurement by loading 5 μL of luciferase (final concentration, 0.2 pM to 50 nM). The spectra were collected using a BioTek Synergy Mx microplate reader. Sensitivity of the photon-multiplier-tube in the plate reader was adjusted per manufacturer specifications to optimize acquisition.

IV.4.5 *Steady state kinetics parameters for luciferin and F_2-luciferin.*

To investigate luciferin and F_2-luciferin affinity and inhibition constants the methods followed were the same as Chapter II, Section II.4.3.

IV.4.6 *Preliminary docking*

The crystal structure of luciferase and adenylated-luciferin analog from *P. pyralis* was obtained from the Protein Data Bank (PBD code 4G36) and used for docking simulations.

The amino acids of luciferase 10 Å away from the luciferin, were modeled without solvents, counterions, and substrates. Affinity grids on the active site were constructed using AutoGrid4. The isotropic grid map consisted of 40-x, y, z grid points with 0.603 Å spacing.

AutoDock4 was used to simulate docking of luciferin or F_2-luciferin into the active site of luciferase. The following constraints were used for docking: (i) the active site structure was kept rigid and the luciferin bond C3-C6 was allowed to rotate; and, (ii) five amino acids (His245, Phe247, Arg218, Ser347, Ala348) within proximity of the benzothiazoline moiety were left able to rotate and adjust to simulate some of the enzyme plasticity.[30] Docking was performed using a global genetic algorithm combined with local minimization (VEGA ZZ Software) and Lamarckian genetic algorithm to explore the ligand conformational space. Final docking conformations were clustered with a 2 Å tolerance as root mean square deviation. Of the resulting conformations, we selected those which resembled the crystal structure of the bound ligand-receptor pair.

IV.5 References

1.   Ando, Y.; Niwa, K.; Yamada, N.; Enomot, T.; Irie, T.; Kubota, H.; Ohmiya, Y.; Akiyama, H., Firefly bioluminescence quantum yield and colour change by pH-sensitive green emission. *Nature Photonics* **2008,** *2* (1), 44-47.

2.   White, E. H.; Worther, H.; Seliger, H. H.; McElroy, W. D., Amino analogs of firefly luciferin and biological activity thereof. *Journal of the American Chemical Society* **1966,** *88* (9), 2015-2019.

3.   Seliger, H. H.; McElroy, W. D., Colors of firefly bioluminescence: enzyme configuration and species specificity. *Proceedings of the National Academy of Sciences of the United States of America* **1964,** *52* (1), 75-81.

4.   Branchini, B. R.; Hayward, M. M.; Bamford, S.; Brennan, P. M.; Lajiness, E. J., Naphthyluciferin and quinolyluciferin - green and red light emitting firefly luciferin analogs. *Photochemistry and Photobiology* **1989,** *49* (5), 689-695.

5.   White, E. H.; Worther, H.; Field, G. F.; McElroy, W. D., Analogs of firefly luciferin. *Journal of Organic Chemistry* **1965,** *30* (7), 2344-2348.

6.   Denburg, J. L.; Lee, R. T.; McElroy, W. D., Substrate-binding properties of firefly luciferase: I. luciferin-binding site. *Archives of Biochemistry and Biophysics* **1969,** *134* (2), 381-394.

7.   Morton, R. A.; Hopkins, T. A.; Seliger, H. H., Spectroscopic properties of firefly luciferin and related compounds: an approach to product emission. *Biochemistry* **1969,** *8* (4), 1598-1607.

8.   Rhodes, W. C.; McElroy, W. D., Synthesis and function of adenyl-luciferin and adenyl-oxyluciferin. *Federation Proceedings* **1958,** *17* (1), 295-295.

9.   Seliger, H. H.; McElroy, W. D., Spectral emission and quantum yield of firefly bioluminescence. *Archives of Biochemistry and Biophysics* **1960,** *88* (1), 136-141.

10.   Seliger, H. H.; McElroy, W. D.; Field, G. F.; White, E. H., Stereospecificity and firefly bioluminescence, a comparison of natural and synthetic luciferins. *Proceedings of the National Academy of Sciences of the United States of America* **1961,** *47* (7), 1129-1134.

11.   Seliger, H. H.; McElroy, W. D., Chemiluminescence of firefly luciferin without enzyme. *Science* **1962,** *138* (3541), 683-685.

12.   White, E. H.; Worther, H., Analogs of firefly luciferin .3. *Journal of Organic Chemistry* **1966,** *31* (5), 1484-1488.

13.   Takakura, H.; Kojima, R.; Ozawa, T.; Nagano, T.; Urano, Y., Development of 5 '- and 7 '-substituted luciferin analogues as acid-tolerant substrates of firefly luciferase. *Chembiochem* **2012,** *13* (10), 1424-1427.

14.   Reddy, G. R.; Thompson, W. C.; Miller, S. C., Robust light emission from cyclic alkylaminoluciferin substrates for firefly luciferase. *Journal of the American Chemical Society* **2010,** *132* (39), 13586–13587.

15.   Sun, W. C.; Gee, K. R.; Klaubert, D. H.; Haugland, R. P., Synthesis of fluorinated fluoresceins. *Journal of Organic Chemistry* **1997,** *62* (19), 6469-6475.

16.   Sun, W. C.; Gee, K. R.; Haugland, R. P., Synthesis of novel fluorinated coumarins: excellent UV-light excitable fluorescent dyes. *Bioorganic & Medicinal Chemistry Letters* **1998,** *8* (22), 3107-3110.

17.   Kakiuchi, M.; Ito, S.; Yamaji, M.; Viviani, V. R.; Maki, S.; Hirano, T., Spectroscopic properties of amine-substituted analogues of firefly luciferin and oxyluciferin. *Photochemistry and Photobiology* **2017,** *93* (2), 486-494.

18.   Gandelman, O. A.; Brovko, L. Y.; Ugarova, N. N.; Chikishev, A. Y.; Shkurimov, A. P., Oxyluciferin fluorescence is a model of native bioluminescence in the firefly luciferin luciferase system. *Journal of Photochemistry and Photobiology B-Biology* **1993,** *19* (3), 187-191.

19.   Kajiyama, N.; Nakano, E., Isolation and characterization of mutants of firefly luciferase which produce different colors of light. *Protein Engineering* **1991,** *4* (6), 691-693.

20.   Kajiyama, N.;   Masuda, T.;   Tatsumi, H.; Nakano, E., Purification and characterization of luciferases from fireflies, *Luciola cruciata* and *Luciola lateralis*. *Biochimica Et Biophysica Acta* **1992,** *1120* (2), 228-232.

21.   Hirokawa, K.;   Kajiyama, N.; Murakami, S., Improved practical usefulness of firefly luciferase by gene chimerization and random mutagenesis. *Biochimica Et Biophysica Acta-Protein Structure and Molecular Enzymology* **2002,** *1597* (2), 271-279.

22.   Naoki Kajiyama, E. N. Thermostable luciferase of firefly, thermostable luciferase gene of firefly, novel recombinant DNA, and process for the preparation of thermostable luciferase of firefly. US patent 5,229,285 filed June 23, 1992 and issued July 20,. 1993.

23.   Valley, M. P.;   Cali, J. J.;   Binkowski, B.;   Eggers, C. T.; Wood, K. V., Stabilized formulation for luminescent detection of luciferase and nucleoside phosphates. US patent 9,487,814 B2 filed February 21, 2014 and issued November 8,. **2016**.

24.   Branchini, B. R.;   Hayward, M. M.;   Bamford, S.;   Brennan, P. M.; Lajiness, E. J., Naphthyluciferin and quinolyluciferin - green and red light emitting firefly luciferin analogs. *Photochemistry and Photobiology* **1989,** *49* (5).

25.   Viviani, V. R.;   Simoes, A.;   Bevilaqua, V. R.;   Gabriel, G. V. M.;   Arnoldi, F. G. C.; Hirano, T., Glu311 and Arg337 stabilize a closed active-site conformation and provide a critical catalytic base and countercation for green bioluminescence in beetle luciferases. *Biochemistry* **2016,** *55* (34), 4764-4776.

26.   Branchini, B. R.;   Southworth, T. L.;   Fontaine, D. M.;   Murtiashaw, M. H.;   McGurk, A.;   Talukder, M. H.;   Qureshi, R.;   Yetil, D.;   Sundlov, J. A.; Gulick, A. M., Cloning of the orange light-producing luciferase from *Photinus scintillans*, a new proposal on how bioluminescence color is determined. *Photochemistry and Photobiology* **2017,** *93* (2), 479-485.

27.   Pirrung, M. C.;   Biswas, G.;   De Howitt, N.; Liao, J., Synthesis and bioluminescence of difluoroluciferin. *Bioorganic & Medicinal Chemistry Letters* **2014,** *24* (20), 4881-4883.

28.   Steinhardt, R. C.; Rathbun, C. M.; Krull, B. T.; Yu, J. M.; Yang, Y.; Nguyen, B. D.; Kwon, J.; McCutcheon, D. C.; Jones, K. A.; Furche, F.; Prescher, J. A., Brominated luciferins are versatile bioluminescent probes. *Chembiochem* **2017,** *18* (1), 96-100.

29.   Green, A. A.; McElroy, W. D., Crystalline firefly luciferase. *Biochimica Et Biophysica Acta* **1956,** *20* (1), 170-176.

30.   Branchini, B. R.; Magyar, R. A.; Marcantonio, K. M.; Newberry, K. J.; Stroh, J. G.; Hinz, L. K.; Murtiashaw, M. H., Identification of a firefly luciferase active site peptide using a benzophenone-based photooxidation reagent. *Journal of Biological Chemistry* **1997,** *272* (31), 19359-19364.

31.   Fraga, H.; Fernandes, D.; Novotny, J.; Fontes, R.; da Silva, J. C. G., Firefly luciferase produces hydrogen peroxide as a coproduct in dehydroluciferyl adenylate formation. *Chembiochem* **2006,** *7* (6), 929-935.

Chapter V: The characterization of iodinated oxyluciferin analogues as sensitizers of molecular oxygen.

V.1 Introduction

Efforts in the luciferase-luciferin system are focused on creating versatile luciferase-luciferin pairs that broaden the scope for cell and molecular research. Currently, most of the technology developed for cell and molecular research is based on external energy excitation of chromophores. Indeed, there are applications where external energy excitation remains the method of choice, e.g. generating singlet oxygen ($^1O_2$); however, these applications also present an opportunity to implement the luciferase-luciferin system. Many studies have shown that $^1O_2$ is an important intermediate in the detrimental oxidation of biomolecules, which has great potential for targeted biomolecule removal strategies.[1, 2] In fact, the generation of $^1O_2$ within cells has been broadly used for cell ablation (i.e. selective cell death).[3-6] Cell ablation is used to investigate the role of a cell within a given environment. This technique expands the knock-out gene strategy where, instead of determining the role of an absent gene, the absence of ablated cell(s) is investigated. Selective killing of cells has been useful to investigate cell and tissue development or function.[3, 7-14] Thus, the unprecedented use of the BL reaction to produce $^1O_2$ could help broaden the scope of BL.

133

Localization of $^1O_2$ is a key challenge in cell ablation studies. The high reactivity, high cytotoxicity, and short life of $^1O_2$ detrimentally reacts with any biomolecule within a 20-nanometer radius from where it is generated.[15-17] Photodynamic therapy (PDT), a cell ablation application, relies on generating $^1O_2$ within cells and is currently used to kill cancer cells.[18-20] PDT uses a photosensitizer that, upon excitation, undergoes intersystem crossing to triplet excited state and interacts with molecular oxygen to form $^1O_2$.[6, 21, 22] Known challenges for PDT are target specificity and localized delivery of the photosensitizers in order to avoid affecting healthy cells or tissue.[23] Furthermore, PDT faces the challenge associated with light penetration through tissue to excite the photosensitizer, which limits its applications to superficial treatments. A homolog of green fluorescent protein, KillerRed, was the first fully genetically-encoded photosensitizer described to kill 40-60% HEK293T cells upon excitation *in vitro*. Follow-up studies focused on developing fluorescence-based genetically-encoded probes to increase the generation of $^1O_2$ per excitation period.[4, 24-27]

Currently, the available probes capable of producing $^1O_2$ to selectively kill cells need an external energy source, such as laser excitation or energy transfer, to excite a photosensitizer. For example, probes have used the energy from the BL reaction to excite hypericin and Rose Bengal photosensitizers.[28-31] Carpenter et al. reported that BL induced activation of hypericin had an antiviral effect on equine infectious anemia virus. Similarly, Theodossiou et al. investigated excitation of Rose Bengal by BL for PDT on cancer cells *in*

vitro. They reported that luciferase-expressing-cancer-cells incubated with Rose Bengal (3 hours at 10 µM) and subjected to BL for 24 hours showed approximately 75% decrease in cell survival. Furthermore, in a more recent study, Yun et al. used a *Renilla* luciferase mutant (RLuc8.6) and Rose Bengal to produce $^1O_2$ through bioluminescence resonance energy transfer (BRET). The authors conjugated 2-5 molecules of RLuc8.6 and 2 Rose Bengal molecules to bovine serum albumin (BSA), verified the production of $^1O_2$ using singlet oxygen sensor green (SOSG), and utilized a cell-penetrating-peptide delivery system to facilitate cell internalization of the conjugate. SOSG is commonly used to probe $^1O_2$ since the FL of SOSG is proportional to $^1O_2$ concentration. The results from this study showed a 40% decrease in cell survival from the BRET-produced $^1O_2$. Similarly, Wu et al. demonstrated the potential of PDT using BRET with *P. pyralis* luciferase linked to a biodegradable nanoparticle carrying Rose Bengal, which significantly decreased tumor growth *in vivo*.[31] Despite the efficacy shown, these systems are limited by the complexity of the photosensitizer systems as well as the energy transfer mechanisms.

Here we take preliminary steps for the concept of luciferase-luciferin reaction system that could generate highly localized $^1O_2$ through a genetically encoded probe. To our knowledge, the development of a firefly luciferin analogue to produce $^1O_2$ is unknown. We envisioned a 5′,7′-diiodo-luciferin (I_2-luciferin) to promote intersystem crossing from an excited singlet state into a triplet excited state when oxidized to 5′,7′-diiodo-oxyluciferin (I_2-oxyluciferin) by luciferase. We hypothesized that a double iodination to

oxyluciferin could provide the "heavy atom effect" that promotes intersystem crossing and generate triplet state emission.[32] Ideally, the energy from the triplet excited state of I_2-oxyluciferin is transferred directly to molecular oxygen in the triplet ground state, resulting in the production of $^1O_2$. Compared with previous strategies that involve BL to produce $^1O_2$, our system reduces the convoluted challenges associated with multi-molecule conjugates and multi-step energy transfer processes. Furthermore, our system also avoids known challenges of current $^1O_2$ sensitizers: energy transfer for excitation, photobleaching, and intracellular delivery of a conjugated molecules. We started our work with I_2-oxyluciferin to help pave the road to develop luciferin analogue 5',7'-diiodoluciferin (I_2-luciferin) and the necessary mutated luciferase to maximize the production of $^1O_2$ using a luciferase-luciferin pair.[33]

We designed and synthesized additional oxyluciferins to systematically evaluate the production of $^1O_2$. First, a known challenge with oxyluciferin is its triple chemical equilibrium, where six different ionization states of the molecule are possible. However, the current accepted emitter from the BL reaction is the keto-phenolate. Therefore, we designed and synthesized 5,5-dimethyl-5',7'-diiodo-oxyluciferin (Me_2-I_2-oxyluciferin) which constrains the molecule to the keto form. Second, recent studies showed that luciferin analogues with bromine substitutions at the C5' or C7' lose approximately 97% or 54%, respectively, of luciferase activity (see Chapter 4, Section VI.3). Likewise, Prescher et al. suggested that luciferin analogues with single C4' or C7' substitutions lose

approximately 90% of activity with luciferase.[34] Thus, there was also motivation to study the production of $^1O_2$ caused by a single iodine substitution on oxyluciferin in addition to the double-substituted I_2-oxyluciferin. We also synthesized 7'-iodo-oxyluciferin (I-oxyluciferin). The synthesis of 5'-iodo-oxyluciferin and of the dimethylated derivative of I-oxyluciferin is more challenging but should also be studied in the future.

In this study, we systematically evaluated the production of $^1O_2$ by several oxyluciferins under UV irradiation to identify key molecular aspects that influence production of $^1O_2$. Figure **V**.1 shows the molecular structure of oxyluciferin and the oxyluciferins discussed in this Chapter. We used a photoreactor to irradiate oxyluciferins, rather than using luciferase to convert the the luciferin analogues to oxyluciferin, to simplify the production of $^1O_2$ and to demonstrate proof-of-concept. Our results showed that I_2-oxyluciferin, Me_2-I_2-oxyluciferin, and I-oxyluciferin produced $^1O_2$ when irradiated. Furthermore, $^1O_2$ production was highest with Me_2-I_2-oxyluciferin compared with the other oxyluciferins evaluated. Our results from iodinated oxyluciferins demonstrated a first step towards the development of iodinated luciferin analogues.

oxyluciferin

5',7'-diiodo-oxyluciferin

5,5-dimethyl-5',7'-diiodo-oxyluciferin

7'-iodo-oxyluciferin
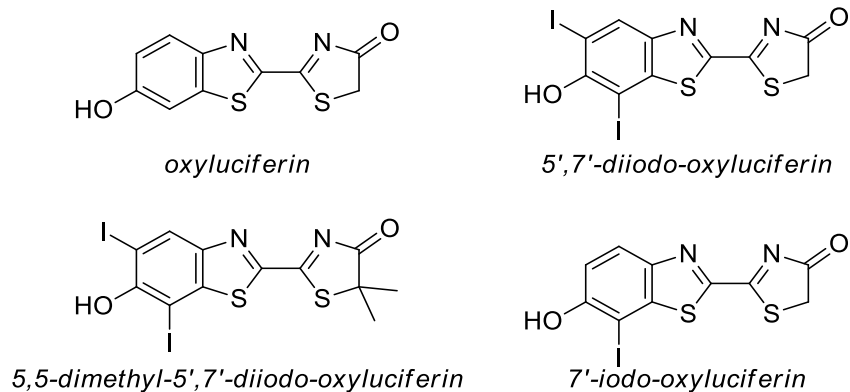
Figure V.1 Chemical structures of oxyluciferin, I$_2$-oxyluciferin, Me$_2$-I$_2$-oxyluciferin, and I-oxyluciferin.

V.2 Results

We studied the optical properties of three oxyluciferin analogues: I$_2$-oxyluciferin, Me$_2$-I$_2$-oxyluciferin, and I-oxyluciferin, to evaluate the heavy atom effect conferred by the iodine substitution. The iodine substitution should promote intersystem crossing followed by energy transfer to molecular oxygen from the excited triplet state. The effect on the FL emission spectra of the oxyluciferin analogues and sensitization of molecular oxygen was used to study relaxation from the triplet state. Alternatively, emission from the triplet state can occur competitively through phosphorescence. Thus, the emission spectra were also analyzed for phosphorescence and the ability to sensitize $^1O_2$.

V.2.1 *Keto-enol tautomerization analysis of I$_2$-oxyluciferin and Me$_2$-I$_2$-oxyluciferin by ^{1}H NMR.*

We started work with I$_2$-oxyluciferin by verifying its chemical form and by investigating the keto-enol tautomerization using the ^{1}H NMR method established by Naumov et al. Naumov et al. used the integration of the 5-C<u>H</u> singlet peaks at 4 and 6 ppm for the keto and enol forms, respectively, and quantified a keto-to-enol ratio for oxyluciferin.[35] In acetonitrile, a polar aprotic solvent, Naumov et al. reported 40% keto form of oxyluciferin, which was the highest percentage among all solvents evaluated. We obtained ^{1}H NMR spectra for I$_2$-oxyluciferin and confirmed single peaks around 4 and 6 ppm (Figure **V.2**). Integration of 2H peak at 4.11 ppm resulted in 0.18 per proton, whereas integration of the 6.48 ppm peak resulted in 0.97. Thus, the keto-to-enol ratio corresponded to 0.18:0.97 or approximately 20% keto to 80% enol form of I$_2$-oxyluciferin in our solution. Since our goal was to study the optical properties of the I$_2$-oxyluciferin analogue in its emitter form, we also synthesized and characterized Me$_2$-I$_2$-oxyluciferin. The Me$_2$-I$_2$-oxyluciferin enabled us to study the molecule in its emitter form. Thus, we characterized the optical properties of both I$_2$-oxyluciferin and Me$_2$-I$_2$-oxyluciferin as well as their ability to generate singlet oxygen.
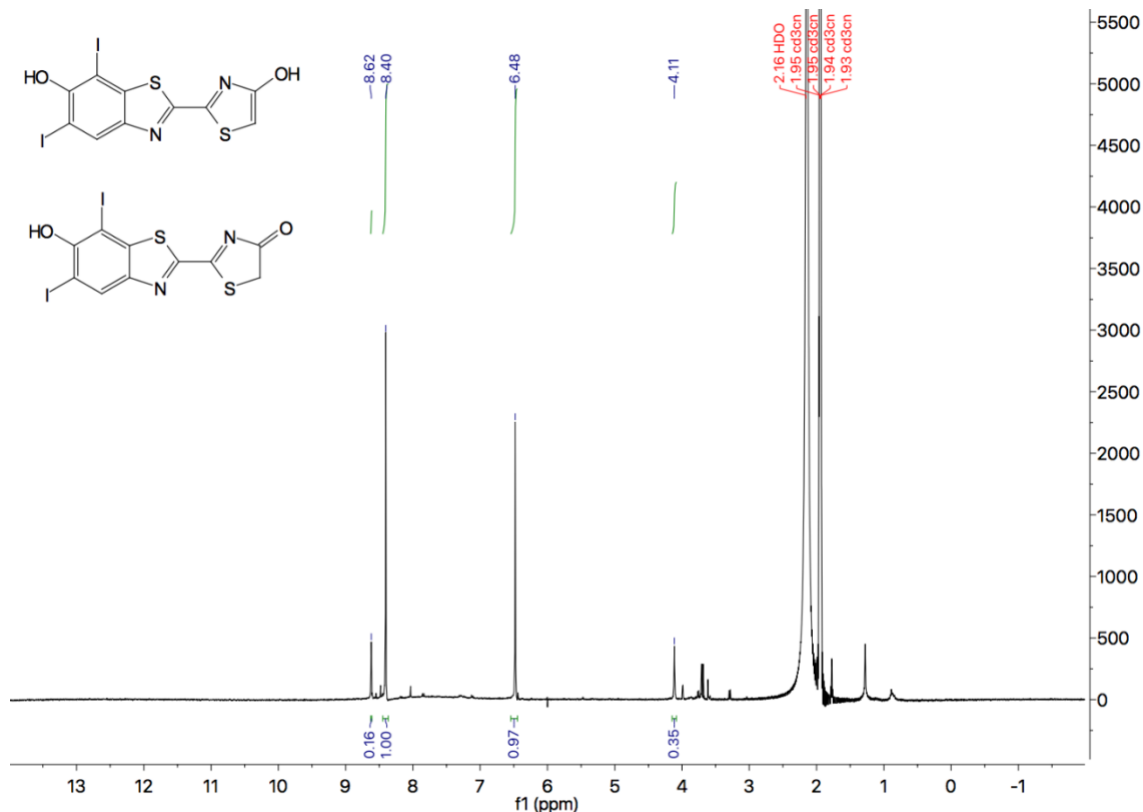
Figure V.2 ¹H NMR spectrum of I₂-oxyluciferin in acetonitrile-d₃.

V.2.2 *Absorbance spectra of oxyluciferin, I₂-oxyluciferin, Me₂-I₂-oxyluciferin, and I-oxyluciferin.*

We measured the absorbance of our oxyluciferin analogues in acetonitrile since it favors the keto form of oxyluciferin, I₂-oxyluciferin, and I-oxyluciferin. Our results showed a similar trend to oxyluciferin, the absorbance of the iodinated oxyluciferin analogues shows a small hypsochromic shift of the analogues relative to oxyluciferin (Figure **V**.3). The absorbance λ_{max} were: 369 nm for oxyluciferin (Figure **V**.3, A), 368 nm for I₂-

oxyluciferin ((Figure **V**.3, B), 364 nm for Me$_2$-I$_2$-oxyluciferin (Figure **V**.3, C), and 366 nm for I-oxyluciferin (Figure **V**.3, D). Thus, the iodinated oxyluciferin analogues did not show a significant difference in λ_{max} compared with oxyluciferin. The absorbance intensity of Me$_2$-I$_2$-oxyluciferin (Figure **V**.3, C) showed a decrease compared with the other oxyluciferins. To continue characterization of the iodinated oxyluciferin analogues, the absorbance maximum for each molecule was used to excite FL emission and $^1O_2$ production studies. Table **V**.1 summarizes the absorbance λ_{max} of each molecule.
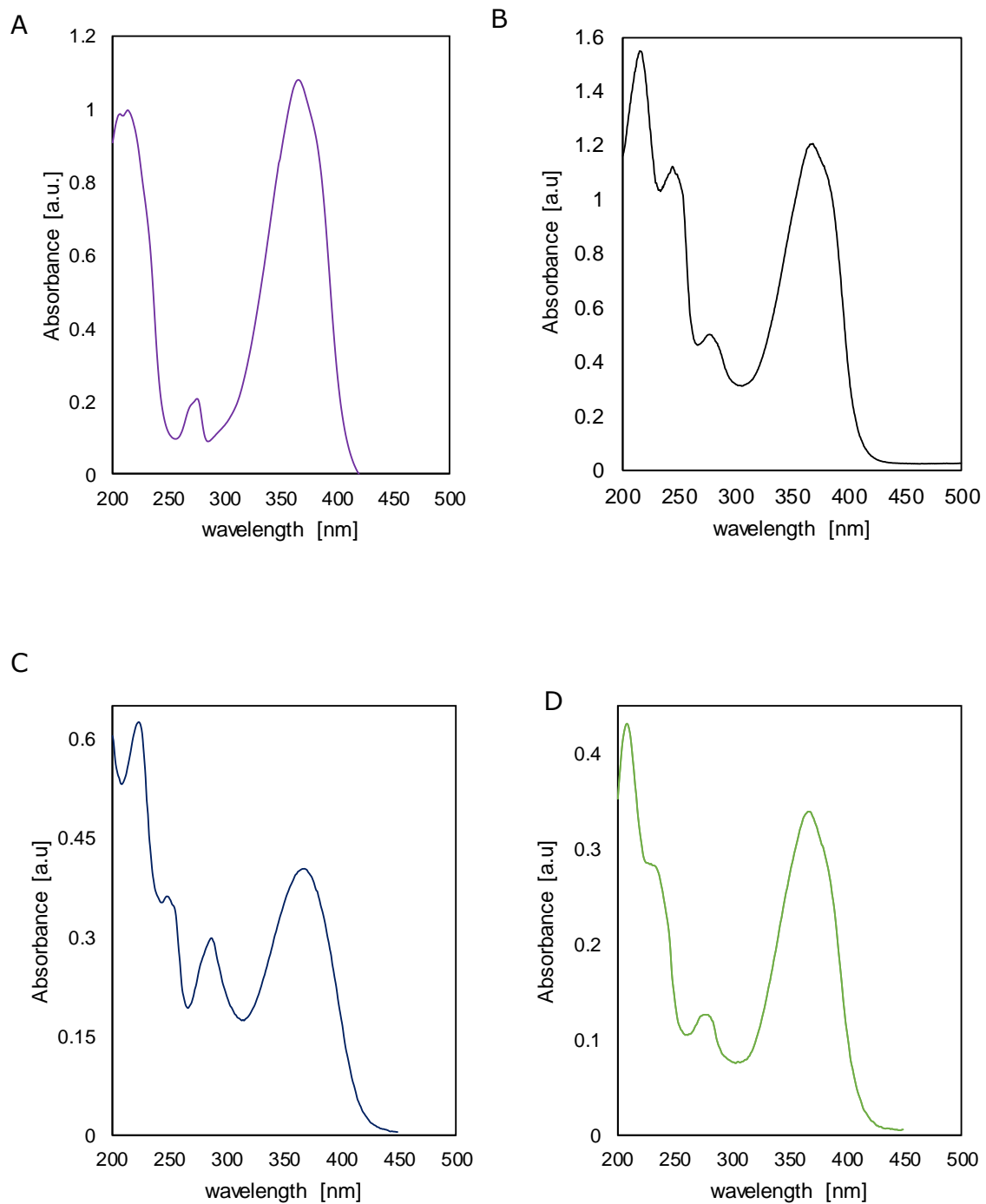
Figure V.3 Absorbance spectra for oxyluciferin (A), I$_2$-oxyluciferin (B), Me$_2$-I$_2$-oxyluciferin (C), I-oxyluciferin (D) in acetonitrile.

The concentration for all molecules was 50 μM.

V.2.3 *Fluorescence emission of oxyluciferin, I$_2$-oxyluciferin and Me$_2$-I$_2$-oxyluciferin.*

We studied the FL emission of our oxyluciferin analogues for indication of the heavy atom effect induced by the iodine substitution. Emission from the triplet state can be identified by a bathochromic shift, a phosphorescence signal, and a reduce emission intensity. Therefore, we evaluated the FL emission of I$_2$-oxyluciferin and Me$_2$-I$_2$-oxyluciferin in acetonitrile. Characterization of the FL emission of I-oxyluciferin was omitted since it was synthesized specifically to evaluate $^1O_2$ production. The FL spectra showed that I$_2$-oxyluciferin and Me$_2$-I$_2$-oxyluciferin lost a significant amount of FL emission intensity compared with oxyluciferin. (Figure **V**.4) Since the FL emission of Me$_2$-I$_2$-oxyluciferin was weak, we increased the integration time and slit opening to obtain finer detail of the spectral characteristics. The spectrum for each molecule was then normalized to facilitate comparison. Results for the normalized spectra showed a bathochromic shift of 34 nm in the emission maximum for Me$_2$-I$_2$-oxyluciferin compared with oxyluciferin. (Figure **V**.5) In contrast, the emission maximum for I$_2$-oxyluciferin overlapped with oxyluciferin. Furthermore, the emission spectrum for Me$_2$-I$_2$-oxyluciferin had a broader maximum peak compared with oxyluciferin and I$_2$-oxyluciferin. A peak at 738 nm was seen for Me$_2$-I$_2$-oxyluciferin, but not for oxyluciferin, and only an extremely small trace obtained for I$_2$-oxyluciferin. (Figure **V**.5)
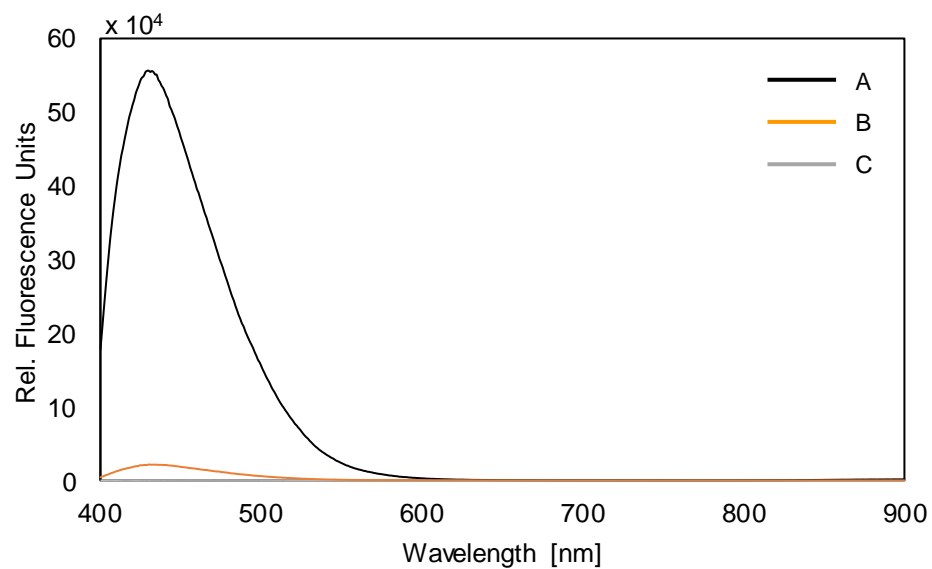
Figure V.4 Fluorescence emission spectra for oxyluciferin (A), I$_2$-oxyluciferin (B), and Me$_2$-I$_2$-oxyluciferin (C) in acetonitrile.
The concentration for all molecules was 50 μM.
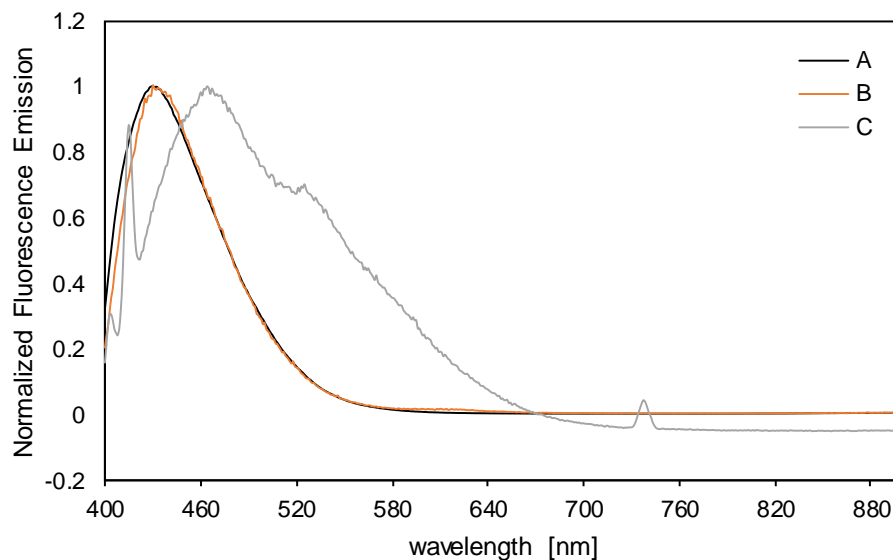
Figure V.5 Normalized fluorescence emission spectra for oxyluciferin (A), I$_2$-oxyluciferin (B), and Me$_2$-I$_2$-oxyluciferin (C) in acetonitrile.
The spectrum for Me$_2$-I$_2$-oxyluciferin was obtained using increased integration time and slit opening. The concentration for all molecules was 50 μM.

Subsequently, we investigated the FL emission of I$_2$-oxyluciferin in oxygen-free solvent to eliminate the possibility of interaction of the excited triplet state with dissolved molecular oxygen, by using acetonitrile that had been bubbled with nitrogen. Results for the FL emission of I$_2$-oxyluciferin showed a similar emission peak at 430 nm in both acetonitrile and deoxygenated acetonitrile but higher intensity in acetonitrile. (Figure **V**.6, A) In contrast, shoulder peaks at approximate 612 nm and 738 nm had an increase in emission intensity when measured in deoxygenated acetonitrile. (Figure **V**.6, B) We speculate that these bathochromic peaks could come from either a weak phosphorescence or an overtone from the monochromator of the instrument.

145
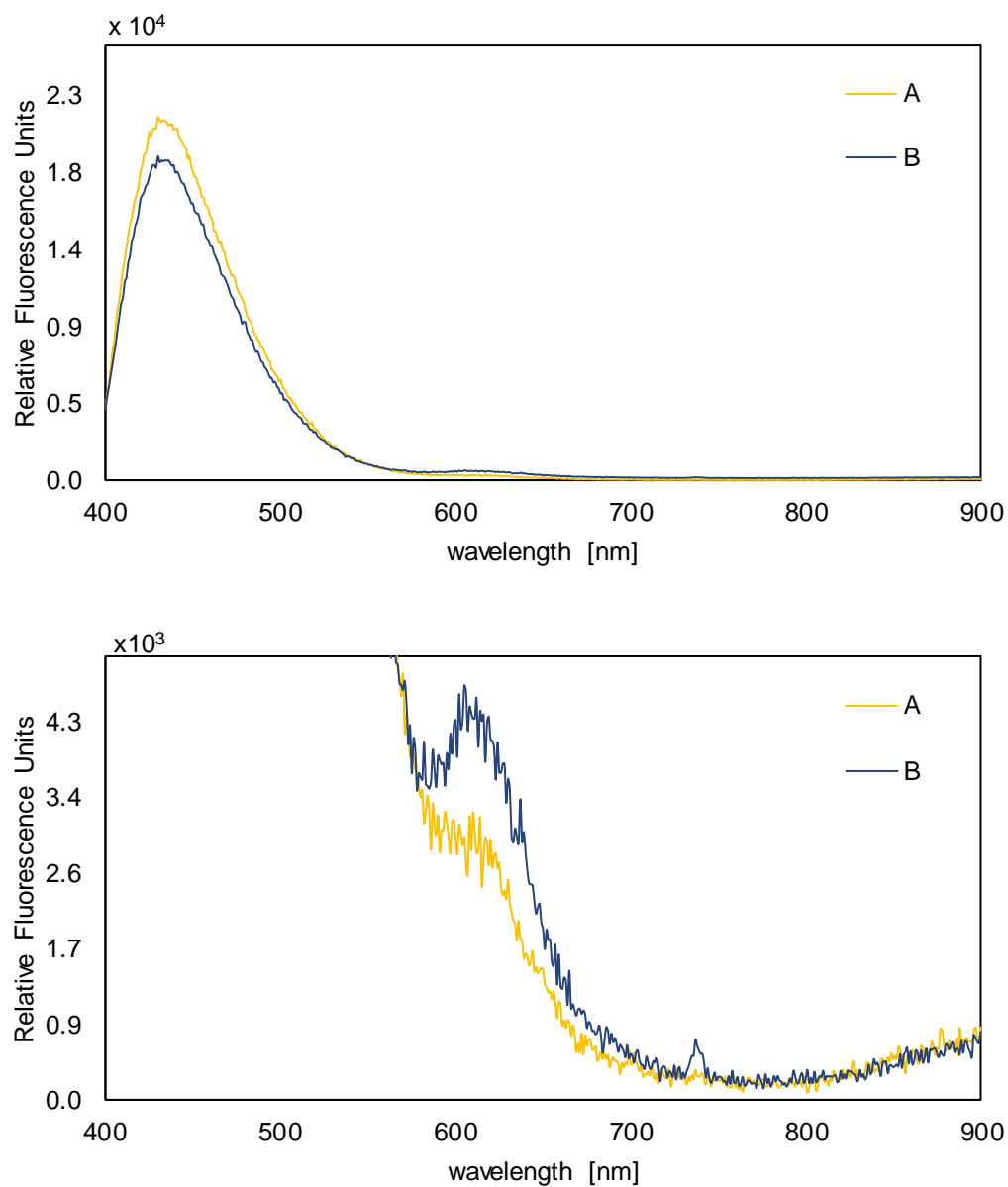
Figure V.6 Fluorescence emission spectra of I₂-oxyluciferin in acetonitrile (A) and deoxygenated acetonitrile (B), bottom graph highlights the peaks above 600 nm.

The concentration for I₂-oxyluciferin was 50 μM in all measurements. Deoxygenated acetonitrile was obtained by bubbling acetonitrile with nitrogen for 30 minutes.

Likewise, we measured the FL emission of Me$_2$-I$_2$-oxyluciferin in acetonitrile and deoxygenated acetonitrile. Our results showed a dramatic increase in emission intensity of Me$_2$-I$_2$-oxyluciferin at 464 and 738 nm in deoxygenated acetonitrile (Figure **V**.7. The peaks at 464 and 738 nm showed a 40% and 83% emission increase, respectively. These results supported our initial hypothesis, where the removal of oxygen from the solvent should decrease the possible $^1O_2$ production by triplet state energy transfer to molecular oxygen, thereby increasing the FL intensity. Due to the molecular oxygen dependence, we speculate that the emission peak at 738 nm in deoxygenated acetonitrile could be phosphorescence emission of the oxyluciferin analogue. Comparison of the emission intensity at 738 nm for I$_2$-oxyluciferin and Me$_2$-I$_2$-oxluciferin in deoxygenated acetonitrile showed a much higher emission for Me$_2$-I$_2$-oxluciferin. This difference could be due to the exclusive keto form of Me$_2$-I$_2$-oxluciferin. As discussed in section V.2.1, the keto-to-enol ratio of I$_2$-oxyluciferin was 20:80 in acetonitrile. Therefore, it is reasonable to speculate that the higher emission intensity for Me$_2$-I$_2$-oxyluciferin compared with I$_2$-oxyluciferin could be related to the 100% and 20% keto form percentage for each molecule, respectively. The absorbance maxima as well as the emission peaks for oxyluciferin, I$_2$-oxyluciferin, Me$_2$-I$_2$-oxyluciferin, I-oxyluciferin measured in acetonitrile are tabulated in Table **V**.1.
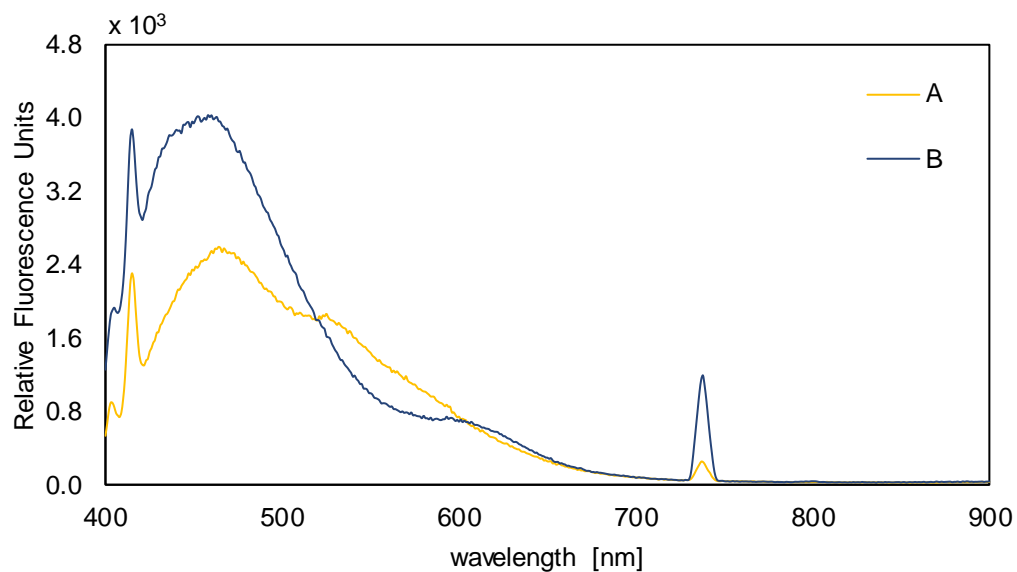
Figure V.7 Fluorescence emission spectra of Me₂-I₂-oxyluciferin in acetonitrile and deoxygenated acetonitrile.

The concentration for Me₂-I₂-oxyluciferin was 50 μM in all measurements. Deoxygenated acetonitrile was obtained by bubbling acetonitrile with nitrogen for 30 minutes.

Table V.1 Summary of absorbance λ_{max} and emission peaks for oxyluciferin, I₂-oxyluciferin, Me₂-I₂-oxyluciferin, I-oxyluciferin measured in acetonitrile.

	Absorbance [nm]	Fluorescence [nm]
Oxyluciferin	369	430
I₂-oxyluciferin	368	430, sh 612, 738
Me₂-I₂-oxyluciferin	364	464, 738
I-oxyluciferin	366	---

148

V.2.4 *Singlet oxygen formation by I$_2$-oxyluciferin and Me$_2$-I$_2$-oxyluciferin*

To assess the production of $^1O_2$ for our oxyluciferin analogues we used the SOSG assay which is highly selective to $^1O_2$. The SOSG reagent has a weak blue FL emission, and upon interaction with $^1O_2$ the chromophore yields a strong green (526 nm) FL emission. Consequently, is able to quantify the $^1O_2$ produced by sensitizers. We optimized the SOSG assay using a known photosensitizer, Rose Bengal, to evaluate the production of $^1O_2$. We then use it to measure $^1O_2$ productions with the iodinated oxyluciferin analogues. As a first step, we measured the production of $^1O_2$ using SOSG as a function of green LED irradiation time and Rose Bengal concentration. Our results showed that the production of $^1O_2$ increased with LED irradiation time and concentration of Rose Bengal (Figure **V**.8). The proportional response for Rose Bengal was observed even at low concentrations of 0.5 μM and much higher for 2.5 to 10 μM.

Figure V.8 Singlet oxygen produced by Rose Bengal during irradiation over time.
Singlet oxygen production was measured by the FL of SOSG, which was at constant concentration of 1 μM. Rose Bengal was excited using green LEDs (emission at 510-520 nm) in a photoreactor. Rose Bengal used at concentrations: 0 μM (A), 0.5 μM (B), 1 μM (C), 2.5 μM (D), 5 μM (E), and 10 μM (F).

Sensitization of molecular oxygen to produce $^1O_2$ by I_2-oxyluciferin and Me_2-I_2-oxyluciferin was evaluated using SOSG and UV irradiation within a photoreactor. To irradiate I_2-oxyluciferin we used UV-black light fluorescence lamps, with a similar setup to the irradiation of Rose Bengal, to investigate the concentration dependence and irradiation time for $^1O_2$ produced. Like the results for Rose Bengal, results for I_2-oxyluciferin showed that the production of $^1O_2$ increased with increasing analogue concentration and irradiation time (Figure **V**.9). However, the proportional increase with irradiation time and concentration of I_2-oxyluciferin was only true for concentrations from 2.5 μM to 10 μM but not for 0.5 and 1 μM. Note that data is not shown for low concentrations because the inability to generate $^1O_2$ leaves SOSG unoxidized and susceptible to UV irradiation which changes its photochemical properties.[36, 37] Results for Me_2-I_2-oxyluciferin also showed an increase in $^1O_2$ with increasing analogue concentration and UV irradiation time (Figure **V**.10). The fact that a lower concentration of Me_2-I_2-oxyluciferin can produce $^1O_2$ indicated that Me_2-I_2-oxyluciferin is a good oxygen sensitizer. It should be noted that our results for I_2-oxyluciferin and Me_2-I_2-oxyluciferin cannot be directly compared with the results for Rose Bengal due to differences in the irradiation source and associated source intensity.
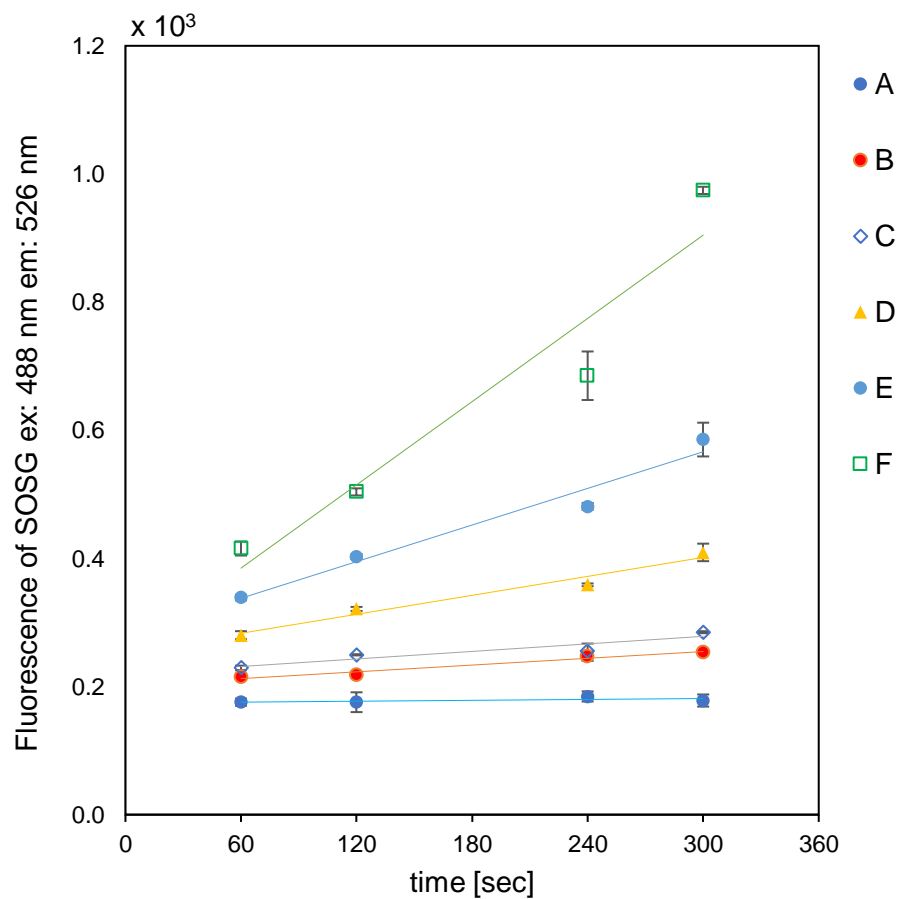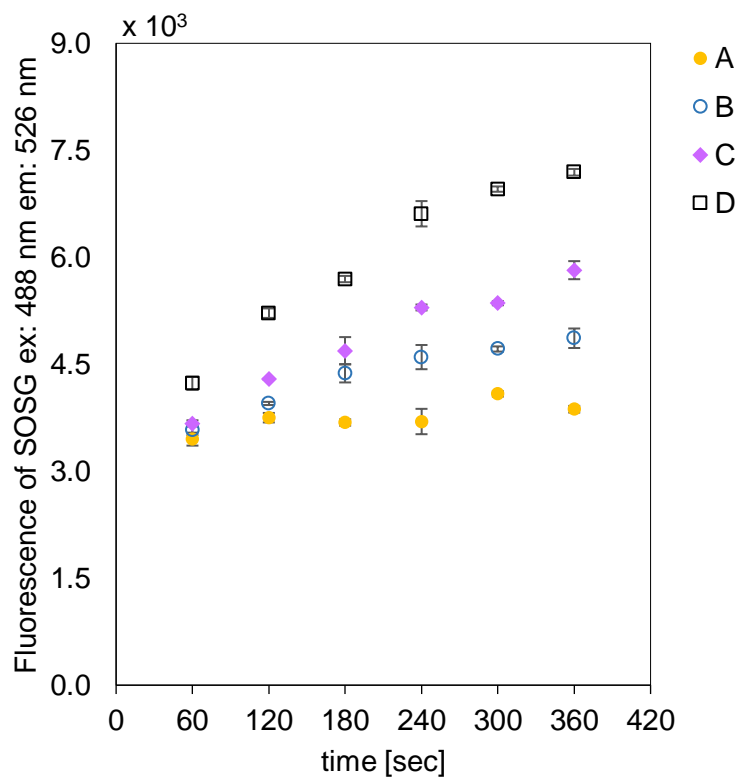
Figure V.9 Singlet oxygen produced by I₂-oxyluciferin during irradiation.
Singlet oxygen production was measured by the FL of SOSG, which was at a constant concentration of 1 μM. A photoreactor with UV-black light fluorescence lamps was used to excite I₂-oxyluciferin at concentrations of 0 μM (A), 2.5 μM (B), 5 μM (C), and 10 μM (D).
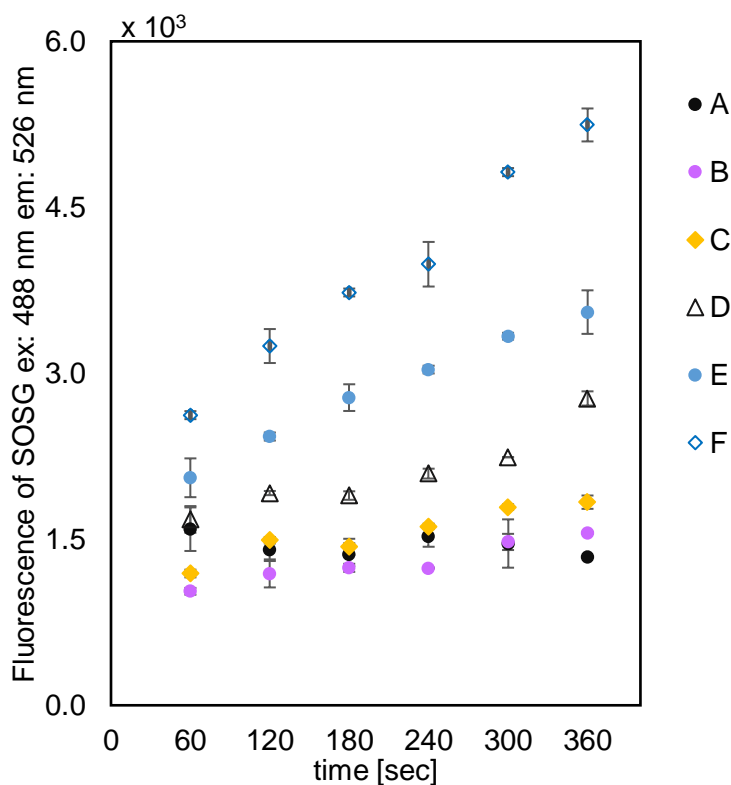
Figure V.10 Singlet oxygen produced by Me$_2$-I$_2$-oxyluciferin during irradiation.
Singlet oxygen production was measured by the FL of SOSG, which was at a constant concentration of 1 μM. A photoreactor with UV- black light fluorescence lamps was used to excite Me$_2$-I$_2$-oxyluciferin at concentrations of 0 μM (A) 0.5 μM (B), 1 μM (C), 2.5 μM (D), 5 μM (B), and 10 μM (F).

V.2.5 *Evaluation of I-oxyluciferin as a molecular oxygen sensitizer.*

Production of $^1O_2$ by I-oxyluciferin was measured using SOSG and UV irradiation, and compared with I$_2$-oxyluciferin to investigate the effect of a single iodine compared with double iodination. We first measured the production of $^1O_2$ by both oxyluciferins at concentrations of 2, 5 and 10 μM with a fixed irradiation time of 300 seconds. Our results

showed a much higher production of $^1O_2$ by the double iodinated compound compared with the single iodinated analogue at all concentrations (Figure **V**.11). Specifically, at a concentration of 10 µM for both sensitizers, I-oxyluciferin produced 57% of $^1O_2$ compared with I$_2$-oxyluciferin. Furthermore, the production of $^1O_2$ by 2 and 5 µM of I-oxyluciferin was similar, indicating that the assay is not sensitive enough to distinguish between these concentrations. Thus, we evaluated the dependence of $^1O_2$ production on irradiation time at a fixed concentration of 10 µM for both oxyluciferins. Our results showed a lower $^1O_2$ yield for I-oxyluciferin compared with I$_2$-oxyluciferin (Figure **V**.12). Collectively, these results indicated that a double iodination at the 5' and 7' positions of oxyluciferin is associated with a much higher oxygen sensitization ability compared with the oxyluciferin substituted with a single iodine at the 7' position. However, as discussed in Chapter 4, Section IV.3, the double substitutions at the 5' and 7' positions of luciferin could interfere with the overall activity of the enzyme. Thus, to maximize the heavy atom effect demonstrated by the double iodination of oxyluciferin, engineering of luciferase will be required to accommodate the luciferin analogue and promote catalysis for sensitization of oxygen.
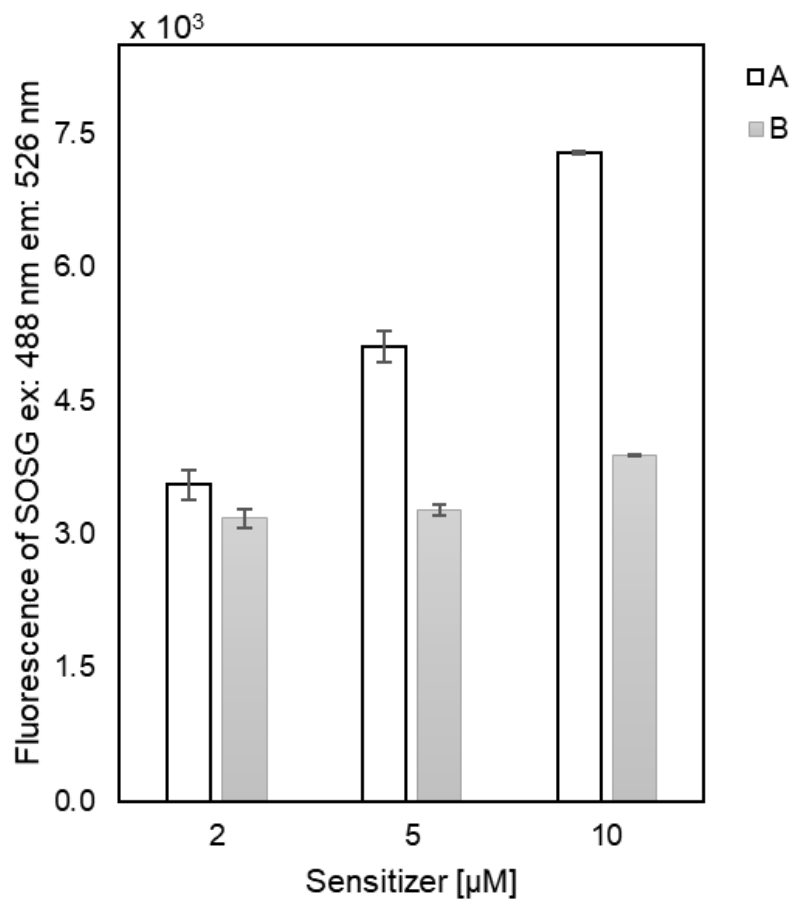
Figure V.11 Singlet oxygen produced by I₂-oxyluciferin and I-oxyluciferin for fixed irradiation time.
Singlet oxygen production was measured by the FL of SOSG, which was at a constant concentration of 1 µM. I₂-oxyluciferin (A) and I-oxyluciferin (B) were excited for 300 seconds using UV- black light fluorescence lamps in a photoreactor.
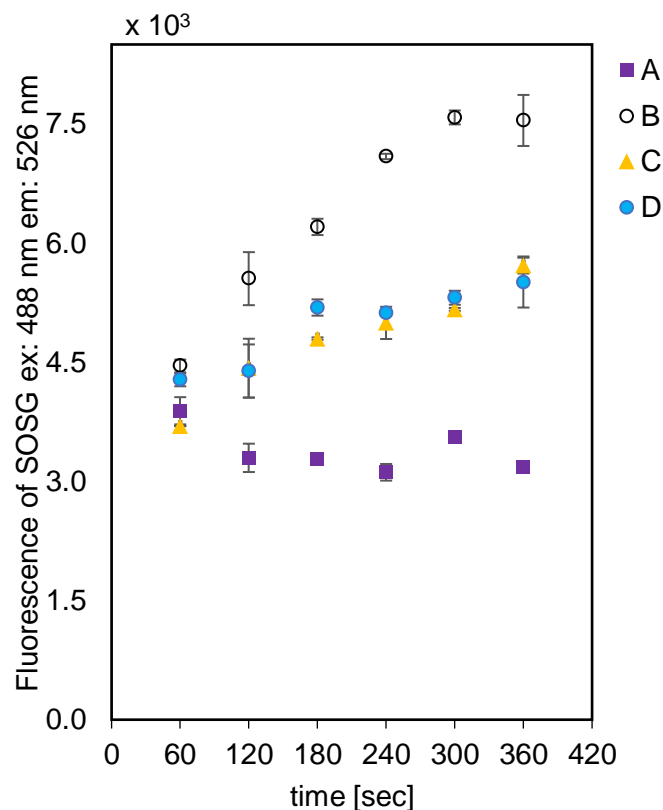
Figure V.12 Singlet oxygen produced by 10 μM of I$_2$-oxyluciferin and I-oxyluciferin during irradiation.
Singlet oxygen production was measured by the FL of SOSG, which was at a constant concentration of 1 μM. I2-oxyluciferin at 0 μM (A), 10 μM (B) and 5 μM (C), and I-oxyluciferin at 10 μM (D) were excited using UV- black light fluorescence lamps in a photoreactor.

V.3 Discussion

We demonstrated proof-of-concept of the oxyluciferin triplet state energy transfer to molecular oxygen to sensitize oxygen. To do so, we systematically evaluated the production of $^1O_2$ by several oxyluciferins under UV irradiation. Irradiation with a photoreactor allowed us to simplify the pathway required to produce $^1O_2$. We showed

that the oxyluciferins: I_2-oxyluciferin, Me_2-I_2-oxyluciferin, and I-oxyluciferin, were all able to produce $^1O_2$ when irradiated in the photoreactor. The significance of oxyluciferin analogue generation of $^1O_2$ demonstrates the feasibility of generating $^1O_2$ through the luciferase-luciferin reaction.

We showed that iodine substitution on oxyluciferin introduces a heavy atom effect that allowed the molecule to generate $^1O_2$. From our oxyluciferin analogues, Me_2-I_2-oxyluciferin showed the strongest bathochromic shift, reduced emission intensity, and highest sensitization of molecular oxygen. We attribute the behavior of Me_2-I_2-oxyluciferin to its tautomerization state, which is by design entirely in the keto form. Interesting, I_2-oxyluciferin, which exists primarily in the enol state, had a poor performance at these conditions. Furthermore, although a single iodination is more likely to work without the need to modify luciferase, we demonstrated that the heavy atom effect is improved for a double iodination compared with a single iodination of oxyluciferin. Collectively, we demonstrated successful sensitization of oxygen by our oxyluciferin analogues. However, to translate this capability to the luciferase-luciferin system, an engineered luciferase will be required to promote catalysis of I_2-oxyluciferin for maximum sensitization of oxygen.

We speculate that a luciferase-luciferin system comprised of an iodinated luciferin analogue and mutant luciferase can be developed to generate $^1O_2$, thereby broadening the use of BL reaction in biomedical or biological research. Recent advances in the BL field

have focused on developing luciferin analogues and mutated luciferase pairs to broaden the scope of BL.[34, 38-40] Key work with brominated luciferin analogues also showed that catalysis from wild-type luciferase can be nearly eliminated [34], suggesting that the iodine-substituted analogues may have no activity with the wild-type luciferase. Nevertheless, an iodinated luciferin and mutant luciferase pair could potentially enable *in vivo* deep tissue ablation studies, which are currently very challenging using the common fluorescence-based probes.[41-44] Moreover, future work with the iodinated oxyluciferins can create the opportunity to selectively target luciferase-expressing cells and permit novel investigations using 2D and 3D *in vitro* assays, and *in vivo* models.

V.4 Materials and methods

V.4.1 *General methods*

Solvents were obtained from commercial suppliers and used without purification. Oxyluciferin, I_2-oxyluciferin, Me_2-I_2-oxyluciferin and I-oxyluciferin were synthesized and spectroscopically characterized by Zhijian Han, Ph.D. Stocks of oxyluciferin and iodinated oxyluciferins were prepared at 1 mM in acetonitrile and stored at -20 °C. Before each experiment, working stocks for all oxyluciferins were prepared at 0.1 mM with sonication to dissolve visible particles, and wrapped in aluminum foil to protect them from light. All experiments were carried out at room temperature and away from direct light.

V.4.2 *^{1}H NMR keto-enol tautomerization evaluation.*

The ^{1}H NMR (400 MHz) spectra of I_2-oxyluciferin and Me_2-I_2-oxyluciferin were obtained by Dr. Han. For estimation of the keto-enol tautomerization the 5-C$\underline{H}$ was used following a method established by Naumov et al. Briefly, we used the integration of the 5-C$\underline{H}$ singlet peaks at 4 ppm corresponding to the keto and 6 ppm to the enol form. The integration was then used to quantify a keto-to-enol ratio of oxyluciferin.[35]

V.4.3 *Optical spectroscopy*

Absorbance measurements for oxyluciferin and iodinated oxyluciferins were obtained as described in Chapter II, Section II.4. Each oxyluciferin was diluted in acetonitrile to 50 μM from its respective 1 mM solution.

Fluorescence measurements for oxyluciferin and iodinated oxyluciferin samples were obtained using quartz cuvettes in a QM-400 Fluorometer from Horiba. Each oxyluciferin was diluted in acetonitrile to 50 μM from its respective 1 mM solution. A separate dilute solution of I_2-oxyluciferin or Me_2-I_2-oxyluciferin was bubbled with nitrogen gas for 30 minutes to prevent the interaction of the triplet state with molecular oxygen. Excitation for each oxyluciferin was set based on absorbance λ_{max} of each molecule (Table **V**.1). Fluorescence measurements for oxyluciferin and I_2-oxyluciferin were carried out using an integration time of 0.1 seconds and 0.5 nm slit. Fluorescence measurements for Me_2-I_2-oxyluciferin were carried out using an integration time of 1 second and 2 nm slit.

V.4.4 *Singlet oxygen measurement using SOSG*

We used Singlet Oxygen Sensor Green (SOSG; absorbance λ_{max} = 488 nm) to quantify the production of $^1O_2$ by Rose Bengal, I_2-oxyluciferin, Me_2-I_2-oxyluciferin and I-oxyluciferin. A stock solution of SOSG was prepared by adding 330 μL of methanol to commercial no-weigh vials containing 100 μg of SOSG obtained from Thermo Fisher. The stock solution

was prepared at an approximate concentration of 500 μM and stored at -20 °C. Stock solutions of SOSG were further diluted in methanol to a working solution of 12 μM for Rose Bengal experiments or 100 μM solutions for I_2-oxyluciferin and Me_2-I_2-oxyluciferin experiments.

To excite Rose Bengal, we used a box with an array of green LEDs with 510 nm to 520 nm emission. Samples were prepared by adding 60 μL solution of 1 mM PBS containing 1 μM SOSG and Rose Bengal at the desired concentration into a 384-black well plate. The Rose Bengal sample concentrations ranged from 0 to 10 μM. The black plates containing the samples were then irradiated by placing the LEDs box on top of the plate for the specified time. In contrast, iodinated oxyluciferins were excited using a Rayonet photoreactor with UV light provided by eight 8W black light fluorescent lamps (NEC. FL8 BL-B) and fitted with a mechanical carousel able to hold and rotate Pyrex-9820 culture tubes. The oxyluciferin analogues: I_2-oxyluciferin, Me_2-I_2-oxyluciferin, or I-oxyluciferin concentrations ranging from 0.5 to 10 μM and SOSG at a fixed concentration of 1 μM were combined into 100 μL of 1mM PBS and added into the Pyrex tubes for irradiation for the specified time. After irradiation, the tubes were removed, the samples collected and transferred to 384-black well plates. Finally, the FL of SOSG with Rose Bengal, I_2-oxyluciferin, Me_2-I_2-oxyluciferin or I-oxyluciferin was measured in a plate reader set to an excitation of 488 nm and with emission intensity acquired at 525 nm.

V.5 References

1.   Kearns, D. R., Physical and chemical properties of singlet oxygen. *Chemical Reviews* **1971,** *71* (4), 395-427.

2.   Briviba, K.; Klotz, L. O.; Sies, H., Toxic and signaling effects of photochemically or chemically generated singlet oxygen in biological systems. *Biological Chemistry* **1997,** *378* (11), 1259-1265.

3.   Bhatta, N.; Anderson, R. R.; Flotte, T.; Schiff, I.; Hasan, T.; Nishioka, N. S., Endometrial ablation by means of photodynamic therapy with photofrin II. *American Journal of Obstetrics and Gynecology* **1992,** *167* (6), 1856-1863.

4.   He, J. J.; Wang, Y.; Missinato, M. A.; Onuoha, E.; Perkins, L. A.; Watkins, S. C.; St Croix, C. M.; Tsang, M.; Bruchez, M. P., A genetically targetable near-infrared photosensitizer. *Nature Methods* **2016,** *13* (3), 263-268.

5.   Qi, Y. C. B.; Garren, E. J.; Shu, X. K.; Tsien, R. Y.; Jin, Y. S., Photo-inducible cell ablation in *Caenorhabditis elegans* using the genetically encoded singlet oxygen generating protein miniSOG. *Proceedings of the National Academy of Sciences of the United States of America* **2012,** *109* (19), 7499-7504.

6.   Wilson, B. C.; Patterson, M. S., The physics of photodynamic therapy. *Physics in Medicine and Biology* **1986,** *31* (4), 327-360.

7.   Bar-On, L.; Jung, S., Defining dendritic cells by conditional and constitutive cell ablation. *Immunological Reviews* **2010,** *234*, 76-89.

8.   Choi, T. Y.; Khaliq, M.; Ko, S.; So, J.; Shin, D. S., Hepatocyte-specific ablation in zebrafish to study biliary-driven liver regeneration. *Jove-Journal of Visualized Experiments* **2015,** (99), e52785.

9.   Cione, E.; Caroleo, M. C.; Cannataro, R.; Perri, M.; Pingitore, A.; Genchi, G., Vitamin A and diabesity: new insight for drug discovery. *Mini-Reviews in Medicinal Chemistry* **2016,** *16* (9), 738-742.

10.   Nast, A. R.; Extavour, C. G., Ablation of a single cell from eight-cell embryos of the amphipod crustacean parhyale hawaiensis. *Jove-Journal of Visualized Experiments* **2014,** (85), 51073.

11.   Pajoohesh-Ganji, A.; Miller, R. H., Oligodendrocyte ablation as a tool to study demyelinating diseases. *Neural Regeneration Research* **2016,** *11* (6), 886-889.

12.   Smith, L. B.; O'Shaughnessy, P. J.; Rebourcet, D., Cell-specific ablation in the testis: what have we learned? *Andrology* **2015,** *3* (6), 1035-1049.

13.   Thorsness, M. K.; Nasrallah, J. B., Cell-specific ablation in plants. *Methods in Cell Biology, Vol 50* **1995,** *50*, 439-448.

14.   Xu, S. H.; Chisholm, A. D., Highly efficient optogenetic cell ablation in *C. elegans* using membrane-targeted miniSOG. *Scientific Reports* **2016,** *6*.

15.   Nauta, J. M.; vanLeengoed, H.; Star, W. M.; Roodenburg, J. L. N.; Witjes, M. J. H.; Vermey, A., Photodynamic therapy of oral cancer - a review of basic mechanisms and clinical applications. *European Journal of Oral Sciences* **1996,** *104* (2), 69-81.

16.   Bachowski, G. J.; Pintar, T. J.; Girotti, A. W., Photosensitized lipid peroxidation and enzyme inactivation by membrane bround merocyanine-540 reaction mechanisms in the absence and presence of ascorbate. *Photochemistry and Photobiology* **1991,** *53* (4), 481-491.

17.   Calixto, G. M. F.; Bernegossi, J.; de Freitas, L. M.; Fontana, C. R.; Chorilli, M., Nanotechnology-based drug delivery systems for photodynamic therapy of cancer: a review. *Molecules* **2016,** *21* (3), 342-360.

18.   Ge, R. F.; Ahn, J. C.; Shin, J. I.; Bahk, C. W.; He, P.; Chung, P. S., An *in vitro* and *in vivo* study of combination therapy with photogem (R)-mediated photodynamic therapy and cisplatin on mouse cancer cells (CT-26). *Photomedicine and Laser Surgery* **2011,** *29* (3), 155-160.

19.   Zuluaga, M. F.; Lange, N., Combination of photodynamic therapy with anti-cancer agents. *Current Medicinal Chemistry* **2008,** *15* (17), 1655-1673.

20.   Szacilowski, K.; Macyk, W.; Drzewiecka-Matuszek, A.; Brindell, M.; Stochel, G., Bioinorganic photochemistry: frontiers and mechanisms. *Chemical Reviews* **2005,** *105* (6), 2647-2694.

21.   Moan, J., On the diffusion length of singlet oxygen in cells and tissues. *Journal of Photochemistry and Photobiology B-Biology* **1990,** *6* (3), 343-347.

22.   Juzeniene, A.; Peng, Q.; Moana, J., Milestones in the development of photodynamic therapy and fluorescence diagnosis. *Photochemical & Photobiological Sciences* **2007,** *6* (12), 1234-1245.

23.   Mehraban, N.; Freeman, H. S., Developments in PDT Sensitizers for Increased Selectivity and Singlet Oxygen Production. *Materials* **2015,** *8* (7), 4421-4456.

24.   Sarkisyan, K. S.; Zlobovskaya, O. A.; Gorbachev, D. A.; Bozhanova, N. G.; Sharonov, G. V.; Staroverov, D. B.; Egorov, E. S.; Ryabova, A. V.; Solntsev, K. M.; Mishin, A. S.; Lukyanov, K. A., KillerOrange, a genetically encoded photosensitizer activated by blue and green light. *Plos One* **2015,** *10* (12), e0145287.

25.   Bulina, M. E.; Chudakov, D. M.; Britanova, O. V.; Yanushevich, Y. G.; Staroverov, D. B.; Chepurnykh, T. V.; Merzlyak, E. M.; Shkrob, M. A.; Lukyanov, S.; Lukyanov, K. A., A genetically encoded photosensitizer. *Nature Biotechnology* **2006,** *24* (1), 95-99.

26.   Ryumina, A. P.; Serebrovskaya, E. O.; Staroverov, D. B.; Zlobovskaya, O. A.; Shcheglov, A. S.; Lukyanov, S. A.; Lukyanov, K. A., Lysosome-associated miniSOG as a photosensitizer for mammalian cells. *Biotechniques* **2016,** *61* (2), 92-94.

27.   Ryumina, A. P.; Serebrovskaya, E. O.; Shirmanova, M. V.; Snopova, L. B.; Kuznetsova, M. M.; Turchin, I. V.; Ignatova, N. I.; Klementieva, N. V.; Fradkov, A. F.; Shakhov, B. E.; Zagaynova, E. V.; Lukyanov, K. A.; Lukyanov, S. A., Flavoprotein miniSOG as a genetically encoded photosensitizer for cancer cells. *Biochimica Et Biophysica Acta-General Subjects* **2013,** *1830* (11), 5059-5067.

28.   Theodossiou, T.; Hothersall, J. S.; Woods, E. A.; Okkenhaug, K.; Jacobson, J.; MacRobert, A. J., Firefly luciferin-activated Rose Bengal: *in vitro* photodynamic therapy by intracellular chemiluminescence in transgenic NIH 3T3 cells. *Cancer Research* **2003,** *63* (8), 1818-1821.

29.   Carpenter, S.; Fehr, M. J.; Kraus, G. A.; Petrich, J. W., Chemiluminescence activation of the antiviral activity of hypericin - a molecular flashlight. *Proceedings of the National Academy of Sciences of the United States of America* **1994,** *91* (25), 12273-12277.

30.   Kim, S.; Jo, H.; Jeon, M.; Choi, M. G.; Hahn, S. K.; Yun, S. H., Luciferase-Rose Bengal conjugates for singlet oxygen generation by bioluminescence resonance energy transfer. *Chemical Communications* **2017,** *53* (33), 4569-4572.

31.   Yang, Y. K.; Hou, W. Y.; Liu, S. Y.; Sun, K.; Li, M. Y.; Wu, C. F., Biodegradable polymer nanoparticles for photodynamic therapy by bioluminescence resonance energy transfer. *Biomacromolecules* **2018,** *19* (1), 201-208.

32.   Rodriguez-Serrano, A.; Rai-Constapel, V.; Daza, M. C.; Doerr, M.; Marian, C. M., Internal heavy atom effects in phenothiazinium dyes: enhancement of intersystem crossing via vibronic spin-orbit coupling. *Physical Chemistry Chemical Physics* **2015,** *17* (17), 11350-11358.

33.   Harwood, K. R.; Mofford, D. M.; Reddy, G. R.; Miller, S. C., Identification of mutant firefly luciferases that efficiently utilize aminoluciferins. *Chemistry & Biology* **2011,** *18* (12), 1649-1657.

34.   Steinhardt, R. C.; Rathbun, C. M.; Krull, B. T.; Yu, J. M.; Yang, Y.; Nguyen, B. D.; Kwon, J.; McCutcheon, D. C.; Jones, K. A.; Furche, F.; Prescher, J. A., Brominated luciferins are versatile bioluminescent probes. *Chembiochem* **2017,** *18* (1), 96-100.

35.   Maltsev, O. V.; Nath, N. K.; Naumov, P.; Hintermann, L., Why is firefly oxyluciferin a notoriously labile substance? *Angewandte Chemie-International Edition* **2014,** *53* (3), 847-850.

36.   Ragas, X.; Jimenez-Banzo, A.; Sanchez-Garcia, D.; Batllori, X.; Nonell, S., Singlet oxygen photosensitisation by the fluorescent probe Singlet Oxygen Sensor Green (R). *Chemical Communications* **2009,** (20), 2920-2922.

37.   Kim, S.; Fujitsuka, M.; Majima, T., Photochemistry of Singlet Oxygen Sensor Green. *Journal of Physical Chemistry B* **2013,** *117* (45), 13985-13992.

38.   Rathbun, C. M.; Porterfield, W. B.; Jones, K. A.; Sagoe, M. J.; Reyes, M. R.; Hua, C. T.; Prescher, J. A., Parallel screening for rapid identification of orthogonal bioluminescent tools. *ACS Central Science* **2017,** *3* (12), 1254-1261.

39.   Mofford, D. M.; Adams, S. T.; Reddy, G.; Reddy, G. R.; Miller, S. C., Luciferin amides enable *in vivo* bioluminescence detection of endogenous fatty acid amide hydrolase activity. *Journal of the American Chemical Society* **2015,** *137* (27), 8684-8687.

40.   Adams, S. T.; Mofford, D. M.; Reddy, G.; Miller, S. C., Firefly luciferase mutants allow substrate-selective bioluminescence imaging in the mouse brain. *Angewandte Chemie-International Edition* **2016,** *55* (16), 4943-4946.

41.   Muthiah, M.; Park, S. H.; Nurunnabi, M.; Lee, J.; Lee, Y. K.; Park, H.; Lee, B. I.; Min, J. J.; Park, I. K., Intracellular delivery and activation of the genetically encoded photosensitizer Killer Red by quantum dots encapsulated in polymeric micelles. *Colloids and Surfaces B-Biointerfaces* **2014,** *116*, 284-294.

42.   Abrahamse, H.; Hamblin, M. R., New photosensitizers for photodynamic therapy. *Biochemical Journal* **2016,** *473*, 347-364.

43.   Shirmanova, M. V.; Serebrovskaya, E. O.; Snopova, L. B.; Kuznetsova, M. M.; Ryumina, A. P.; Turchin, I. V.; Sergeeva, E. A.; Ignatova, N. I.; Klementieva, N. V.; Lukyanov, K. A.; Lukyanov, S. A.; Zagaynova, E. V., KillerRed and miniSOG as genetically encoded photosensitizers for photodynamic therapy of cancer. In *Medical Laser Applications and Laser-Tissue Interactions Vi*, Lilge, L. D.; Sroka, R., Eds. 2013; Vol. 8803.

44.   Serebrovskaya, E. O.; Stremovsky, O. A.; Chudakov, D. M.; Lukyanov, K. A.; Deyev, S. M., Genetically encoded immunophotosensitizer. *Russian Journal of Bioorganic Chemistry* **2011,** *37* (1), 123-129.

Chapter VI: Conclusion

Efforts to expand the BL scope through the luciferase-luciferin system from the firefly have been describe in this work. We have designed luciferin analogues aimed to improve the efficiency of luciferase, use the reaction a for thiol/disulfide redox probe, achieve higher BL at neutral pH, and investigated the possibility of $^1O_2$ production from the reaction. These aims were studied with d_2-luciferin, S-luciferin, F_2-luciferin, and the iodinated oxyluciferins analogues, I_2-oxyluciferin, Me_2-I_2-oxyluciferin, I-oxyluciferin, which are discussed in the previous chapters.

More specifically, our results with d_2-luciferin showed that the deuteration was successful in decreasing the production of dehydroluciferin, a known inhibitor of the BL reaction.[1, 2] The BL reaction with d_2-luciferin has a new ratio of 1 to 11 dehydroluciferin to oxyluciferin produced, compared to 1 to 5.25 with luciferin. However, these results did not reflect a high BL emission intensity as expected, when compared to luciferin. BL emission studies showed that over time there is a lower decay in BL from d_2-luciferin compared to luciferin. Our results suggest that long-term BL *in vivo* or *in vitro*, where addition of Coenzyme A is not feasible, might benefit from using d_2-luciferin.

Many BL analyte probes have been created over the years using the luciferase-luciferin reaction from the firefly.[3-11] However, to our knowledge there is no thiol-disulfide BL

probe that could be used in intact cell studies. Therefore, we designed S-luciferin which possesses the ability to interact with other sulfides within the cells and decrease BL as a signal of a reductive environment. Interestingly, S-luciferin proved to be a poor chromophore and poor substrate of luciferase. These results were explained through the thiol substitution that causes a decrease in the electron donating capacity necessary for emission. Furthermore, our results showed that S-luciferin is a strong inhibitor to luciferase and its BL intensity is 0.01% to that of luciferin.

A known challenge of the luciferase-luciferin reaction is the pH dependence of both, the enzyme and the substrate. Previous studies have focused on targeting the pH dependence through luciferase mutants and luciferin analogues. However, most of them resulted in a decrease of enzymatic activity.[12-14] Our studies with F_2-luciferin, which was designed to drastically lower the pK_A of the 6'-hydroxyl group and allow the molecule to be ionized during neutral pH, showed that it is a better chromophore at neutral pH compared to luciferin. However, as a substrate of luciferase, F_2-luciferin has a high affinity but has a low turn-over rate, which translate to a low BL emission intensity.

After our experience with the first three luciferin analogues, d_2-luciferin, S-luciferin, and F_2-luciferin, our next aim to broaden the scope of luciferase-luciferin reaction targeted the production of $^1O_2$ as a product of the reaction. Our strategy to investigate the production of $^1O_2$ through the luciferase-luciferin reaction started by using oxyluciferin analogues for proof-of-concept. Therefore, we designed iodinated oxyluciferin analogues and studied

their $^1O_2$ production capacity independent of the enzyme environment and by UV irradiation. Our results showed that the iodinated oxyluciferin analogues were capable of generating $^1O_2$. Furthermore, our overall experience with the luciferase-luciferin reaction will help us engineer a novel luciferase-luciferin pair capable of generating $^1O_2$ using iodinated luciferin analogues.

VI.1 References

1. Fontes, R.; Dukhovich, A.; Sillero, A.; Sillero, M. A. G., Synthesis of dehydroluciferin by firefly luciferase: effect of dehydroluciferin, coenzyme A and nucleoside triphosphates on the luminescent reaction. *Biochemical and Biophysical Research Communications* **1997,** *237* (2), 445-450.

2. da Silva, L. P.; da Silva, J. C. G. E., Kinetics of inhibition of firefly luciferase by dehydroluciferyl-coenzyme A, dehydroluciferin and L-luciferin. *Photochemical & Photobiological Sciences* **2011,** *10* (6), 1039-1045.

3. Ioka, S.; Saitoh, T.; Maki, S. A.; Imoto, M.; Nishiyama, S., Development of a luminescence-controllable firefly luciferin analogue using selective enzymatic cyclization. *Tetrahedron* **2016,** *72* (47), 7505-7508.

4. Zheng, Z.; Wang, L.; Tang, W.; Chen, P. Y.; Zhu, H.; Yuan, Y.; Li, G. Y.; Zhang, H. F.; Liang, G. L., Hydrazide d-luciferin for *in vitro* selective detection and intratumoral imaging of Cu2+. *Biosensors & Bioelectronics* **2016,** *83*, 200-204.

5. Hsu, H. T.; Trantow, B. M.; Waymouth, R. M.; Wender, P. A., Bioorthogonal catalysis: a general method to evaluate metal catalyzed reactions in real time in living systems using a cellular luciferase reporter system. *Bioconjugate Chemistry* **2016,** *27* (2), 376-382.

6. Mofford, D. M.; Adams, S. T.; Reddy, G.; Reddy, G. R.; Miller, S. C., Luciferin amides enable *in vivo* bioluminescence detection of endogenous fatty acid amide hydrolase activity. *Journal of the American Chemical Society* **2015,** *137* (27), 8684-8687.

7. Henkin, A. H.; Cohen, A. S.; Dubikovskaya, E. A.; Park, H. M.; Nikitin, G. F.; Auzias, M. G.; Kazantzis, M.; Bertozzi, C. R.; Stahl, A., Real-time noninvasive imaging of fatty acid uptake *in vivo*. *Acs Chemical Biology* **2012,** *7* (11), 1884-1891.

8. Yuan, Y.; Wang, F. Q.; Tang, W.; Ding, Z. L.; Wang, L.; Liang, L. L.; Zheng, Z.; Zhang, H. F.; Liang, G. L., Intracellular self-assembly of cyclic d-luciferin nanoparticles for persistent bioluminescence imaging of fatty acid amide hydrolase. *ACS Nano* **2016,** *10* (7), 7147-7153.

9. Ke, B. W.; Wu, W. X.; Liu, W.; Liang, H.; Gong, D. Y.; Hu, X. T.; Li, M. Y., Bioluminescence probe for detecting hydrogen sulfide *in vivo*. *Analytical Chemistry* **2016,** *88* (1), 592-595.

10. Ke, B. W.; Wu, W. X.; Wei, L.; Wu, F. B.; Chen, G.; He, G.; Li, M. Y., Cell and *in vivo* imaging of fluoride ion with highly selective bioluminescent probes. *Analytical Chemistry* **2015,** *87* (18), 9110-9113.

11. Van de Bittner, G. C.; Bertozzi, C. R.; Chang, C. J., Strategy for dual-analyte luciferin imaging: *in vivo* bioluminescence detection of hydrogen peroxide and caspase activity in a murine model of acute inflammation. *Journal of the American Chemical Society* **2013,** *135* (5), 1783-1795.

12. Hirokawa, K.; Kajiyama, N.; Murakami, S., Improved practical usefulness of firefly luciferase by gene chimerization and random mutagenesis. *Biochimica Et Biophysica Acta-Protein Structure and Molecular Enzymology* **2002,** *1597* (2), 271-279.

13. Jathoul, A.; Law, E.; Gandelman, O.; Pule, M.; Tisi, L.; Murray, J., Development of a pH tolerant thermostable *Photinus pyralis* luciferase for brighter *in vivo* imaging. In *Bioluminescence - Recent Advances in Oceanic Measurements and Laboratory Applications*, Lapota, D., Ed. InTech: **2012**; pp 119-136.

14. Takakura, H.; Kojima, R.; Ozawa, T.; Nagano, T.; Urano, Y., Development of 5 '- and 7 '-substituted luciferin analogues as acid-tolerant substrates of firefly luciferase. *Chembiochem* **2012,** *13* (10), 1424-1427.